UNIVERSITA' DEGLI STUDI DI MILANO

Facoltà di Medicina e Chirurgia

Dipartimento di Biotecnologie Mediche e Medicina Traslazionale

CORSO DI DOTTORATO DI RICERCA IN

PATOLOGIA E NEUROPATOLOGIA SPERIMENTALI, CICLO XXVII

MED/04

TESI DI DOTTORATO DI RICERCA

Role of microRNA in the regulation of TLR signaling pathway

Tiziana Ada RENZI

Matr. R09503

Tutor: Prof. Massimo LOCATI

Anno Accademico 2013-2014

INDEX

Abbreviations

Ab	antibody
Ag	antigen
Ago	Argonaute
APC	antigen presenting cell
-APC	allophycocyanin
BLIMP1	B lymphocyte-induced maturation protein-1
BM	bone marrow
BSA	bovine serum albumin
CD40L	CD40 ligand
ChIP	Chromatin immunoprecipitation
chr	chromosome
C.I.	confidence interval
CTL	cytotoxic T lymphocytes
DAMP	damage- associated molecular pattern
DC	dendritic cell
DGCR8	DiGeorge Syndrome Critical Region 8
DNA	deoxyribonucleic acid
eIF	eukaryotic initiation factor
ELISA	enzyme linked immunosorbent assay

ER	endoplasmic reticulum
FACS	fluorescence activated cell sorting
FCS	fetal calf serum
Fig	figure
FITC	fluorescein-isothiocyanate
Fc	fragment crystallisable
IFNγ	interferon-γ
Ig	immunoglobulin
IL	interleukin
i.p.	intra-peritoneal
IRAK	IL1R associated kinase
LN	lymph node
lncRNA	Long non-coding RNA
LPS	lipopolysaccharide
mAb	monoclonal antibody
MAPK	mitogen-activated protein kinase
Mϕ	macrophages
MHC	major histocompatibility complex
MMR	macrophage mannose receptor
MNC	mononuclear cell
MiRNA	MicroRNA

MRE	miR- responsive element
mRNA	Messenger RNA
MSR	macrophage scavenger receptor
MyD88	myeloid differentiation factor 88
ncRNA	Non-coding RNA
NF-κB	nuclear factor – kappa B
NK	natural killer
NLR	NOD-like receptor
NP-CGG	4-hydroxy-3-nitrophenyl-chicken gamma globulin
OD	optical density
o.n.	overnight
PAMP	pathogen-associated molecular pattern
Pam3CSK4	palmitoyl-3-cysteine-serine-lysine-4
PBMC	peripheral blood mononuclear cells
PBS	phosphate buffered saline
PBL	peripheral blood lymphocytes
PCR	Polymerase chain reaction
PE	phycoerythrin
PMN	polymorphonucleated granulocytes
Pre-miRNA	Precursor miRNA
Pri-miRNA	Primary miRNA

PRR	pathogen-recognition receptor
Pol II	RNA polymerase II
poly(I:C)	polyinosinic-polycytidylic acid
qPCR	Quantitative PCR
RAN-GTP	RAS- related nuclear protein-guanosine triphosphate
RIP	RNA immunoprecipitation
RISC	RNA-induced silencing complex
RLR	Rig-I-like receptor
RNA	ribonucleic acid
ROS	reactive oxygen species
rRNA	Ribosomal RNA
RT	room temperature
SD	standard deviation
SEM	Standard error of the mean
SLE	systemic lupus erythematosus
SnoRNA	small nucleolar RNA
SOCS	Suppressor of cytokine signaling
STAT	signal transducers and activators of transcription
TCR	T cell receptor
TD	thymus-dependent
TGFβ	transforming growth factor-β

Th	T helper type 1
TLR	toll-like receptor
TNF	tumor necrosis factor
TRAF6	Tumor necrosis factor receptor-associated factor 6
TRBP	Tar RNA binding protein
TRIF	TIR domain-containing adaptor protein inducing IFNβ
tRNA	transfer RNA
UTR	untranslated region
WT	wild-type

ABSTRACT

Toll-like receptors (TLRs) play key roles in detecting pathogens and initiating inflammatory responses via the activation of specific signaling pathways. The TLRs activity must be tightly regulated to avoid excessive inflammation and consequent immunopathology, ranging from autoimmunity to cancer. MicroRNAs (miRNAs) are a new class of negative regulators involved in setting the balance of the immune response to inflammatory triggers. In this study, we identified miR-125a~99b~let-7e cluster and miR-146b as miRNAs that, after LPS engagement on human monocytes, are induced by the anti-inflammatory IL-10 and TGFβ, but are inhibited by the pro-inflammatory IFNγ.

Bioinformatic analysis predicted and experimental evidence demonstrated that miR-125a-5p, let-7e-5p and miR-146b directly target the TLR pathway at multiple levels, including receptors (TLR4, CD14), signaling molecules (IRAK1, MyD88, TRAF6), and effectors (TNFα, IL-6, CCL3, CCL7, CXCL8).

We showed that over-expression or inhibition of miR-125a, let-7e and miR-146b expression with lentiviral vector in human monocytes had a significant impact on the production of pro-inflammatory cytokines in response to LPS. In particular, we identified a role for miR-125a-5p and miR-146b in mediating the LPS hyporensponsiveness observed after IL-10 or TGFβ priming or during the endotoxin tolerance, the phenomenon of reduced sensitivity to subsequent challenge of LPS. The up-regulation of miR-125a-5p and miR-146b into THP-1 cells mimicked the LPS, IL-10 or TGFβ priming, whereas the inhibition of them by lentiviral vector or a pre-treatment with IFNγ reverted, partially, the tolerant phenotype.

In an *in vivo* model of acute inflammatory response, we obtained that miR-125a-5p, miR-99b-5p and miR-146b were induced in macrophages recruited at the site of inflammation during the resolution process, and this was impaired in macrophages of IL-10 KO mice. Our studies indicated that miRNA cluster and miR-146b represent a new negative feedback mechanism of the TLR signaling pathway.

1. INTRODUCTION

1.1 The immune system

The human body provides a perfect habitat for many germs, such as bacteria, viruses, fungi, and parasites, so the immune system has been evolved to recognize and to distinguish them from the organism's health tissues. The immune system can be divided in subsystems with increasing specificity: the *innate immune system* offers an immediate, but non-specific response and it is found in all animals and plants; and the *adaptive immune system*, activated by the innate immune cells if the infection could not be cleared. It is extremely specific, relying on antigen-specific receptors and results in immunological memory which allows a better response after a re-infection of the same pathogen.

Both adaptive and innate immune systems are needed for an optimal response against pathogens because, other than chronologically subsequent, they are also highly integrated: the innate responses stimulate and direct the adaptive ones, while the adaptive responses react against pathogens by stimulating also effector mechanisms of innate immunity.

1.1.2 The innate immune system

The innate immune system is formed by a group of cells or molecules which recognize elements conserved and used in a large group of pathogens, called pathogen associated molecular patterns (PAMPs), by germline-encoded pattern-recognition receptors (PRR). These PRRs have evolved to recognize what is infectious non-self from non-infectious self, a vital distinction [1].

The innate immune system is made of both humoral components, composed by soluble proteins as the complement system, and cellular components, that include

macrophages, monocytes, polymorphonucleated granulocytes (PMN; neutrophils, basophils, mast cells, and eosinophils), natural killer (NK) cells and dendritic cells (DCs). These cells are activated during and inflammatory response and clear the infection; but subsequently migrate to lymphoid organs and present microbial antigens, as antigen presenting cells (APCs), to specific T lymphocytes trigger adaptive immune response.

- ***Neutrophils***

Neutrophils are the most abundant leukocytes in mammals. During the acute phase of inflammation, they are the first cells that arrive at the site of inflammation. Once in the inflammatory tissue, the hallmark functions of neutrophils are: the ability to act as phagocytes, the release of anti-microbial mediators from their granules, and the production of reactive oxygen intermediates (ROI) with anti-microbial potential [2]. Another described mechanism of killing bacteria is the formation of neutrophil extracellular traps (NET), a net of fibers composed by chromatin and serine proteases that trap and kill bacteria with a high concentration of anti-inflammatory mediators, preventing the spread of pathogens and of damaging molecules [3]. All of these processes are highly regulated by the signals they receive from different PRRs, including almost all members of Toll-like receptor (TLR) family with the exclusion of TLR3 [4]. The resting neutrophils have a very short average lifespan in the circulation, of about 5.4 days [5], and after the activation they survive only 1-2 days. It has been hypothesized that the short lifetime of neutrophils derived from an evolutionary adaption, because reduce the diffusion of pathogens that have been phagocytized and because limits the damage of antimicrobial products released by neutrophils during the inflammatory response. Usually, after the ingestion of pathogens, neutrophils undergo apoptosis and are phagocytosed by macrophages, an important step for the resolution of inflammation.

- ***Monocytes***

Monocytes, macrophages and DC are mononuclear phagocytes that were universally considered as related cell types that arise from a continuum of differentiation, established by van Furth's *mononuclear phagocyte system* (MPS) concept in 1968 [6]. However, although monocytes can originate DCs and macrophages during inflammation, recent studies have demonstrated that most of tissue macrophages do not derive from differentiated monocytes in the steady state and rather originate from yolk sac of fetal liver and populate organs at birth [7]. Monocytes have an essential role in antimicrobial immune defense but they are also implicated in many inflammatory diseases and they can be recruited to tumor sites and can inhibit tumor-specific immune defense mechanisms [8].

Monocytes represent 10% of leukocytes in human blood and 4% of leukocytes in mouse blood, with a marginal pool in the spleen and lungs that can be mobilized in certain conditions [9, 10]. Monocytes arise from myeloid precursor cells in primary lymphoid organs, including the fetal liver and bone marrow, during both embryonic and adult haematopoiesis [11]. There are two main phenotypically and functionally distinct subsets of monocytes: the first subset — defined as $LY6C^{low}$ cells in mice and as $CD14^{low}CD16^{+}$ cells in humans — seems to be dedicated to the surveillance of endothelial integrity and these cells effectively act as luminal blood macrophages; the second main subset — defined as $LY6C^{hi}$ cells in mice and as $CD14^{+}$ cells in humans — have classical monocyte functions, such as rapid extravasation at sites of injury and replenishment of peripheral DC and macrophage compartments [12]. A peculiar feature of monocytes is their plasticity that can be recapitulated *in vitro* with different stimuli: human and mouse monocytes cultivate with IL-4 and granulocyte- macrophage colony- stimulating factor (GM-CSF) differentiate them into DCs; stimulation with M-CSF differentiate them into macrophages [13].

- ***Macrophages***

Macrophages are haematopoietic cells that populate every tissue including the brain. They play a major role in tissue homeostasis and development, through clearance of foreign and damaged cells and participate in the induction and resolution of the inflammation [14]. Recently, fate-mapping studies revealed that adult microglia, alveolar macrophages, splenic red pulp macrophages and F4/80^{hi} peritoneal cavity macrophages do not derive from blood monocytes for their replenishment but have a fetal origin, at least under steady-state conditions [7]. In normal mice, these cells exist togheter with 'F4/80^{lo} macrophages', that have haematopoietic origin [15]. Macrophages are divided into two classes: the 'M1-M2 paradigm'. Classically activated M1 macrophages are induced by interferon γ (IFNγ) alone or with microbial stimuli (e.g. LPS) or cytokines (e.g. TNF and GM-CSF). Alternative M2 activation can be induced by IL-4 and IL-13 [16] and many other cytokines like IL-33 [17] and IL-21 [18]. Macrophages can also be polarized into an 'M2-like' state, by different stimuli as transforming growth factor-β (TGFβ), glucocorticoids, IL-10 and Wnt5a [19]. This 'M2-like' macrophages share some characteristics of M2 cells, as high expression of IL-10, mannose receptor, and angiogenic factors [20]. In general, M1 cells produce more inflammatory cytokines (IL-1β, TNF, IL-6) and reactive oxygen species and mediate defense against intracellular parasites and tumors. Instead, M2 cells have more anti-inflammatory properties and mediate parasite clearance, angiogenesis, tissue remodelling, tumour progression and immunoregulation [21].

1.2 Pattern recognition receptors

The innate immune cells express different pattern recognition receptors (PRR) to identify PAMPs, associated to microbial and viral pathogens, as well as damage-associated molecular patterns (DAMPs), associated with molecules released by the damaged cell. The PRRs can be in intracellular compartments, on cell surface or secreted into bloodstream and tissue fluids [22] with different functions, as opsonization, activation of complement, phagocytosis and induction of pro-inflammatory signaling pathways.

The secreted PRRs, as complement receptors, collectins and pentraxins, are released immediately after the infection [23-25]. The collectins belongs to the C-type lectins superfamily and form a family of collagenous Ca^{2+}- dependent lectins which can bind to oligosaccharide structures or lipids present on the surface of microorganism. One of the member of this family is mannan-bindig lectin (MBL) that binds specifically mannose residues at the terminal portion, which are abundant on many microorganisms, and associates with MBL-associated serine proteases (MASP). The binding of MBL to MASP1 and MASP2 activates them that initiate the lectin complement pathway [26]. The pentraxin superfamily are composed of serum proteins known as acute phase proteins. C-reactive protein (CRP) and serum amyloid P (SAP) are the short pentraxins and PTX3 is the long pentraxin. They can induce the activation of the classical pathway of complement and facilitate pathogen recognition by DCs and macrophages.

There are some cell surface receptors that function as PRRs and mediate phagocytosis of microorganism. Macrophage mannose receptor (MMR) is a member of C-type lectin family and interacts with fungal pathogens and different gram-negative and gram-positive bacteria. It can induce phagocytosis of pathogens and delivery into the lysosomal compartment. Macrophage scavenger receptor (MSR) is another phagocytic PRRs that has specificity to LTA, LPS and double-stranded RNA (dsRNA) [27]. Another scavenger receptor is MARCO, which binds to LPS and bacterial cell walls and induces phagocytosis [28].

Several PRRs are presented in the cytoplasm where they detect virus and bacteria penetrated in the intracellular compartment. NOD-like receptors (NLR) contain and N-terminal CARD domain, a nucleotide binding domain (NBD) and a C-terminal leucine-rich repeat (LRR). The CARD domains of NOD1 and NOD2 bind a protein kinase, RIP2, which in replay activates NF-κB and MAPK signaling pathways [29]. Rig-I-like receptors (RLR) are another class of intracellular PRRs, which recognize viral RNA. Two of the RLRs, MDA-5 and RIG-I sense ds-RNA and induce a cellular response via CARD domain; instead LGP-2 does not expressed CARD domains so it fails to induce signaling alone but has been found to be necessary for effective RIG-I and MDA5-mediated responses [30]. Toll like receptors are the best characterized among the PRRs and thus will be discussed in further detail.

1.2.1 Toll like receptors (TLRs)

The TLRs are a type of PRRLs, homologues of the *Drosophila* Toll protein. They are transmembrane proteins composed of an extracellular domain containing leucine-rich repeats (LRRs), that mediate the recognition of PAMPs, and a cytoplasmic tail that contains a conserved region called the Toll/IL-1 receptor (TIR) domain, required for signaling transduction [31]. In human, there are 10 TLRs, with TLR1 to TLR9 being conserved in humans and mice; mouse TLR10 is not functional for a retrovirus insertion, and the genes coding for TLR11, TLR12 and TLR13 are not present in the human genome. They differ from each other in PAMP ligands and their cellular localization. TLR1, TLR2, TLR4, TLR5, TLR6 and TLR11 are exposed on cell membrane and recognize mainly lipoproteins, lipids and protein expressed on microbial surface; TLR3, TLR7, TLR8 and TLR9 recognize nuclear acids and are exposed on intracellular compartments, as endosomes, endoplasmic reticulum and lysosomes [32].

- ***TLR4***

TLR4 was the first discovered human homologue of *Drosophila* Toll [33]. Its main ligand is the lypopolisaccharide (LPS), an element present on the outer membrane of the Gram-negative bacteria. On cell surface, TLR4 complexes with MD-2, which lacks a transmembrane domain but is associated with the extracellular part of TLR4 [34]. The LPS in the serum is bound by LPS-binding protein (LBP) that transfer LPS monomer to CD14, a glycosylphosphatidylinositol-linked protein that delivers LPS-LBP to TLR4-MD-2 complex [35]. TLR4, in addition to LPS, has been implicated in the recognition of the fusion protein of the respiratory syncytial virus, lipoteichoic acid (LTA) and the heat shock protein hsp60 [36, 37].

- ***TLR2***

TLR2 is a cell surface TLR that recognize the largest number of ligands among all PRRs, derived from fungi, bacteria, viruses and parasites. These include peptidoglycan from Gram-positive bacteria, lipopeptides from bacteria and zymosan from fungi [38]. TLR2 can not recognize PAMPs alone, but assembles with either TLR1 or TLR6 to form heterodimers, and this increase repertoire of ligand specificities [39]. TLR2 can interact with other cell surface receptors present on the cell membrane, as CD36 and dectin-1, a C-type lectin that detects fungus β-glucan and causes its internalization [40].

- ***The other TLRs***

TLR3 recognizes double-stranded RNA (dsRNA) generated from the replication of single-stranded RNA (ssRNA) viruses, in intracellular compartments. It can bind polyinosinic-polycytidylic acid (poly(I:C)), a synthetic analog of dsRNA, imitating a viral infection. The antiviral immune response induced leads to the release of inflammatory cytokines and type I interferon [31].

TLR5 is a cell surface TLRs that recognize the bacterial flagellin protein. It is expressed at high level on DCs in the lamina propria of small intestine [41]. In mouse, TLR11 corresponds to TLR5 and it have high expression in kidney and bladder, where recognizes uropathogenic bacterial components [42].

TLR7 is an intracellular TLRs, expresses principally by pDCs at lysosome compartment. It identifies ssRNA of RNA viruses as influenza A virus, vesicular stomatitis virus and human immunodeficiency virus [31]. It also recognizes small interfering RNAs and synthetic poly(U) RNA [43]. *In vitro* and in clinic, it is activated by imiquimod and resiquimod (R-848). Human TLR8 shows high homology to mouse TLR7 even in ligand specificity, but mouse TLR8 appears to be nonfunctional [31].

TLR9 recognizes unmethylated CpG motifs express frequently in viral and bacterial DNA but are unusual in mammalian cells [44]. Synthetic CpG oligodeoxynucleotides work as ligand of TLR9 and active DCs, macrophages and B cells to produce type I IFNs and inflammatory cytokines. TLR9, as TLR7 are sequestered in the ER in rest cells but after a ligand stimulation they can traffic to endolysosomes [45].

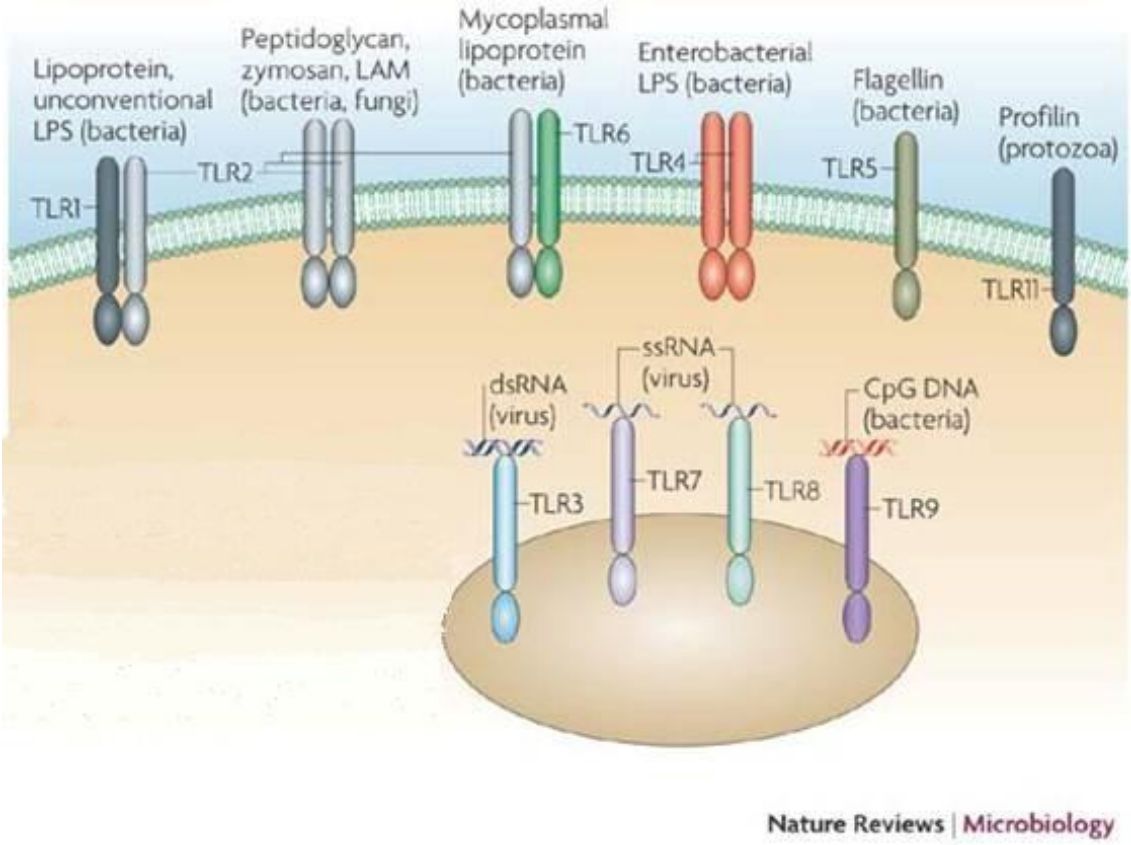

Figure. 1: Toll-like receptors. TLR2, alone or in combination with other TLRs, senses lipoproteins, lipoarabinomannans and lipoteichoic acids; TLR4 senses different lipopolysaccharides of the Enterobacteriaceae; TLR5 recognizes flagellin of flagellated bacteria; TLR3, TLR7 and TLR8 detect viral RNA, whereas TLR9 recognizes low-methylated DNA that contains CpG motifs, which are characteristic of bacterial DNA. Imagine adapted from [46].

1.3 TLRs signaling pathways

Upon recognition of their ligands, TLRs activate specific host defense responses. For example, TLR4 and TLR3 induce type I IFN and inflammatory cytokines expressions, whereas TLR2-TLR1, TLR2-TLR6 and TLR5 induce mainly inflammatory cytokines. These differences are due to different Toll-1-resistence (TIR) domain-containing adaptor molecules, including MyD88, TIRAP (Mal), TRIF and TRAM, which are recruited by different TLRs and activate distinct signaling pathways. MyD88 (myeloid differentiation primary-response protein 88) is used by all TLRs except TLR3, and induces inflammatory cytokines by the activation of NF-κB and mitogen-activated protein kinases (MAPKs). In contrast, TRIF (TIR domain-containing adaptor protein inducing IFNβ) is used by TLR3 and TLR4 and induces alternative pathways, activating the transcription factors NF-κB and IRF3 to produce type I IFN and inflammatory cytokines. TRAM (TRIF-related adaptor molecule) is a sorting adaptors that recruit TRIF to TLR4, instead TIRAP function as sorting MyD88 to TLR4 and TLR2 [32]. Thus, TLRs signaling can be classified in MyD88-dependent pathways or TRIF-dependent pathways.

1.3.1 The MyD88-dependent pathway

When PAMPs bind to the specific TLRs, MyD88 recruits the IL-1 receptor-associated kinase IRAK4, which phosphorylates IRAK1 and IRAK2 sequentially. Activated IRAKs interact with Tumor necrosis factor receptor-associated factor 6 (TRAF6), an E3 ubiquitin protein ligase, which catalyzes the formation of a K63-linked polyubiquitin chain on TRAF6 itself and on IKK-γ/NF-κB essential modulator (NEMO) [47]. A complex formed of TAK1 (TGF-β-activated kinase 1) and TAK1 binding proteins (TAB1, TAB2, and TAB3) is recruited to TRAF6 [48] and IKK-β is phosphorylated, which leads to NF-κB activation. TAK1 simultaneously activates the MAPKs Erk1, Erk2, p38 and JNK, which activate other transcription factors, including AP-1 [48]. In addition to NF-κB activation, the transcription factor IRF-5 is activated and it translocates into the nucleus and

induces expression of inflammatory cytokines [49]. There are other molecules activated downstream the TLRs engagement, as IκBζ, which acts as inducer of the NF-κB p50 subunit to induce IL-6 and IL-12p40 [50], and C/EBPδ, which amplify IL-6 production downstream NF-κB [51].

1.3.2 The TRIF-dependent pathway

The TRIF-dependent pathway stimulates both IRF3 and NF-κB. TRIF forms a complex with TRAF6, Pellino-1, TRADD and RIP-1 that activates TAK1, which in turn activates the NF-κB and MAPK pathways [52]. On the other hand, TRIF activates TBK1 via TRAF3 to induce IRF3 and IRF7 translocation into the nucleus, resulting in the expression of IFN- inducible genes. This signaling pathway is used by TLR4 and by TLR3, when they are internalized in the endosome compartment after the initial trigger [53].

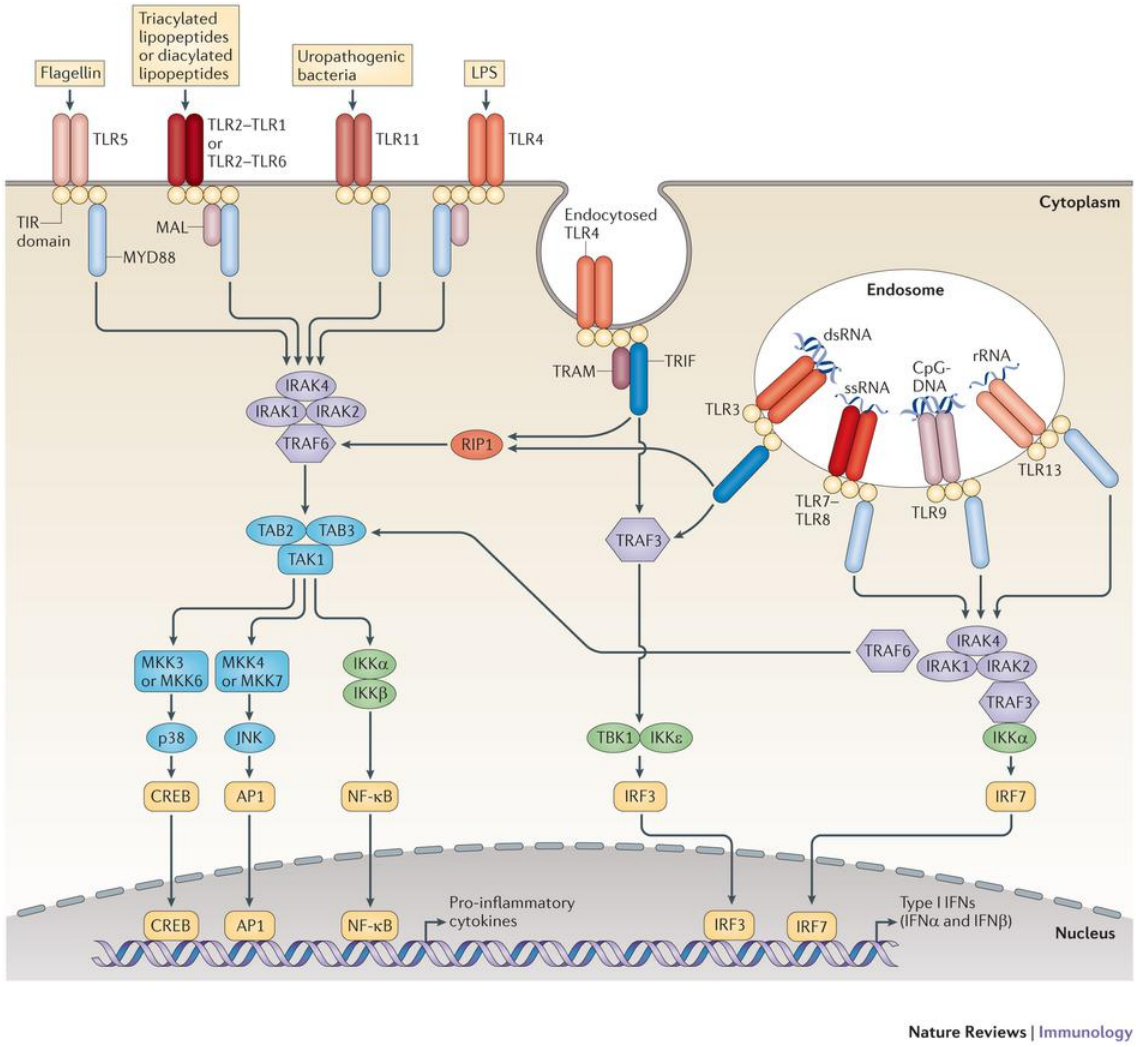

Figure 2: TLRs signaling pathways. TLR signaling is initiated by ligand-induced dimerization of receptors. Following this, the TIR domains of TLRs engage MYD88 and MAL, or TRIF and TRAM. TLR4 moves from the plasma membrane to the endosomes in order to switch signaling from MYD88 to TRIF. Engagement of the signaling adaptor molecules stimulates interactions between IRAKs and TRAFs and that lead to the activation of the MAPKs, JNK and p38, and to the activation of the transcription factors. A major consequence of TLR signaling is the induction of pro-inflammatory cytokines, and in the case of the endosomal TLRs, the induction of type I IFNs. Imagine from [54].

1.4 microRNA

Signaling pathways commonly activated during acute immune responses induce the transcription of coding and non-coding RNAs (ncRNA). For definition, ncRNAs are all RNAs that are not transcribed in proteins and they include ribosomal RNA (rRNA) and transfer RNA (tRNA), involved in the translation process; small nucleolar RNA (snoRNA), which participate in the splicing process; microRNA (miRNA) and long non-coding RNA (lncRNA), that regulate gene expression [55]. The increase identification of non-coding genome functions sheds light on the complexity of eukaryotes and supports a fundamental role to non-conding RNAs on the evolutionary process.

1.4.1 The biogenesis of miRNA

MiRNAs are small, single-stranded non-coding RNAs of 19-23 nucleotides in length. miRNAs are found in animals, plants, and some viruses, with the function in RNA silencing and regulation of gene expression at post-transcriptional level [56]. The first miRNA were identified in 1993 in *Caenorhabditis elegans* worm, in the course of a study of *lin-4* gene, which instead of producing an mRNA encoding a protein, it produced short non-coding RNAs, that contained sequences partially complementary to multiple sequences in the 3' UTR of the *lin-14* mRNA [57]. Presently, there are 28645 mature miRNA listed in miRBase21 (June 2014).

Most miRNAs are produced from intergenic regions or can be found in introns. In some cases, a miRNA gene can be transcribed with its host gene, such as the bic/miR-155 gene [58]. Interestingly, there are miRNA genes formed by multiple hairpins on a single cluster, as the miR-17-92 cluster [59]. miRNAs are transcribed by RNA polymerase II (Pol II) as a long pri-miRNA that is 5’ capped and polyadenylated [60]. A single pri-miRNA may include one or more miRNA precursors that are stem-loop structures, constituted of about 70 nucleotides. The

position of the stem-loop in the pri-miRNA is recognizes by a nuclear protein known as DiGeorge Syndrome Critical Region 8 (DGCR8 or "Pasha" in invertebrates) that, together with Drosha, form the microprocessor complex [61]. Drosha is an RNase III enzyme that, thanks to DGCR8, cleaved the pri-miRNA in a precise position to liberate the hairpins with a 5' phosphate groups and an overhang at its 3' hydroxyl end. This is termed precursor miRNA (pre-miRNA). Some miRNAs that are located in the introns of the mRNA host gene, termed "mirtrons", can bypassed the microprocessor complex and can be spliced out directly by the spliceosome [62].

Pre-miRNAs are then actively exported out of the nucleus by the nucleocytoplasmic Exportin-5. This protein recognizes the 3' overhang of the pre-miRNA hairpins and mediates the transport of the correctly processed stem-loops in a RAS- related nuclear protein-guanosine triphosphate (RAN-GTP)-dependent manner [63].

Once in the cytoplasm, pre-miRNAs are cleaved by Dicer, an RNase III enzyme, to an imperfect miRNA/miRNA* duplex of about 22 nucleotides in length [64]. Dicer acts in conjunction with an RNA-binding protein TRBP (Tar RNA binding protein), needed for Dicer stability, and proteins of Argonaute family, mostly Ago2, to form the RNA-induced silencing complex (RISC). Normally, the strand of the miRNA duplex that is incorporated in the RISC complex is selected depending on its thermodynamic instability or the position of the stem-loop [65]. The miRNA*, or the passenger strand, is generally degraded, but sometimes, both strands of the duplex are functional and target different mRNA populations [66].

1.4.2 The miRNA targeting of mRNA

The RISC complex, once formed with the mature miRNA, will act as gene regulator. Plant miRNAs are usually complementary to coding regions of mRNA targets with perfect base pairing and promote cleavage of the RNA [67]. Conversely, mammalian miRNAs bind the mRNA targets with partial complementarity in the 3' UTR of the mRNA. Only the 'seed region' of the miRNA (nucleotides 2-7 from 5' end) still have to be perfectly complementary [68]. Recently, an alternative RISC assembly have been proposed, in contrast to the consensus view that all miRNAs are associated to Ago proteins. The authors identified the existence of miRNA-mRNA duplexes not bound by Ago proteins and demonstrated that Ago proteins can bind and repress this duplex in a second moment [69].

miRNAs can repress targets in different ways: cleaving of target mRNAs (usually for plant miRNAs), repressing mRNA translation or promoting its degradation. A theory proposes that RISCs repress the initiation step of the translation process by competing with eIF4E (eukaryotic initiation factor-4), which recognizes the 5'UTR of mRNA and initiates ribosome formation, for binding to the 5'cap of mRNA. Moreover, this interaction limit the cooperation among the 5′ cap and 3′ poly(A) tail for a correct translation [70]. An alternative mechanism of miRNA actions propose that Ago proteins prevent the assembly of the 60S subunit of the ribosome on the mRNA [71]. Other studies suggest that mRNAs can be repressed not only at the initiation step of translation but even when they are associated with active polysomes, necessary for translation [72].

Additional studies revealed that miRNAs can induce mRNA degradation by favoring removal of Poly(A) tail. The mRNAs can be degraded by progressive 3'→5' decay, catalysed by exosome, or by the removal of the cap followed by 5'→3' degradation, catalysed by the exonuclease XRN1. The recruitment of the different decay machinery is controlled by the RISC. The final step of degradation is thought to occur in P-bodies, which are structure of the cell enriched of enzymes and translational repressors [73].

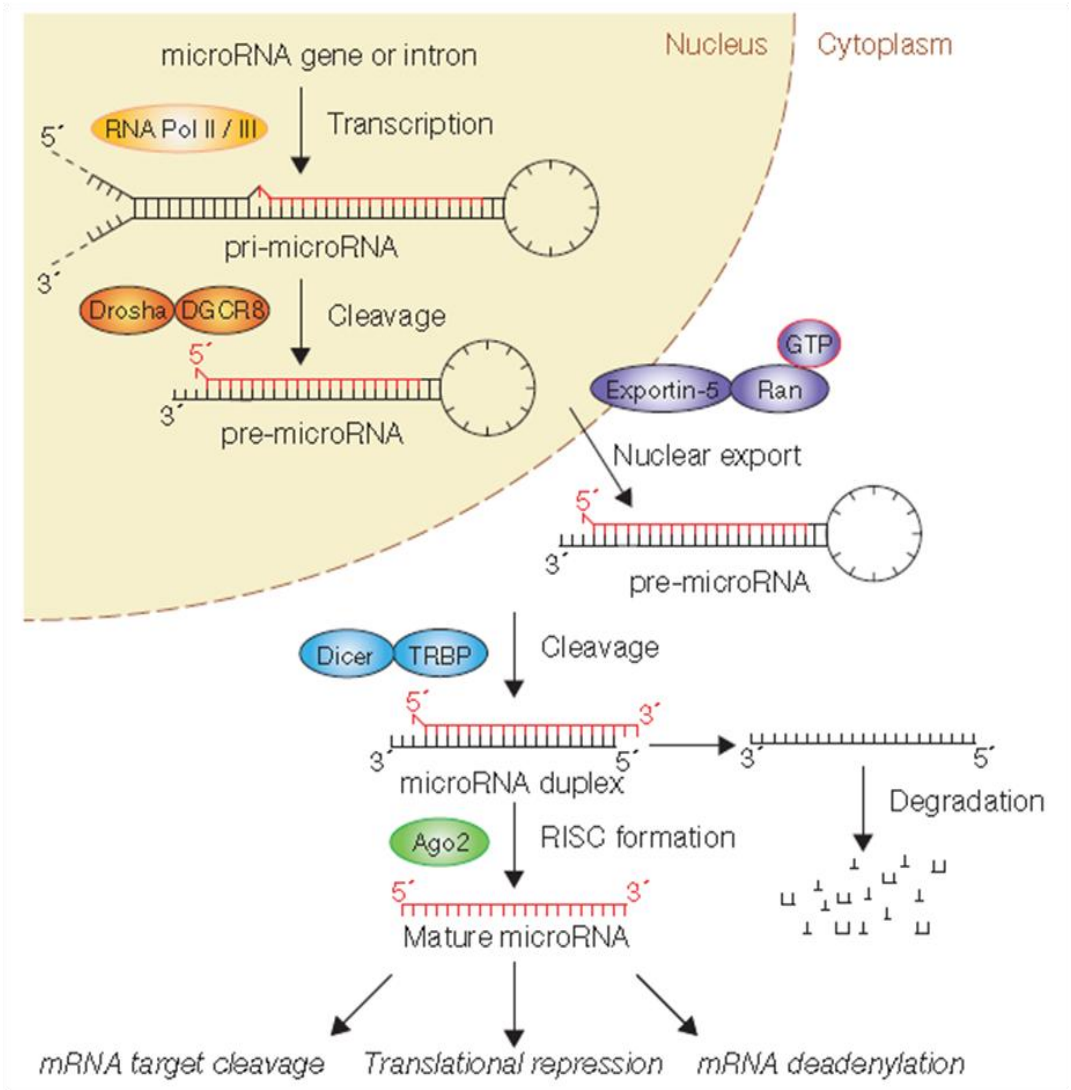

Figure 3: miRNA processing. The pri-miRNA is transcribed by RNA pol II or III and it is cleaved by the microprocessor complex Drosha–DGCR8 (Pasha) in the nucleus. The resulting precursor hairpin, the pre-miRNA, is exported from the nucleus by Exportin-5–Ran-GTP. In the cytoplasm, the RNase Dicer in complex with the double-stranded RNA-binding protein TRBP cleaves the pre-miRNA hairpin to its mature length. The functional strand of the mature miRNA is loaded together with Argonaute proteins (usually Ago2) into the RISC, where it guides RISC to silence target mRNAs through mRNA cleavage, translational repression or deadenylation. Imagine from [74].

1.4.3 The miRNA in innate immune response

MiRNAs are implicated in the regulation of proliferation, maturation, differentiation and activation of the innate and adaptive immune systems.

Following exposure of immune cells to pathogens or to inflammatory signals, hundreds of genes are up- or down-regulated in order to induce an efficient immune response. miRNA transcripts are also dynamically altered during this process, and many of them are strongly involved in TLR signaling. Important miRNAs that are up-regulated after stimulation of TLRs are miR-155 [75] miR-146a [76], miR-9 [77]. Other miRNAs have been reported to be down-regulated by the TLR activation, for example LPS can reduce the expression of let-7i [78] and miR-125b [6]. Many of those TLR-dependent miRNAs are also found dysregulated in cancer [79] thus representing a link between inflammation and cancer progression. As other TLR-responsive genes, also miRNA activity must be negatively regulated. For example, the anti-inflammatory cytokines IL-10 inhibits the activity of miR-155 [80]. Another kind of inhibitor, in particular in tumor, are the long non-coding RNA (lncRNA) that act as miRNA "sponge" and are called 'competing endogenous RNA' (ceRNA) [81]. They contain multiple copies of the miRNA response element, even for a combination of different miRNAs, becoming suitable for miRNA binding and changing in the amount of miRNA that is available. In this way, they can impact the multiple targets of multiple microRNAs.

Now, we focus the discussion on miRNAs that are the argument of this thesis.

- ***miR-125a~99b~let-7e cluster***

In humans, miR-125a, miR-99b and let-7e belong to a cluster present on chromosome (chr) 19. There are other isoforms of this cluster found in a different location within the genome: miR-125b-1, let-7a-2 and miR-100 found on chr 11 and miR-125b-2, miR-99a and let-7c found on chr 21. It is not yet clear whether this different cluster play unique or redundant roles in mammalian biology but it is clear they have a different transcriptional control. MiR-125a has recently found

enriched in mouse and human HSCs, with evidence that it can impact HSC engraftment and output of mature hematopoietic cells [82]. There are evidences that, among the other members of the cluster, miR-125a can decrease the level of apoptosis in hematopoietic progenitors by targeting pro-apoptotic factors, such as Bak1 [83].

An abnormal expression of miR-125a was found in several cancers. In breast cancer, miR-125a was reported down-regulated in biopsy specimens, with the capacity to inhibit ERBB2 and ERBB3 pathway [84]; in hepatocellular carcinoma, decreased miR-125a was found in both cell lines and tissues and over-expression of miR-125a inhibited the proliferation and metastasis of hepatocellular carcinoma by targeting MMP11 and VEGF [85]. In autoimmune diseases, miR-125a has been found down-regulated in T cells of systemic lupus erythematosus (SLE) patients. This contributes to the elevated expression of the inflammatory chemokine RANTES in SLE by the reduced targeting of KLF13 in activated T cells [86]. MiR-125a was also significantly up-regulated in macrophages by oxidized low density lipoprotein (oxLDL) and it was reported to regulate the proinflammatory response, lipid uptake, and ORP9 expression [87].

The let-7e belongs to a big family of microRNAs first discovered in *Caenorhabditis elegans*, and functionally conserved from worms to humans. The human let-7 family contains 13 members located on nine different chromosomes. The members are: let-7a-1, 7a-2, 7a-3, 7b, 7c, 7d, 7e, f7-1, 7f-2, 7g, 7i, mir-98, and mir-202 [88]. These members have been found deregulated in many human cancers. In the macrophage's activity, let-7e has been demonstrated to be Akt1 dependent after LPS stimulation and it can regulate the TLR4 expression, controlling macrophage tolerance and sensitivity to endotoxin [89].

The miR-99 family is composed of miR-99a, miR-99b and miR-100. They were found down-regulated in human prostate tumor tissue and in all prostate cancer cell lines. Ectopic expression of this members blocked the proliferation of prostate cancer cells and reduced the prduction of prostate-specific antigen, by the targeting of the growth regulatory kinase mTOR and the chromatin-remodeling

factors SMARCA5 and SMARCD1[90]. Another study identified miR-99b, together with miR-99a, as new modulators of TGF-β pathway that alter SMAD3 phosphorylation, in turn altering cell migration and adhesion in normal murine mammary gland cells, blocking the epithelial to mesenchymal transition of breast cancer [91].

- ***miR-146 family***

The miR-146 family is composed of two members, miR-146a and miR-146b, located on chromosomes 5 and 10, respectively. miR-146a was initially found during a pivotal study by David Baltimore group who identified miRNAs important in the innate immune response to microbial infection [76]. This study confirmed that many miRNAs were induced following TLR signaling and proposed for the first time the existence of a negative feedback loop between TLR-induced miRNA and TLR signaling pathway. They found that miR-146a was rapidly up-regulated after LPS and PolyI:C, as well as pro-inflammatory cytokines, IL-1β and TNFα, via the transcriptional activity of NF-κB. In turn, miR-146a targets important adaptor of the TLR pathway, as TRAF6 and IRAK1, thereby having a negative feedback effect on the TLR signaling. To better define the function of miR-146a, the miR-146a knockout mice (miR-146a$^{-/-}$) were generated. These mice showed no obvious abnormality early on, but at 6 months of age they developed a progressive myeloproliferative disorder which eventually progressed to splenic myeloid sarcoma, which is likely to be due to chronic inflammation [92]. miR-146a$^{-/-}$ mice exhibited an hyper-responsive reaction to systemic LPS, and bone marrow-derived macrophages from miR-146a$^{-/-}$ showed a significant increase in inflammatory cytokines production upon LPS stimulation, as IL-6, TNFα and IL-1β [92]. The importance of miR-146a in myeloid immune response was also demonstrated in human monocytes in the context of endotoxin-induced tolerance [93]. In addition, mouse macrophages infected with vesicular stomatitis virus up-regulated miR-146a expression, that in turn negatively regulated type I IFN production through a

TLR4/MyD88-independent but RIG-I/NF-κB-dependent pathway [94]. This finding is supported by a study in which miR-146a was detected at reduced level in human peripheral blood mononuclear cells of systemic lupus erythematosus patients and this resulted in increased type I IFNs [95].

miR-146b is the other member of the miR-146 family and its mature form sequence differs only by 2 nucleotides in the 3' end (Figure 4). Although it shares many targets with miR-146a, little is known about its regulation of expression. Recently, miR-146b has been associated in erythroid and megakaryocytic differentiation of HSC via its regulation on platelet-derived growth factor receptor α and its effect on GATA-1 expression [96]. miRNA profiling by microarrays has shown that miR-146b expression is impaired in many cancer types, such as breast cancer [97], lung cancer [98], melanoma [99] and colorectal cancer [100]. Studies on resolution of the inflammation mediated by pro-resolving lipid mediators identified a set of miRNAs that are temporally regulated, among which there is miR-146b [101].

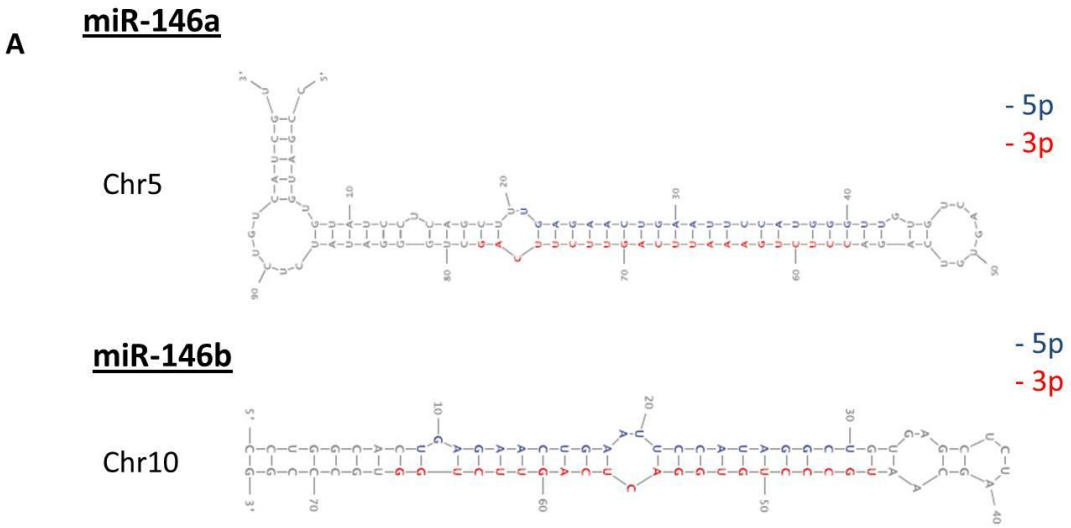

Figure 4: The miR-146 family. (A) Stem-loop sequence and structure of the pre-miR-146a and pre-miR-146b. (B) Identities between the sequence of miR-146a-5p and miR-146b-5p. MiR-146a-5p and miR-146b-5p differ by only two nucleotides located outside the seed region (red box).

1.5 Negative regulation of the immune response

The activation of a robust innate immune response against damaging stimuli, known as acute inflammation, is essential to allow maintenance of homeostasis but it can be deleterious if it is uncontrolled. Sustained inflammation can lead to various metabolic, autoimmune, and inflammatory disorders, such as inflammatory bowel disease, obesity, multiple sclerosis, rheumatoid arthritis, asthma, atherosclerosis, chronic obstructive pulmonary disease (COPD), and also contribute to cancer progression [102]. The resolution of inflammation is an important and active process that involve mediators and signaling pathways that switch pro-inflammatory cell phenotypes and induce pro-resolution phenotypes, control apoptosis of recruited inflammatory cells, and their removal by phagocytosis.

1.5.1 The phases of self-resolving acute inflammation

Macroscopically, the inflammatory reaction is recognized by well known major signs: *calor* (heat), *rubor* (redness), *tumor* (swelling), and *dolor* (pain), described by Cornelius Celsius during the Roman Empire. Microscopically, in response to PAMP or DAMP, the tissue resident immune cells (resident macrophages, dendritic cell and epithelial cells) rapidly release pro-inflammatory mediators, as TNFα and IL-1β, and chemoattractant factors, as IL-8/CXCL8, CCL2, CCL3. Mediators produced in this phase of inflammation increase the permeability of the vessel wall, accompanied by hyperemia, with consequent exudation of plasma proteins and fluid from the blood into tissue (edema). The up-regulation of cell adhesion molecules (selectins and integrins) on endothelial cells and the presence of chemoattractant factors allow the migration of leukocytes from the circulation to the site of injury. Neutrophils are the first cells that extravasate followed by mononuclear cells, mainly monocytes, that become activated and produce more

mediators, including growth factors (G-CSF, GM-CSF), cytokines, chemokines, lipid mediators and reactive oxygen species (ROS). With progression of the inflammatory response, PMN start undergoing apoptosis followed by phagocytosis by macrophages, a phenomenon called efferocytosis. During the resolution phase, macrophages switch toward an anti-inflammatory phenotype and start releasing anti-inflammatory molecules (such as IL-10 and TGFβ) and pro-resolving mediators such as lipid mediators (lipoxins, resolvins, protectins, maresins) [103], glucocorticoids [104] and ROS [105]. In order to mantain a healthy status, both the initiation of acute inflammation and its resolution must be efficient.

1.5.2 The anti-inflammatory cytokine IL-10

IL-10 is the founding member of the class II family of α-helical cytokines, composed of type I interferons, interferon γ (IFNγ), IL-19, IL-20, IL-22, IL-24 (Mda-7), IL-26 and IL-10 [106]. It is released by different cell types including DCs, macrophages, mast cells, eosinophils, NK cells, T reg, T and B cells [107].

IL-10 is recognized by the heterodimeric receptor consisting of IL-10R1 and IL10R2 subunits, which activates the receptor –associated Janus tyrosine kinases JAK1 and Tyk2, resulting in activation of STATs (signal transducers and activators of transcription), principally STAT3 [108]. The activated JAK1 phosphorylates two tyrosine residues of the IL-10R1 and creates binding sites for the Src homology 2 (SH2) domains of STAT3, that becomes phosphorylated, dimerizes and enters into the nucleus to start the anti-inflammatory process [109]. If STAT3 is lacking in neutrophils and macrophages, IL-10 cannot inhibit their production of proinflammatory cytokines [110]. The JAK1/STAT3 signaling is shared by different cytokines receptors as IL-6R, but IL-10 has anti-inflammatory effects and IL-6 does not. This is due to suppressor of cytokine signaling (SOCS) 3, that belongs to SOCS family of SH2-containing E3 ligases, that have a role in suppressing specifically cytokine signaling. SOCS3 is induced after IL-6 and IL-10 stimulation but it binds only to the gp130 subunits of the IL-6R to block it signaling [111].

- ***The IL-10 action***

The hallmark IL-10 action is the selective reduction of pro-inflammatory gene transcription, reducing the expression of inflammatory cytokines as TNFα, IL-6, IL-1, IL-8 and IL-12. However, microarray analysis determined that only ~ 15-20% of genes induced by LPS were decreased by IL-10 in macrophages [112]. Evidence indicates that IL-10 does not induce a direct inhibition of inflammatory gene expression but, rather, induces the expression of transcriptional repressors that mediate the inhibition of promoters of inflammatory genes [113]. Despite numerous groups have investigated the IL-10-inducible genes able to mediate IL-10 anti-inflammatory effects, they have yet to be found. A study identified that PI3K-Akt signaling can augments some of IL-10-inducible gene expression in part by eliminating the repressive effects of GSK3 [114]. Additionally, IL-10 can reduce co-stimulatory and MHC class II molecule expression on macrophage surface, affecting antigen presentation to T cells [115]. In mouse model studies, it has been confirmed the anti-inflammatory activity of IL-10 in different settings, as respiratory virus infections, colitis, ischemia and reperfusion, acute myocarditis, and endotoxic shock [116]. Specifically, mice lacking IL-10 (IL-10 $^{-/-}$) or the IL10R (IL-10R $^{-/-}$) develop severe spontaneous colitis [117]. Moreover, B-cell lymphoma patients have elevated levels of IL-10 and activation of JAK/STAT pathway, suggesting that IL-10, reducing the immune response against the tumor, contributes to tumor proliferation [118].

- ***The IL-10 production in innate immune cells***

The induction of IL-10 in macrophages and DCs represents a way to dampen the pro-inflammatory phenotype and a mechanism of immune escape used by different pathogens, because IL-10 is induced by the activation of specific PRRs: TLR2, TLR4 and TLR9, TLR3 (only in macrophages), DC-SIGN, and dectin 1. Some viruses can produce an homologous of IL-10 (vIL-10) to directly inhibit the

immune system of the host [119]. For an optimal LPS- dependent induction of IL-10 in macrophages, it is necessary the activation of the TRIF- and MYD88-dependent pathways and the production and signaling by type I IFNs [120]. Following TLR stimulation, the activation of the MAPKs Erk and p38, via the activation of the transcription factor Sp1, modulate IL-10 production [121]. As inhibitory mediator of IL-10 expression, there is IFNγ that, in addition to block the activation of the MAPK, induces the release of GSK3 by antagonizing PI3K/Akt activation and suppressing the binding of AP1 on IL-10 promoter [122]. IL-10 itself can feed back to produce dual-specificity protein phosphatase 1 (DUSP1), which prevents the phosphorylation of p38 and thus limits IL-10 production. By contrast, IL-10 can induce the expression of tumour progression locus 2 (TPL2), a MEK kinase required for activation of Erk [112]. After the stimulation of TLR, TPL2 dissociates from the NF-κB inhibitory complex NF-κB1 (p105) and activates Erk.

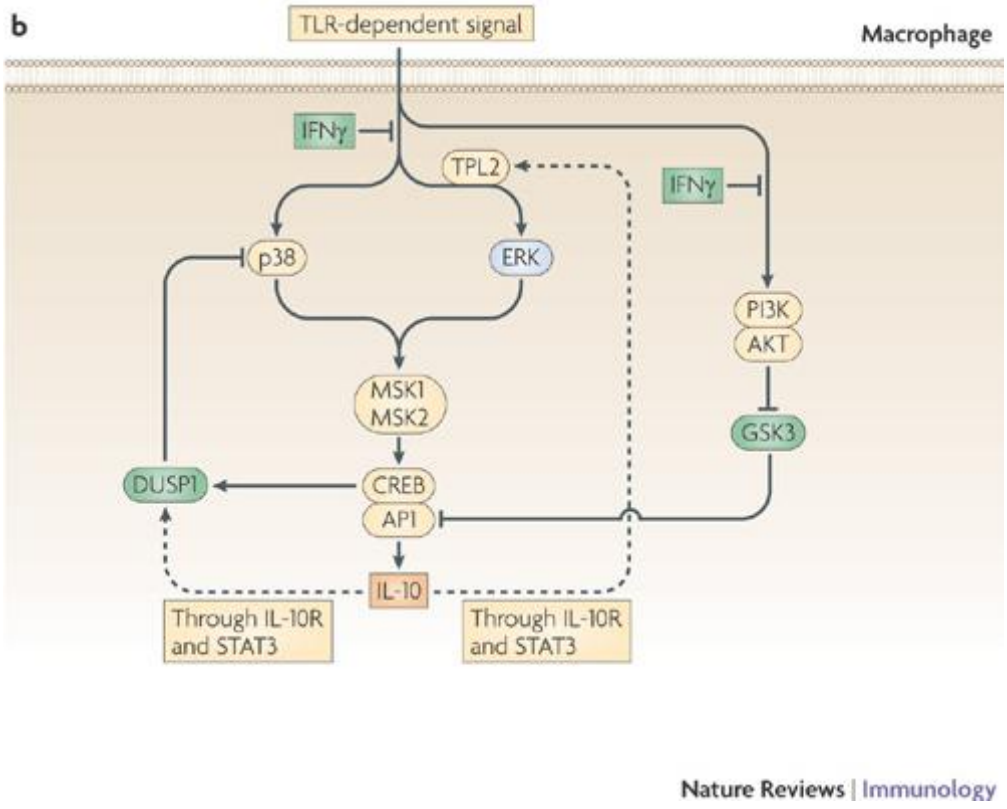

Figure 5: IL-10 production by immune cells. The p38 and ERK pathways activation lead to IL-10 expression. A negative feedback loop to regulate IL-10 production is formed by IFNγ, that blocks the activation of the MAPKs and can also interfere with PI3K/Akt pathway, inducing the release of GSK3, that in turn suppresses the AP1 binding on IL-10 promoter. Even IL-10 can feed back to induce the expression of DUSP1, which negatively regulates p38 phosphorylation and thus limits IL-10 production. IL-10 can also positively feed back to induce TPL2 expression, that is an up-stream activator of ERK, inducing an amplification loop of its own expression [123].

- ***The IL-10 and miRNAs***

Recent studies revealed that IL-10 can be post-transcriptionally regulated by miRNAs, including miR-106a, miR-466l, miR-98, miR-27, let-7 and miR-1423p-5p [124]. For example, miR-106a have the ability to down-regulate IL-10 in vitro and knock-down of this miRNA has the potential to alleviate symptoms in an asthma model, with increased IL-10 levels in the lungs and improved disease phenotype [125]. miR-466l can regulate IL-10 but has a positive effect, because the miRNA binding to the IL-10 3'UTR results in a stabilization and protection from RBP degradation of the transcripts [126]. Other miRNAs can regulate indirectly IL-10 expression, as miR-21. LPS stimulation induces miR-21 that targets PDCD4, a negative regulator of IL-10, thus promoting IL-10 production [127].

On the other hand, IL-10 can also modulate a number of miRNAs, up-regulating those with anti-inflammatory activity such as miR-187 [128] and down-regulating those that contribute to a pro-inflammatory response such as miR-155 [80]. MiR-155 is a LPS-induced miRNA and its repression by IL-10 increases the activity of SHIP1, an important negative regulator of TLR signaling [80]. Furthermore, our lab identified miR-187 as an IL-10-induced miRNA acting in IL-10-mediated suppression of TNFα, IL-6, and the p40 subunit of IL-12 (IL-12p40) produced by primary human monocytes following activation of TLR4. miR-187 targets TNF-α mRNA stability in a direct way and indirectly decreases IL-6 and IL-12p40 expression by targeting IκBζ, an important regulator of these cytokines [128]. As discussed in this thesis the miR-146b is aslo induced by IL-10 [129], indicating that an interplay between IL-10 and miRNA represents a new regulatory network during inflammation.

1.5.3 The anti-inflammatory cytokine TGFβ

Transforming growth factor beta (TGFβ) is a pleiotropic cytokine that regulates differentiation, cell proliferation, survival and migration. It plays a critical role in fibrosis, wound healing, carcinogenesis, development, and immune responses through its regulatory effects on many cell types [130].

The TGF-β superfamily of cytokines contains more than 30 structurally related polypeptide growth factors including TGF-βs (1–3), activins (A, B), inhibins (A, B), bone morphogenetic proteins (BMPs 1–20) and growth differentiation factors including myostatin, nodal, leftys (1,2), and Müllerian-inhibiting substance (MIS) [131]. In mammals, there are three homologous TGF-β isoforms: TGF-β1, TGF-β2, and TGF-β3. The predominant isoform expressed in immune cells is TGF-β1, but *in vitro,* all three isoforms have similar properties, instead *in vivo*, they have both redundant and distinctive functions depending on where and when they are expressed during development [132, 133].

- ***The TGFβ signaling***

TGFβ signals are transmitted via a transmenbrane receptor complex consisting of the TGFβ type I receptor (TβRI) and TGFβ type II receptor (TβRII), that are serine/threonine kinase receptors. TGFβ is secreted by cells as a latent complex, composed of homodimer of mature TGFβ noncovalently associated with an homodimer of latency-associated protein (LAP). TGF-β needs to be liberated for binding to its receptors, but the mechanisms for activation are not clear. However, *in vitro* this can be achieved using heat, several proteases or extremes of pH [134]. The active form of TGFβ initially binds TβRII, that induces recruitment and complex formation with TβRI. The constitutively active serine/threonine kinase activity of TβRII phosphorylates TβRI, which in turn recruits and phosphorylates the transcription factors Smad. The vertebrate Smad family is composed of eight members divided in three groups: R-Smad1, 2, 3, 5, and 8 are receptor-associated Smads, Co-Smad4 is common Smad, I-Smad6 and 7 are the two inhibitory Smads.

R-Smads are located in the cytoplasm and after phosphorylation they associate with Co-Smad4 and translocate into the nucleus. R-Smads bind to specific sequences of the promoter but need other transcription factors to form complexes that control gene expression by recruiting coactivators that contain histone-acetyl transferase activity (e.g., CBP/p300); or histone-deacetylase activity–containing corepressors (e.g., Sno/Ski) [135]. Even if Co-Smad4 is involved in all Smad-mediated transcription, it is not essential for TGFβ response: the traslocation of R-Smad into the nucleus can also take place without Co-Smad4 and some Smad4-deficient cell lines are still sensible to TGFβ signaling [136]. The I-Smads, Smad6 and Smad7, act as inhibitor because they compete with R-Smads for receptor or Co-Smad interaction and target receptors for degradation [137]. Besides the Smad-dependent pathways, TGFβ also activates the JNK, p38, Erk MAPKs and PI3K pathways [138].

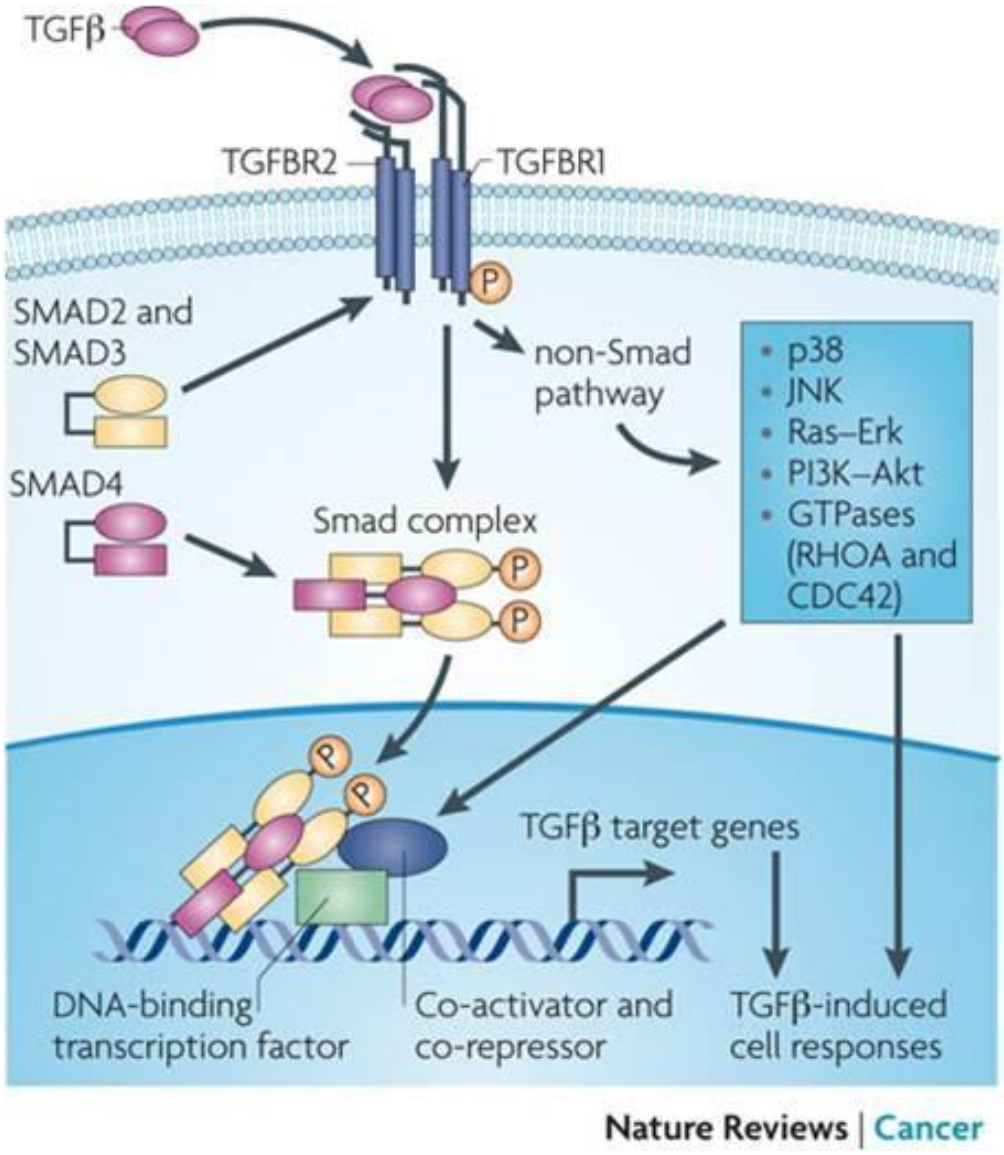

Figure 6. TGFβ signaling. TGFβ signaling is transduced through Smad and non-Smad pathways. TGFβ ligand binds to TGFBR2 and TGFBR1. TGFBR2 phosphorylates (P) TGFBR1, which subsequently phosphorylates and activates SMAD2 and SMAD3. Activated SMAD2 and SMAD3 form a Smad complex with SMAD4 and translocate into the nucleus. In the nucleus, the Smad complex interacts with other DNA-binding transcription factors, and co-activators and co-repressors, binds to the promoter regions of TGFβ target genes and regulates the transcription of target genes. TGFβ stimulation also activates other signalling cascades in addition to the Smad pathway. TGFβ receptors activate p38, JNK, Ras–Erk, PI3K–Akt, and small GTPases such as RHOA and CDC42. From [139]

- ***The TGFβ action***

TGFβ signaling is very important for the immune system because TGFβ1 knockout mice develop a severe lethal inflammatory disease within 3 weeks of birth, with inflammatory cell infiltration and lesions in different organs [140, 141]. The importance of TGFβ in T-cell response it has been made evident in mice that have an impaired TGFβ signaling on T cell [142]. Conversely, the effect of TGFβ signaling on macrophages is not so clear, maybe for the contrasting effects that it has in the monocyte/macrophage lineage. TGFβ reveals pro-inflammatory functions on monocytes: it acts as a chemoattractant to the site of inflammation [143]; it induces adhesion molecules, for adhesion to extracellular matrix; and it induces matrix metalloproteinases (MMPs), which can degrade vascular membranes to allow monocytes migration. In addition, TGFβ potentiates the inflammatory immune response of monocytes by induction of IL-6, IL-1 and leukotriene C4 synthase [138]. On macrophages, TGFβ act as an anti-inflammatory molecule: it prevents the expression of some LPS-induced inflammatory molecules as TNFα and some chemokines including CCL3 and CXCL2; it down-regulates the expression of inducible NO synthase (iNOS) and the production of nitric oxide (NO); it inhibits CD14 expression and MyD88-dependent TLR signaling pathways via degradation of MyD88 [144]. The TGFβ inhibition on macrophages can be mediated by Smad3 because over-expression of Smad3 represses iNOS and MMP-12 promoter activity in macrophages, whereas the blocking of Smad3 activity alleviates the TGFβ inhibition [145]. In addition, TGFβ can inhibit the antigen presentation function of macrophages by the down-regulation of MHCII, the co-stimulatory molecule CD40 and the inflammatory cytokine IL-12p40 expression [146].

- ***The TGFβ and miRNAs***

Using *in silico* miRNA–mRNA target predictions the TGFβ signaling cascade can be targeted by miRNAs but few of this targeting have been experimentally validateted, especially in the immune cells. In tumorigenesis, for example, miR-

146a has been demonstrated to target SMAD4. As in acute pro-myelocytic leukemia cells all transretinoic acid up-regulates SMAD4 and down-regulates miR-146a [147]. During the development process, the targeting by let-7c of TGFβR1 may control TGFβ signaling activity at each developmental stage of the liver to the necessary level [148]. TGFβ has been demonstrated to have a role in the epithelial to mesenchymal transition (EMT) because it down-regulates all the five members of miR-200 family that inhibit E-cadherin transcriptional repressors, ZEB1 and ZEB2, involved in tumor metastasis and EMT. The over-expression of the miR-200 family was enough to block TGFβ-induced EMT, and, to the contrary, the inhibition of miR-200 family was enough to cause EMT [149].

PROJECT AIMS

The overall aim of this project is to investigate the role of miRNAs in the regulation of monocytes/macrophages immune response after the engagement of TLRs. The previously identification of miR-125a~99b~let-7e cluster and miR-146b up-regulation in human monocytes after LPS stimulation forms the basis for this thesis. The specific purposes of the project are:

- Characterization of miR-125a, miR-99b, let-7e and miR-146b expression in human monocytes after pro- and anti-inflammatory stimuli;
- Bioinfomatically analysis of the promoters of miR-125a~99b~let-7e cluster and miR-146b, in order to identify key conserved binding sites to determine the transcriptional regulation of these miRNAs;
- Identification of miR-125a, miR-99b, let-7e and miR-146b targets in the context of LPS-mediated inflammation with *in silico* and experimental approaches;
- Determination of the functional role of these miRNAs in an *in vivo* model of inflammation.

Analysis of the regulation of TLR pathway in monocytes can provide new insights into the mechanistic details of the inflammatory immune response process.

2. MATERIALS AND METHODS

Reagents.

LPS from *E. coli* (serotype 055:B5), Zymosan A from Sigma Aldrich. Pam_3CSK_4, imiquimod, CpG DNA, and poly(I:C) were purchased by Enzo Life Sciences. IL-10 and recombinant murine M-CSF were from R&D System. IFNγ and IL-1β were from Peprotech. The AG-490 inhibitor was purchased from Calbiochem. Rabbit anti-Myd88 antibody was purchased from Enzo Life Science, rabbit anti–IRAK-1 and rabbit anti-TRAF6 antibodies were from Cell Signaling Technology. Ab-anti-Pol II (N-20) and anti-STAT3 (C-20) for ChIP experiments were purchased from Santa Cruz Biotechnology. Anti-SMAD3 ChIP grade from Abcam. Other antibodies were purchased from Biolegend unless specified otherwise. Fluorochrome-conjugated antibodies were from BD Bioscience.

Human monocytes purification and cell culture.

Human monocytes were obtained from healthy donor buffy coats by two-steps gradient centrifugation using Ficoll (Biochrom) and Percoll (Amersham). Monocytes were resuspended in RPMI 1640 medium (Lonza) supplemented with 10% heat-inactivated fetal bovine serum (FBS; Lonza), 100 U/mL penicillin/streptomycin (Lonza) and 25 mM L-glutamine (Lonza). The human THP-1 and murine RAW 264.7 cell lines (American Type Culture Collection, ATCC) were maintained by twice weekly passages in RPMI 1640 medium containing 10% heat-inactivated FBS, 100 U/mL penicillin-streptomycin, 25 mM L-glutamine at 37°C with 5% CO_2. HEK-293T cells (ATCC) were grown in Dulbecco's modified Eagle medium (DMEM) (Cambrex) supplemented with 10% FBS, 100 U/mL penicillin-streptomycin, and 25 mM L-glutamine at 37°C with 5% CO_2. Trypan Blue was used to determine cell viability.

RNA isolation and real-time PCR.

Total RNA was prepared using TRIzol (Ambion) and Direct-zol RNA MiniPrep kit (Zymo Research) and quantitative real-time PCR (qPCR) was conducted using a 7900HT Real-time PCR System (Applied Biosystems). For miRNA quantification, 300 ng of total RNA was reverse transcribed using TaqMan® MiRNA Reverse Transcription kit (Applied Biosystems). For gene quantification, 1 μg of RNA was reverse transcribed with random primers and quantification was performed using Power SYBR Green Mix (Applied Biosystems) with specific primer pairs (Table 1). Experimental data were then analyzed using the SDS2.2 software and the relative expression values were calculated according to the "comparative Ct" method using U6 for human and snor202 for mouse miRNA endogenous control and GAPDH for mRNA endogenous control. The list of oligonucleotides used is reported in Table 1.

Constructs generation.

3'UTR of CCL3, IL-6, CXCL8, TNFα, CCL7, TLR4, TLR2, CD14, MYD88, TRAF6 and IRAK1 was amplified from genomic DNA and was cloned in the biosensor psiCHECK™-2 vector (Promega) for the evaluation of miRNA activity. Pre-miR-125a~99b~let7e, pre-miR-125a, pre-miR-99b, and pre-let-7e were amplified from genomic DNA and subsequently cloned in pcDNA3 expression vector. The pCR2.1 vector (Invitrogen) was used as subcloning vector. To knockdown miRNA expression, sponge constructs (miRT) containing multiple sequential repeats of miRNA imperfect complementary seed site region were cloned into a psiCHECK™-2 vector (Promega), downstream the *renilla* luciferase gene. The fragment containing the SV40 promoter together with the *renilla* luciferase gene fused to the miR sponge fragment was then subcloned into the pRRLSIN.CPPT.PGK.GFP.WPRE vector (plasmid no. 12252; Addgene) in an antisense orientation respect the GFP cassette. The expression of the luciferase reporter gene was checked to assess the efficacy of miR inhibition. A lentiviral construct (miRT-CT/pRRL-CT), encoding for a hairpin yielding a 22-mer RNA designed to lack homology to any human gene, was used as control.

Lentiviral THP1 infection.

HEK293T cells were cultured in DMEM supplemented with 10% FBS, 25 mM L-glutamine but without PenStrep at 37°C with 5% CO_2 and transfected with pRRL or miRT lentiviral vectors plus pLP1, pLP2, pVSVg vectors (necessary for the lentiviral formations) using Lipofectamine 2000 (Invitrogen). After 3 days, we replaced the medium and incubated for at least 24 hours. At 4 day, we collected the supernatant and filtered it in 0,4 μm filter and applied 1 ml directly on THP1 cells plated 1 x 10^6 cells/well in a 6-well plate. We sealed and centrifuged the plate at 1800rpm x 90min at room temperature with reduced break and accelerator. After 8 days from the infections we counted and sorted the cells for the GFP present in the lentiviral construct. Lentiviral infections must be conducted in a P3 room.

Bone-marrow derived macrophages.

Harvest bone marrow cells from femura and tibia of 8- to 12- week old WT and IL-10 KO C57BL/6J mice plated in IMDM with 10% FCS overnight at 37°C. Non-adherent cells were resuspended at 5 x 10^6 cells/dish in complete bone marrow macrophage medium (IMDM, 10% FCS, 150 μM MTG, 1%P/S, 1%Glut, 10 ng/mL M-CSF) in low attachment culture dish (Corning Costar) and cultured for 7 days replacing medium at day 3. To prepare BMDM to further stimulations, cells were detached with 2mL of Accutase and replate at the concentration of 0.5 x10^6 cells/mL in complete bone marrow macrophage medium without M-CSF in multiwell 6 or 24 wells low attachment (500uL/well). After overnight culture BMDM were stimulated with 100 ng/mL LPS (Sigma) plus 20ng/mL mIL-10 (R&D System) or 100 ng/mL LPS for indicated time points.

Murine zymosan A- induced peritonitis.

Male C57BL/6 from 8-10 week old of wild type (Charles River Laboratories) and IL-10 KO mice (The Jackson Laboratory) were administered zymosan A (Sigma-Aldrich) at 1 mg/mouse, suspended in 0.5 ml of sterile saline to initiate peritonitis. At selected time intervals, mice were euthanized, peritoneal exudates were collected with 5 ml of cold Ca^{2+}/Mg^{2+} free PBS (PBS$^{-/-}$). Leukocytes were stained with Turk's solution to exclude erythrocytes and enumerated using a hemocytometer and light microscopy. 1 x 10^6 cells were analyzed by FACS analysis to identify different cell populations and the rest were sorted for macrophages cells.

Murine LPS- induced peritonitis.

Male C57BL/6J from 8-10 week old WT mice (Charles River Laboratories) were administered an intra-peritoneal injection of LPS (2.5 mg/kg) or PBS$^{-/-}$ as control. Peritoneal exudates were collected with 5 ml of cold PBS$^{-/-}$ at 0, 6, 24 and 48 hours from the injections. Leukocytes were stained with Turk's solution to exclude erythrocytes and enumerated using a hemocytometer and light microscopy. 0.2 x 10^6 cells were analyzed by FACS analysis to identify different cell populations. The remaining cells at each time point were pooled and subjected to macrophages purification with Manual MACS Cell Separation (Miltenyi Biotec).

FACS analysis and sorting.

Cells were resuspended in FACS buffer (1% FBS in PBS + 0.1% NaN3 (sodium azide)) were incubated with antibodies for 30 minutes in the dark at 4°C. Cells were washed 3 times with FACS buffer and fixed with 0.1% paraformaldyhyde. Control samples were generated using fluorescence minus one controls. Fluorochrome-conjugated antibodies for flow cytometry were anti-CD11b (clone M1/70), anti-CD45 (clone 30-F11), anti-Ly6G (clone 1A8), anti-Ly6C (clone AL-21),

anti-CD19 (clone 1DE), anti-CD11c (clone HL3) from BD Bioscience; anti-F4/80 (CI:A3-1) from Serotec. All Abs were titrated under assay conditions, and optimal photomultiplier voltages were established for each channel using calibration beads (BD Biosciences). Each murine leukocyte population was identified on the basis of antigen expression, as well as size and granularity on forward-scatter/side-scatter (FSC/SSC) plots, as follows: Macrophages: FSChigh/SSChigh, CD45+, CD11b+, F4/80high, LY6G-; neutrophils: FSCmed/SSChigh, CD45med, CD11bmed, Ly6Ghigh; lymphocytes: FSC/SSClow, CD45high, CD11b−, CD19+.

For sorting procedure, cells were stained with specific antibodies and resuspended at 10 x 10^6 cell/ml in a buffer for sort ($PBS^{-/-}$ + 1% FCS + 2mM EDTA).Flow cytometry was performed using FACSCanto II flow cytometer or sorted with FACSAria (BD Biosciences) and data analyzed with FACSDiva 6.1.1 software (BD Biosciences) or Flowjo6.1 (Treestar).

Bioinformatic analysis.

For each miRNA predicted target genes were defined using the microrna.org database [150] and the relative enrichment of biological functions and associated networks was determined using the Ingenuity Pathway Analysis software (IPA; Ingenuity Systems) by applying the “expression in immune cells” filter and the built-in Fisher exact test. The relationship of miRNA of interest with the 124 genes included in the *Inflammatory response* network was graphically visualized using IPA. The probability score of each conserved human or murine miRNA to be involved in this network was calculated according to the formula: $miR_x = -1/\log_2[(T_x \epsilon N)/124]$, where T = number of predicted target genes of miR_x and N = genes included in the *Inflammatory response* network. The statistical value of the involvement in the TLR signaling pathway, as identified by IPA, was defined by fitting the target distribution to Gaussian functions with mean 25.74/43.82 and SD 11.40/10.59, for human/mouse respectively. Similarly, the distribution of the percentage of common predicted target genes between human miR-125a-5p and 60 random murine miR was fitted to a Gaussian function with mean 23.86 and SD

9.85. Evolutionary conserved regions and transcription factor binding sites were identified using the MULAN software (http://mulan.dcode.org) [151] and visualized using the Jalview 2.8 software (www.jailview.org) [152].

Luciferase reporter assay.

HEK-293T cells were plated in 24-well plates in 500 µl DMEM supplemented with 10% FBS and 1% of L-glutamine at 16 x 10^4/well and after 24 h were transfected with 100 ng psiCHECK™-2-3'-UTR reporter construct and 10µM of mirVana miR mimcs (Life Technologies), using Lipofectamine 2000 (Invitrogen), according to the manufacturer's protocol. After 48 h, cells were lysed and firefly and renilla luciferase activities were determined using the Dual-Glo Luciferase Assay System (Promega). The enzymatic activities of both luciferases were quantified using a MultiDetection Microplate Reader Synergy 2 luminometer (BioTek). The values of renilla luciferase activity were normalized by firefly luciferase activities, which served as internal control. Normalized values were expressed as fold changes relative to the value of the negative control.

Chromatin immunoprecipitation (ChIP) assay.

12x10^6 human monocytes were used for each ChIP. Cells were cross-linked for 10 minutes at room temperature using 1% formaldehyde. Cross-linking was quenched by adding glycine to a final concentration of 0.125M. The cells were then collected, resuspended in lysis buffer (5mM PIPES pH 8, 85mM KCl, 0.5% NP40 and protease inhibitors), and incubated on ice for 30 min. Before proceeding with sonication to generate 200–400 bp fragments, the efficiency of sonication was assessed with agarose gel electrophoresis. Chromatin samples were pre-cleared for 1 hour with protein-G magnetic beads (Life Technologies) and then immunoprecipitated overnight at 4°C with specific antibodies: Ab-anti-Pol II (N-20) (Santa Cruz Biotechnology), anti-STAT3 (C-20) (Santa Cruz Biotechnology), anti-SMAD3 (Abcam). Rabbit IgG (Millipore) was used as negative control. After

incubation, the immunocomplexes were bound to protein-G magnetic beads for 2 hours and subsequently washed with low-salt wash buffer (0.1% SDS, 2mM EDTA, 20mM Tris HCl pH8, 1% Triton X-100, 150mM NaCl and protease inhibitors), high-salt wash buffer (0.1% SDS, 2 mM EDTA, 20mM Tris HCl pH8, 1% Triton x-100, 500mM NaCl and protease inhibitors), and TE buffer. Immunocomplexes were then eluted in elution buffer (1% SDS, 100mM NaHCO3) and cross-linking reverted overnight at 65°C. Samples were then extracted with QIAquick PCR Purification Kit (Qiagen) and qPCR was performed in triplicates using promoter-specific primers (Table 1). 1% of starting chromatin was not immunoprecipitated and used as input. Signals obtained from the ChIP samples were normalized on signals obtained from corresponding input samples, according to the formula: 100 x $2^{\wedge(\text{input Ct - sample Ct})}$. Results were expressed as fold enrichment relative to untreated cells.

Immunoprecipitation of Ago2-bound RNAs (RIP) assay.

5 to 10 x 10^6 of cells for each experimental point were pelletted, washed with $PBS^{-/-}$ 1x and lysed in 300 µl of lysis buffer (150 mM KCL, 25 mM Tris PH 7.4, 5 mM EDTA, 0,5% NP40, 5 mM DTT, protease inhibitor cocktails (Roche), 100 U/ml Superase-In (Ambion)). The cells were lived on ice for 30 min and then centrifuged 14000 rpm for 30 min at 4°C. The supernatants were incubated with protein G sepharose magnetic beads (GE Healthcare) conjugated with anti-Ago2 (EIF2C2 monoclonal antibody, clone 2E12-1C9; Abnova) or isotype IgG_{1k} control Abs (Abnova) ON at 4°C. After the immunoprecipitations, we kept the flow-through which contains the Ago2 unbound fraction, labeled “left over ip”. The beads with the Ago2 bound fraction were washed 3 times with the lyses buffer, before the direct RNA extraction with the TRizol. Sequences of 3’UTR mRNA-specific primers used in qPCR are listed in Table 1.

ELISA assay.

All antibodies and detection reagents were purchased from R&D Systems. The ELISA were carried out according to the manufacturer's instructions. Samples were diluted so that the optical density fell within the optimal portion of a log *st*andard curve.

Western blot.

5 x 10^6 cells were treated as indicated and lysed with a buffer containing 50 mM Tris-HCl (pH 8), 150 mM NaCl, 5 mM EDTA, 1.5 mM $MgCl_2$, 10% glycerol, 1% triton X-100, and protease/phosphatase inhibitors. The proteins were quantified using DC protein assay (Bio-Rad) and same amount for each sample were electrophoresed with a 10% SDS-PAGE gel. The proteins were transferred on a nitrocellulose membrane and immunoblotted with the antibody rabbit anti-human Myd88, rabbit anti-human IRAK1 and rabbit anti-human TRAF6, using standards conditions. Chemiluminescence was acquired by ChemiDoc XRS Imaging System, densitometric analysis was performed by Image Lab software (Bio-Rad) and protein band intensity was calculated by normalization over α-tubulin or actin band intensity reveald on the same blot.

Statistical analysis.

Statistical evaluation was determined using the Student *t*-test or the One-way ANOVA with Prism4. *P* values < 0.05 were considered significant.

Table 1. List of oligonucleotides used

Cloning of miR-cluster:	
TLR4 3'-UTR	5'- AATACAGAGTCTTCCAGGTG-3' 5'-TGTTCAATCACCCTAGACCT-3'
TLR2 3'-UTR	5'- GTTCCCATATTTAAGACCAG-3' 5'- TCTCATCCTGTAAAGTTTAA-3'
CD14 3'-UTR	5'-TGGATAACCTGACACTGGA-3' 5'-ATGAAGAAAGCCTAAGTATG-3'
MYD88 3'-UTR	5'-CTCCTCCTTTCGTTGTAG-3' 5'-GACTCTCTTTGGAGCATA-3'
IRAK1 3'-UTR	5'-ATCATTTATGCTTGGGAGGT-3' 5'-AAGAGGACACTCGGTTACA-3'
IL-6 3'-UTR	5'-GTCAGAAACCTGTCCACT-3' 5'-AATATGTATAAGTTAGCCAT-3'
CXCL8 3'-UTR	5'-CCAAGAGAATATCCGAACT-3' 5'- CAAAGAGAATCCCAATAAGC-3'
TNFα 3'-UTR	5'-GGAGGACGAACATCCAACCT-3' 5'-AGCAATGAGTGACAGTTGGTCA-3'
CCL3 3'-UTR	5'-CTGAGCCTTGGGAACAT-3' 5'-AGAGCATCTTTATTATTTCC-3'
CCL7 3'-UTR	5'-ACATTCATGACTGAACTGA-3' ACAAAAATCTATTTTAT
hsa-miR-125a	5'-TGCCTATCTCCATCTCTGACC -3' 5'-TGGTGGTCAAATGTCATGCT -3'
hsa-let-7e	5'-CTGTCTGTCTGTCGGGTCTG -3' 5'-GCAGGGACAAGGACAGAAAA -3'
Cloning of miR-146b:	

TLR4 3’-UTR	5’-GTCAGAAACCTGTCCACT-3’ 5’-TGTGCCTAATTCAGAAGATG-3’
TLR2 3’-UTR	5’- GTTCCCATATTTAAGACCAG-3’ 5’- TCTCATCCTGTAAAGTTTAA-3’
IL-6 3’-UTR	5’-GTCAGAAACCTGTCCACT-3’ 5’-AATATGTATAAGTTAGCCAT-3’
IRAK1 3’-UTR	5’-ATCATTTATGCTTGGGAGGT-3’ 5’-AAGAGGACACTCGGTTACA-3’
MyD88 3’-UTR	5’-GCAAATATCGGCTTTTCTCA-3’ 5’-GACTCTCTTTGGAGCATA-3’
TRAF6 3’-UTR	5’-TTGCCCTCACTTGCTCAA-3’ 5’-AGATGCTACTTCGTAACCTC-3’
miR-146b	5’-TGGAATAGGAGTTCTCTTG-3’ 5’-TAGTGGCAGGTTATGAGCA-3’
Seed mutagenesis (*hsa* targets):	
miR125a-5p TLR4-3’UTR	5’-AAGGACAATCAGGATGTCATAAATGAAAATAAAAACCACAATG-3’ 5’- CATTGTGGTTTTTATTTTCATTTATGACATCCTGATTGTCCTT-3’
let-7e-5p TLR4-3’UTR	5’- CCATGACAAAGAAAGTCATTTCAACTCTTATCAAGTTGAATAA-3’ 5’-TTATTCAACTTGATAAGAGTTGAAATGACTTTCTTTGTCATGG -3’
miR146b TLR4-3’UTR	5’-TGTCTATGGCTGTTTGAGATTCTCTACTCTTGTGCTTG-3’ 5’-CAAGCACAAGAGTAGAGAATCTCAAACAGCCATAGACA-3’
miR125a-5p CD14-3’UTR	5’-CTGCCTTGGCTTCGAGTCCCGTCAGG -3’ 5’-CCTGACGGGACTCGAAGCCAAGGCAG-3’
miR146b IRAK1-3’UTR seed1	5’-GATCCCCCAAATCCGGCAAAGTTCTCATGGTC-3’ 5’-GACCATGAGAACTTTGCCGGATTTGGGGGATC-3’
miR146b IRAK1-3’UTR seed 2	5’-GCAAAGTTCTCATGGTCGTTCTCATGGTGCACGA-3’ 5’-TCGTGCACCATGAGAACGACCATGAGAACTTTGC-3’
miR125a-5p IRAK1-3’UTR seed 1	5’-CAGACAGGGAAGGGAAACATTTTGAAAAGACATGTATCAC -3’ 5’-GTGATACATGTCTTTTCAAAATGTTTCCCTTCCCTGTCTG-3’
miR125a-5p IRAK1-3’UTR	5’-CAGGGAAGGGAAACATTTTGGACATGTATCACATGTCTTC -3’

seed 2	5’-GAAGACATGTGATACATGTCCAAAATGTTTCCCTTCCCTG-3’
let-7e-5p MyD88-3’UTR seed1	5’-AGGAGGAATCTGTGCTCTACCTCTCAATTCCTGG -3’ 5’-CCAGGAATTGAGAGGTAGAGCACAGATTCCTCCT-3’
let-7e-5p MyD88-3’UTR seed2	5’-CAAACTCTGGAAAGGACCCTACCAGTATTTATACCTCTA-3’ 5’-TAGAGGTATAAATACTGGTAGGGTCCTTTCCAGAGTTTG-3’
let-7e-5p MyD88-3’UTR seed3	5’-CTGAGTTTATAATAATAAATAATATCTTGGAAACTTGTGTGTG -3’ 5’-CACACACAAGTTTCCAAGATATTATTTATTATTATAAACTCAG-3’
miR146b MyD88-3’UTR	5’-GAACTGCAGACACAGCTTCTCCCTCTCTCCTT-3’ 5’-AAGGAGAGAGGGAGAAGCTGTGTCTGCAGTTC-3’
miR146b TRAF6-3’UTR seed 1	5’-CCTGGAGAAAACAGTGTCCTTGCCCTGTTCTC-3’ 5’-GAGAACAGGGCAAGGACACTGTTTTCTCCAGG-3’
miR146b TRAF6-3’UTR seed 2	5’-CTCGAGAAGAGTTATTGCTCTAGTTGAGTTCTCATTTTTTTAACC-3’ 5’-GGTTAAAAAAATGAGAACTCAACTAGAGCAATAACTCTTCTC-3’
miR146b TRAF6-3’UTR seed 3	5’-ATTTGAACCATAATCCTTGGATTAAGTTCTCATTCACCCCAG-3’ 5’-CTGGGGTGAATGAGAACTTAATCCAAGGATTATGGTTCAAAT-3’
miR125a-5p TNFα-3’UTR	5’-TCTGGAATCTGGAGACAGCCTTTGGTTCTGGC -3’ 5’-GCCAGAACCAAAGGCTGTCTCCAGATTCCAGA-3’
let-7e-5p IL6-3’UTR	5’-GTCAGAAACCTGTCCACT-3’ 5’-AATATGTATAAGTTAGCCAT-3’
miR125a-5p CCL3-3’UTR	5’-AAATGTGTATCGGATGCTTTTGTGGCTGTGATCGG -3’ 5’-CCGATCACAGCCACAAAAGCATCCGATACACATTT-3’
let-7e-5p CCL3-3’UTR	5’-GTGTGACCTCCACAGCTTTCTATGGACTGGTTGT-3’ 5’-ACAACCAGTCCATAGAAAGCTGTGGAGGTCACAC-3’
miR125a-5p CXCL8-3’UTR	5’-GATGTTTTATTAGATAAATTTCGGGTTTTTAGATTAAAC-3’ 5’-GTTTAATCTAAAAACCCGAAATTTATCTAATAAAACATC-3’
let-7e-5p CXCL8-3’UTR	5’-AAGTATTAGCCACCATCTCACAGTGATGTTGTGAGG -3’ 5’-CCTCACAACATCACTGTGAGATGGTGGCTAATACTT-3’
let-7e-5p CCL7-3’UTR	5’-ATGCTCCTCCCTTCTCCATGGGGGTATTGTA-3’ 5’-TACAATACCCCCATGGAGAAGGGAGGAGCAT-3’
Q-PCR:	

hsa-TLR4	5’-CACCTGATGCTTCTTGCTG-3’ 5’-TCCTGGCTTGAGTAGATAA-3’
hsa-CD14	5’-GCAACACAGGAATGGAGA-3’ 5’-ACAGATTGAGGGAGTTCA-3’
hsa-IRAK1	5’-TGAAGAGGCTGAAGGAGAA-3’ 5’-CACAATGTTTGGGTGACGAA-3’
hsa-MyD88	5’-GCACATGGGCACATACAGAC-3’ 5’-GACATGGTTAGGCTCCCTCA-3’
hsa-TRAF6	5’-GTCCCTTCCAAAAATTCCAT-3’ 5’-CACAAGAAACCTGTCTCCTT-3’
hsa-IL-6	5’-TACCCCCAGGAGAAGATTCC-3’ 5’-TTTTCTGCCAGTGCCTCTTT-3’
hsa-CCL3	5’-TGACTACTTTGAGACGAGCA-3’ 5’-CTGACATATTTCTGGACCC-3’
hsa-CCL7	5’-CTGCTGCTACAGATTTATCA-3’ 5’-TCCTTGTCCAGTTTGGTCTT-3’
hsa-CXCL8	5’-GCCAGGAAGAAACCACCGGAAGGA-3’ 5’-GGGTCCAGACAGAGCTCTCTTCC-3’
hsa-TNFα	5’-GCTGCACTTTGGAGTGATCG-3’ 5’-GAGGTACAGGCCCTCTGATG-3’
hsa-GAPDH	5’-GATCATCAGCAATGCCTCCT-3’ 5’-TGTGGTCATGAGTCCTTCCA-3’
ChIP assay:	
hsa-STAT3cluster	5’-AACGCCTTGTCCAGTGACCTT-3’ 5’-GTGGGGGTGGTTTGAGAA-3’
SP1-200bp-site/ Pol II-cluster	5’-AGGGAAGGGGGAAGAGA-3’ 5’-GTGGGGGTGGTTTGAGAA-3’
SP1-320bp-site/ STAT3-cluster	5’-TTCTCGGCTTCCCCTCT-3’ 5’-CAACCTCCCAGACCCTCAG-3’
SP1-770bp-site/NFkB-	5’-TCCCCACCTCCTCTTTAG-3’

cluster	5’-GCCCATAGCCCCGCTTTG-3’
Pol-II miR-155	5’-ACCATTTCTTCCTCTCTTAG-3’ 5’-GGCTCCAACCTTTGTTCTT-3’
Pol-II miR-146b	5’-AATAGGAGTTCTCTTGGTAT-3’ 5’-AATTCAGTTCTCAGTGCC-3’
Pol-II miR-146a	5’-GAGGAAGTGACATTGAAAGC-3’ 5’-TGTATGGTAGACACACACAT-3’
Pol-II miR-155	5’-ACCATTTCTTCCTCTCTTAG-3’ 5’-GGCTCCAACCTTTGTTCTT-3’
STAT3 miR-146b	5’-CTCGGCTGAACTCTCCAGA-3’ 5’-GCAAACCAAGGGGCTTTCT-3’
STAT3 miR-146a	5’-GCACTTGAAAAGCCAACAGG-3’ 5’-CACAGCGAGGGAGGAAGA-3’
STAT3 IL-10	5’-GCAGAAGTTCATGTTCAACCAA -3’ 5’-AGGCCTCTTCATTCATTAAAA -3’
RIP assay:	
hsa-TLR4-RIP	5’-CCTCCTCAGAAACAGAACAT-3’ 5’-TCATAACGGCTACACCATTT-3’
hsa-CD14-RIP	5’-CTAACTCCCTAAGAAACCC -3’ 5’-ACCTTTTAATCCAGATGCCA -3’
hsa-IRAK1-RIP	5’-CTCTTTGCCCATCTCTTTG-3’ 5’-GCCACACTTTTCCAAATTGT-3’
hsa-MYD88-RIP	5’-GCTTGGGCTGCTTTTCATT-3’ 5’-CCTGCTCACATCATTACAGT-3’
hsa-TRAF6-RIP	5’-TAAGTTCTCATTCACCCCAG-3’ 5’-AGGAAATAAGTAAGCAAGGC-3’
hsa-TNFα-RIP	5’-CTGACATCTGGAATCTGGA-3’ 5’-TCTGGAAACATCTGGAGAG -3’
hsa-IL6-RIP	5’-GCATTCCTTCTTCTGGTCA-3’ 5’-ATAGTGTCCTAACGCTCATA-3’

hsa-CXCL8-RIP	5’-TACTCCCAGTCTTGTCATTG-3’ 5’-TTCCGTAATTCAACACAGCA -3’
hsa-CCL3-RIP	5’-AAGCCACCAGACTGACAAA-3’ 5’-CCTTTTAAAAGAGCATCTTT-3’
hsa-CCL7-RIP	5’-GGATTTTGGTGGGTTTTGAA-3’ 5’-TGAGGTAGAGAAGGGAGG-3’

3. RESULTS

3.1 The miR-125a~99b~let-7e cluster and miR-146b are induced by IL-10 and TGFβ

To identify miRNA potentially involved in the monocytes-mediated response to stimuli of bacterial origin in humans, we previously analyzed their miRNA expression profile after stimulation with 100 ng/ml LPS using a TaqMan-based Low Density Array [77]. Under this conditions, we confirmed the induction of LPS-dependent miRNAs described in monocytic cell lines or mouse macrophages, such as miR-146a [76] and miR-155 [75], and we identified previously unrecognized miRNAs, including miR-9 [77], miR-187 [128], miR-125a-5p, let-7e-5p, miR-99b-5p and miR-146b. For miR-9 [77] and miR-187 [128], we described their involvement in the regulation of monocytes activation by the direct targeting of a specific gene involved in the NFKB pathway (p50 NFKB and NFKBIZ respectively). We here report our study regarding the second group of LPS-dependent miRNA in order to identify a potential role in the innate immune response: miR-125a-5p, let-7e-5p, miR-99b-5p and miR-146b.

MiR-125a-5p, let-7e-5p and miR-99b-5p belong to a cluster encoded by a conserved region hosted in the first intron of the *linc00085* gene and we will refer to it as 'miRNA cluster'.

3.1.1 Regulation of miR-125a, miR-99b, let-7e and miR-146b by pro-inflammatory stimuli.

We stimulated human monocytes with different TLR ligands and with the proinflammatory cytokines IL-1β. IL-1β and the TLR2 agonist palmitoyl-3-cysteine-serine-lysine-4 (Pam3CSK4) induced miR-125a-5p, let-7e-5p, miR-99b-5p and miR-146b to similar extent as LPS, while the TLR3 agonist poly(I:C), the TLR7

agonist imiquimod, and a CpG oligodeoxynucleotide (agonist of TLR9) were inactive (Fig. 1A to D).

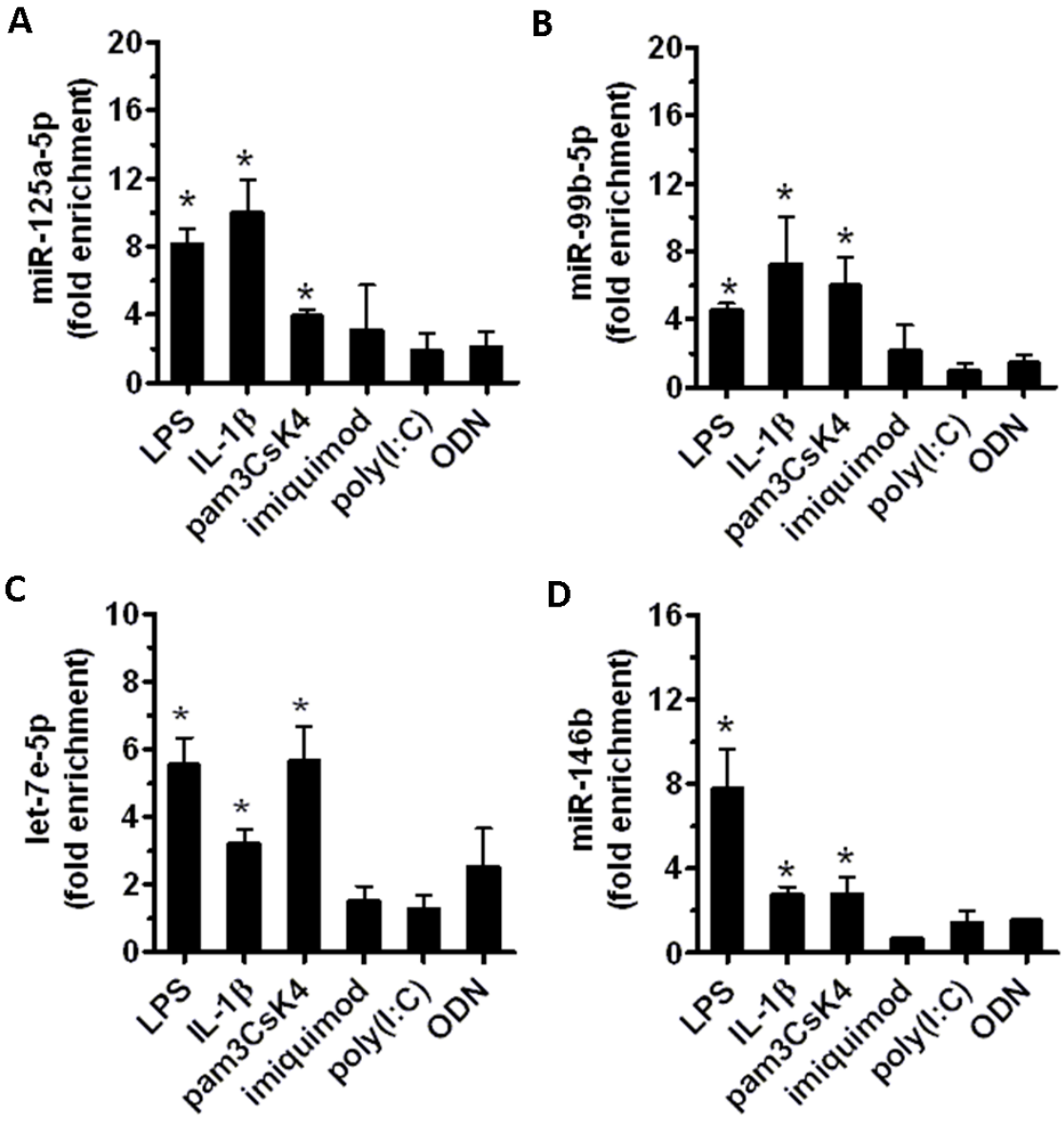

Figure 1: Regulation of miR-125a, miR-99b, let-7e and miR-146b by pro-inflammatory stimuli. Human purified monocytes were cultured with different stimuli (100 ng/mL LPS, 25 ng/mL IL-1β, 2 µg/mL Pam3CSK4, 3 µg/mL imiquimod, 50 µg/mL poly(I:C), 1 µM ODN) for 24 h. Levels of miR-125a-5p (A), miR-99b-5p (B), let-7e-5p (C) and miR-146b (D) were measured by qPCR in triplicate samples. Results are expressed as fold change over control (mean ± SEM; n = 3; * $p < 0.05$).

3.1.2 IL-10 induces miR-125a~99b~let-7e cluster and miR-146b expression.

Differently from miR-146a, rapidly induced in response to LPS (detectable after 2 hours of stimulation), miR-125a, miR-99b, let-7e and miR-146b showed instead a delayed kinetics of expression (Fig. 2 A-D), suggesting the involvement of IL-10, which is late induced in monocytes after LPS exposure [123, 153, 154]. We stimulated human monocytes with LPS, IL-10 alone and LPS plus IL-10 and we measured miRNAs expression levels at different time points. Recombinant IL-10 induced the expression of miR-125a-5p, miR-99b-5p, let-7e-5p and miR-146b, and potentiated their expression by LPS (Fig. 2). Instead, IL-10 stimulation had no effect on the expression of miR-146a, that is only LPS-dependent (Fig. 2 E).

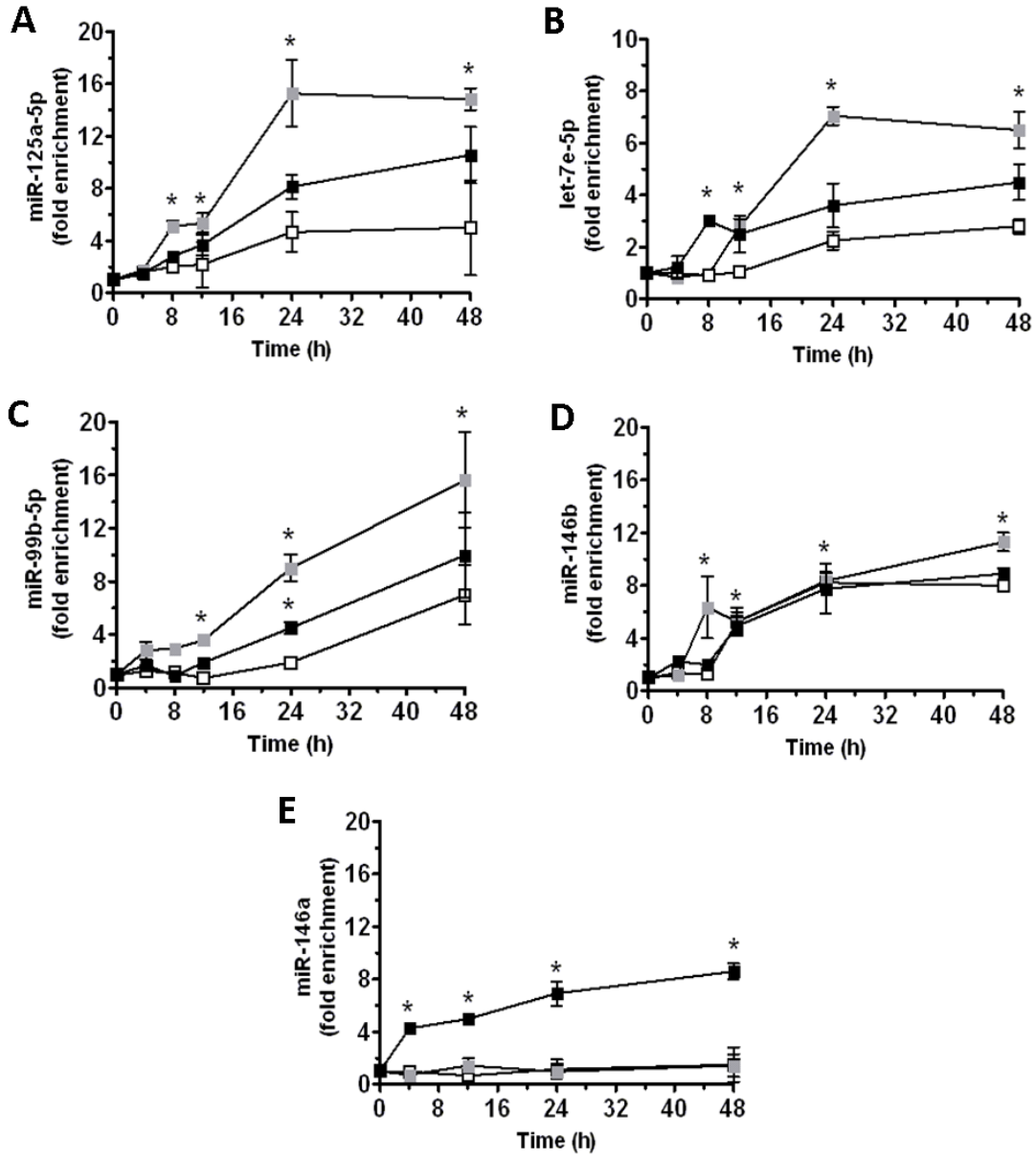

Figure 2: IL-10 induces miR-125a~99b~let-7e cluster and miR-146b expression. Human purified monocytes were cultured with 100 ng/mL LPS (black), 20 ng/mL IL-10 (white), or both stimuli (grey) for the indicated times. Levels of miR-125a-5p (A), let-7e-5p (B), miR-99b-5p (C), miR-146b (D) and miR-146a (E) were measured by qPCR in triplicate samples. Results are expressed as fold change over control (mean ± SEM; n = 3; * $p < 0.05$).

3.1.3 Inhibition of IL-10 signaling pathway leads to a reduction of miR-125a, miR-99b, let-7e and miR-146b expression

To investigate whether endogenously produced IL-10 played a role in the expression of miR-125a-5p, miR-99b-5p, let-7e-5p and miR-146b induced by LPS, monocytes were pretreated by an anti-IL-10R blocking monoclonal antibody (and isotype-specific control IgG) or the JAK/STAT signaling pathway inhibitor AG-490 compound [155]. MiRNAs expression were analyzed 24 h after LPS stimulation. The activity of the inhibitor AG-490 was confirmed by the reduced detection of IL-10 after 24 h LPS in monocytes pre-treated with the inhibitor (data not shown). Blocking endogenous IL-10 signaling or its production, we observed a significant reduction of miR-125a-5p, miR-99b-5p, let-7e-5p and miR-146b expression after LPS stimulation, whereas miR-146a induction was not affected (Fig. 3).

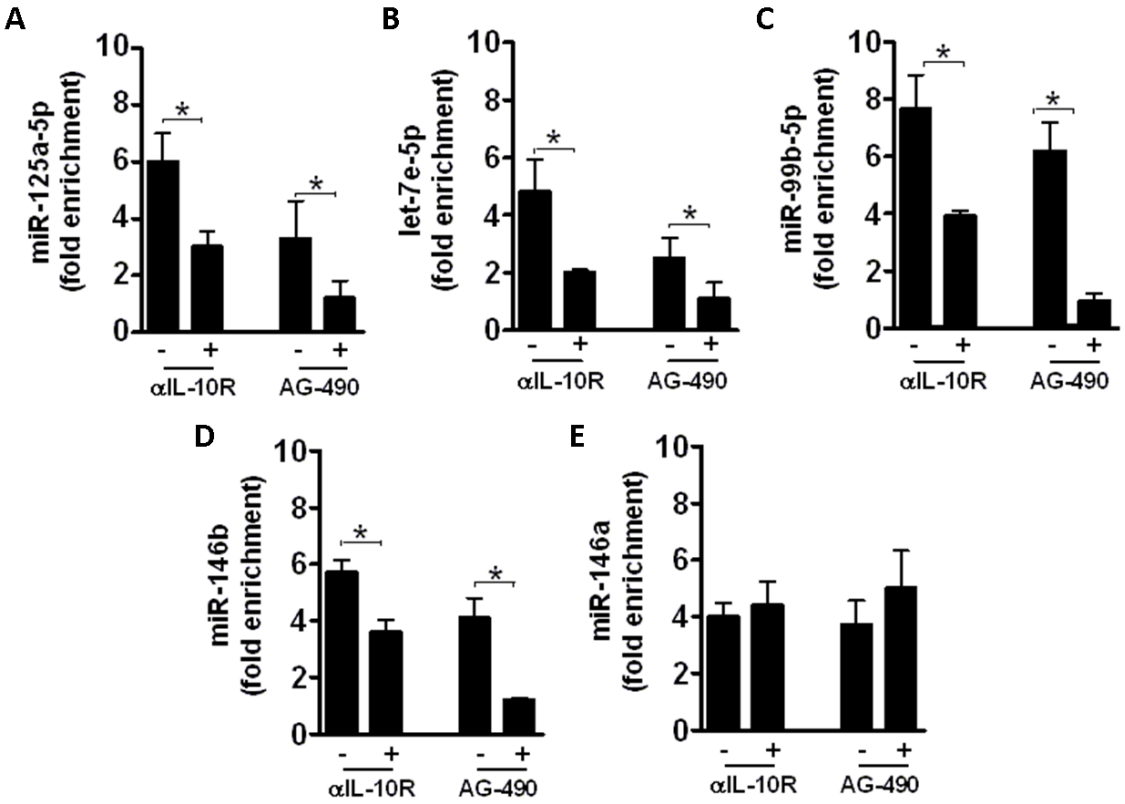

Figure 3: miR-125a~99b~let-7e cluster and miR-146b induction after LPS challenge is driven by IL-10. Human monocytes were pre-treated or not for 30 min with 5 μM of the JAK/STAT inhibitor AG-490 and then stimulated for 24 h with 100 ng/ml LPS. Alternatively, monocytes stimulated for 24 h with 100 ng/ml LPS were cultured in the presence of 10 μg/ml anti-IL-10R or isotype control MoAb. MiRNAs levels were measured by qPCR in triplicate samples and results expressed as fold change over control (mean ± SEM; n = 3; * $p < 0.05$).

3.1.4 Regulation of miR-125a, miR-99b, let-7e and miR-146b by anti-inflammatory stimuli.

We then investigated the regulation of these miRNAs by other anti-inflammatory mediators in order to define if they were only relevant for IL-10-mediated anti-inflammatory action or also induced by other anti-inflammatory signals. Interestingly, we found that, in addition to IL-10, TGFβ but not glucocorticoids (Dex), IL-4 and IL-13 increased miRNA cluster and miR-146b expression (Fig. 4).

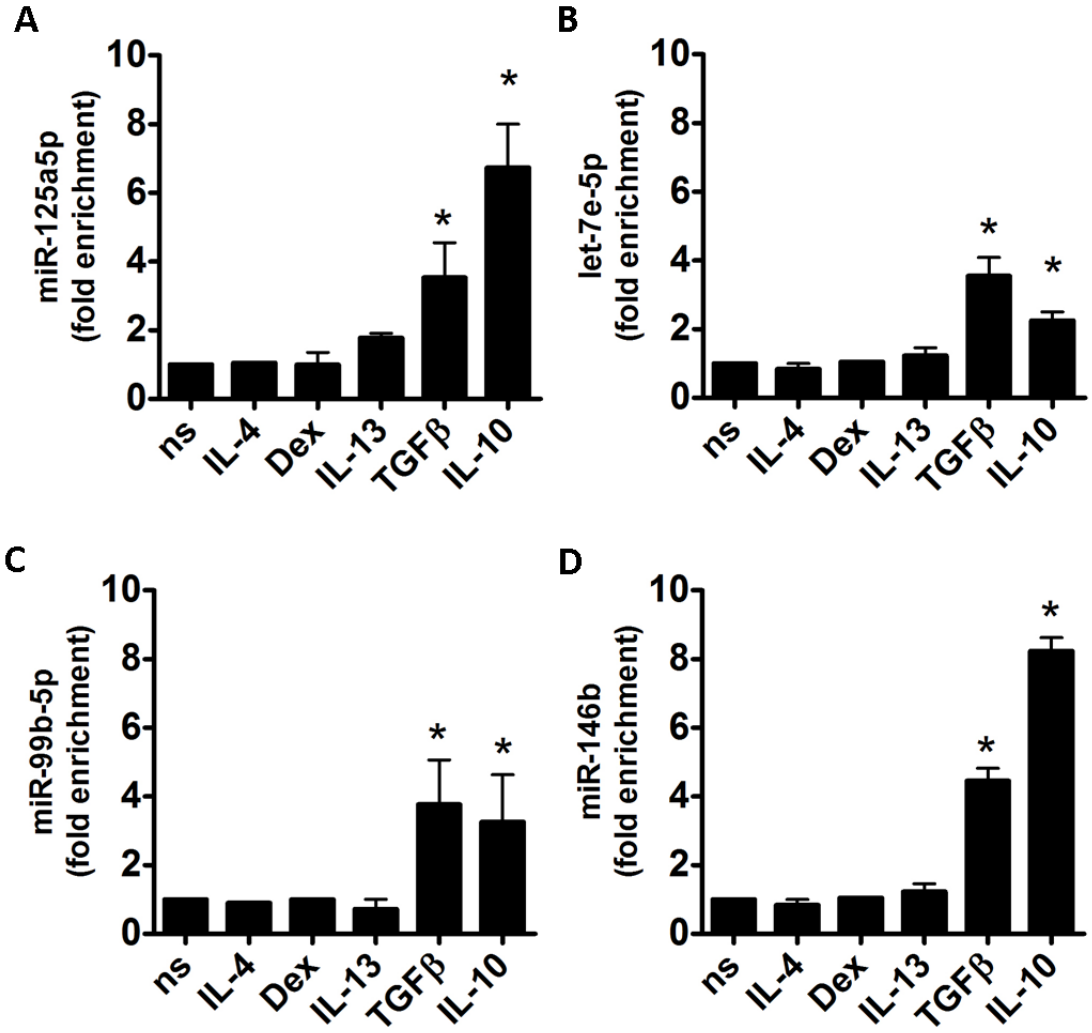

Figure 4: miR-125a~99b~let-7e cluster and miR-146b induced by TGFβ. Human purified monocytes were cultured with 20 ng/mL Dex, 50 ng/mL TGFβ, 20 ng/mL IL-4, 50 ng/ml IL-13 or 20 ng/ml IL-10 for 24 hours. MiRNAs levels were measured by qPCR in triplicate samples and results expressed as fold change over control (mean ± SEM; n = 3; * $p < 0.05$).

3.1.5 miRNA cluster and miR-146b enriched in RISC of LPS-, IL-10-, TGFβ stimulated human monocytes

To demonstrate the functional activity of these miRNAs we checked their presence into the RISC complex upon different stimulation conditions. To this aim, we performed a RNA-induced silencing complex (RISC) immunoprecipitation, using Ago2 antibody. Indeed, to be functional miRNA must be incorporated into a RISC-complex, composed of specific RNA-binding protein, miRNA and the mRNA target. Ago2 is an essential components of the complex [156]. Consistent with the expression data, we obtained miRNA cluster and miR-146b loading in the RISC only when the cells were treated with LPS, IL10 and TGFβ but not with dex (Fig.5).

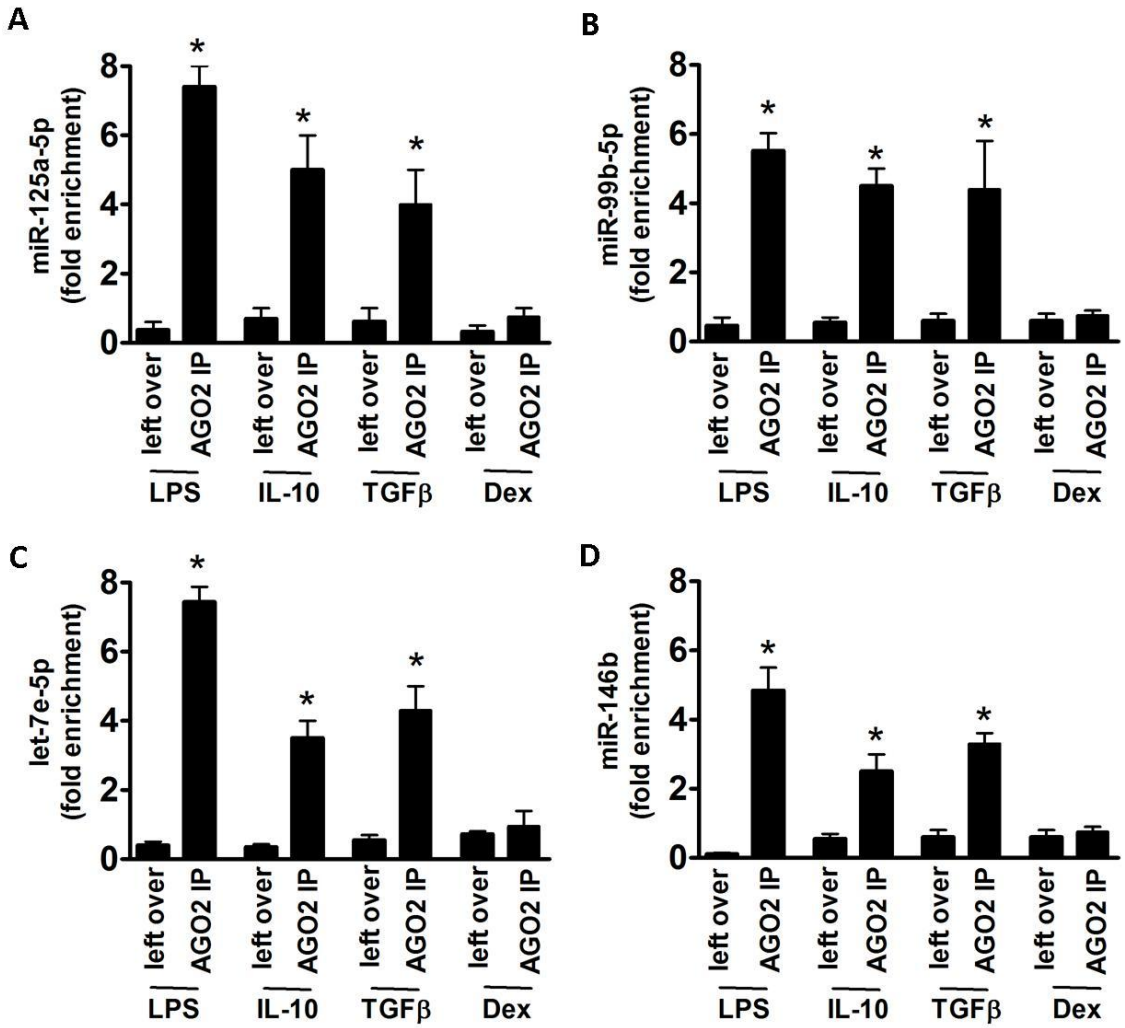

Figure 5: miRNA cluster and miR-146b enriched in RISC of LPS-, IL-10-, TGFβ stimulated human monocytes. Human purified monocytes were cultured with 100 ng/ml LPS, 20 ng/mL Dex, 50 ng/mL TGFβ or 20 ng/mL IL-10 for 24 hours. Cell extracts were subjected to RIP assay using anti-Ago2 or IgG control Abs. Levels of miR-125a-5p (A), miR-99b-5p (B), let-7e-5p (C) and miR-146b (D) were measured by qPCR in triplicate samples. Results are expressed as fold change over control (mean ± SEM; n = 3).

3.1.6 IFNγ blocks miRNA cluster and miR-146b expression

IL-10 and TGFβ primarily operate as feedback inhibitors of the LPS-mediated inflammatory response and are part of a more complex network of regulation in which also operates IFNγ, as a coadiuvator of LPS activatory stimulus [157]. Therefore we studied the effect of IFNγ stimulation on miR-125a~99b~let-7e cluster expression and miR-146b. We found that IFNγ was able to reduce miR cluster expression at early time points and it also abolished the effect of LPS-mediated upregulation when monocytes were challenged with both LPS and IFNγ (Fig.6).

Taken together, these data identify the miR-125a~99b~let-7e cluster and miR-146b as an LPS, IL-10, and TGFβ-responsive gene, negatively modulated by IFNγ, therefore suggesting a complex feedback loop regulatory mechanism that orchestrates the inflammatory response upon TLR engagement.

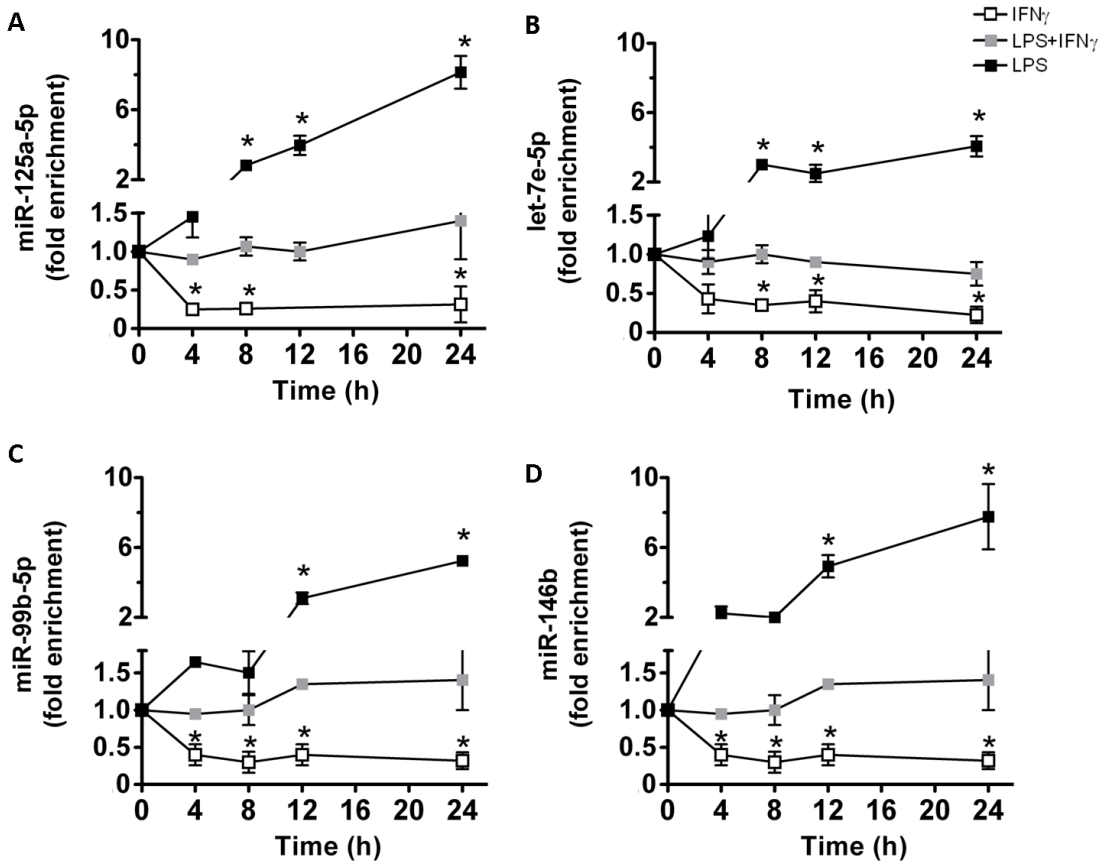

Figure 6: IFNγ blocks miRNA cluster and miR-146b expression. Human purified monocytes were culture with 100 ng/mL LPS (black), 20 ng/mL IFNγ (white) or both stimuli (grey) for 4, 8, 12 and 24 hours. MiRNAs levels were measured by qPCR in triplicate samples and results were expressed as fold change over control (mean ± SEM; n = 3; * $p < 0.05$).

3.2 Transcriptional regulation of miR-125a~99b~let-7e cluster and miR-146b in human monocytes

3.2.1 Genomic organization and bioinformatic analysis of miR-125a~99b~let-7e cluster promoter.

MiR-125a-5p, let-7e-5p and miR-99b-5p represent the mature products of the miR-125a~99b~let-7e cluster, encoded by a conserved region hosted in the first intron of the *linc00085* gene in human chromosome 19 (Fig. 7). To investigate the transcriptional regulation of these miR we performed a bioinformatics analysis, scanning a 2kb region upstream the predicted transcription start site of the gene. We identified putative binding sites for transcription factors, known to be LPS-, IL-10-, and TGFβ- sensitive, more exactly: NFκB, STAT3 and SMAD respectively. (Fig. 7).

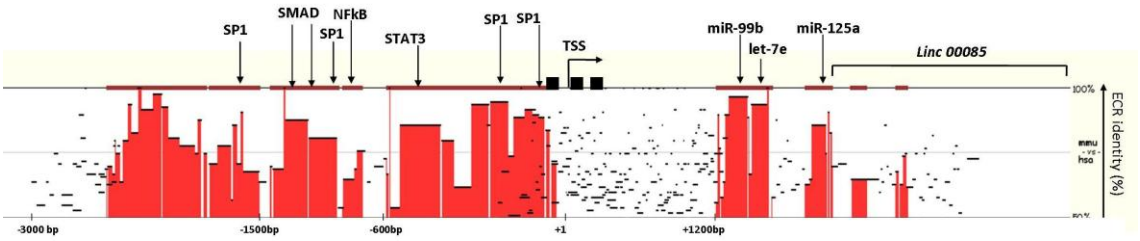

Figure 7: Genomic organization and bioinformatic analysis of the miR-125a~99b~let-7e cluster promoter. Pairwise sequence local alignments of human (chr.19: 52191745-52196592) and murine (chr.17: 17827604-17832451) cluster miR-125a~99b~let-7e *loci* are visualized as a conservation plot generated by Mulan using the TBA alignment program (see Materials and Methods). Black blocks identify evolutionary conserved regions (ECR) with >50% identity between the two species over 100 bp segments. The transcription start site [158], TATA boxes (black squares), and the putative binding sites for transcription factors are indicated.

3.2.2 Direct transcriptional induction of miR-125a~99b~let-7e cluster by LPS, IL-10 and TGFβ.

To study the transcriptional regulation of the miR-125a~99b~let-7e cluster upon TLR4/TLR2, IL-10 and TGFβ stimulation, we analyzed the recruitment of RNA polymerase II (Pol II) to its promoter region in the presence of different stimuli.

Chromatin immunoprecipitation (ChIP) experiments on human monocytes stimulated with LPS, IL-10 and TGFβ showed a recruitment of the Pol II on the promoter of miR-125a~99b~let-7e cluster, confirming a direct transcriptional induction of the miRNA cluster by this stimuli (Fig. 8A). We used miR-155 as a positive control for the LPS stimulation because it is a very well-known LPS-responsive miRNA [75], for whom we obtained a consistent Pol II recruitment on its promoter. Instead we did not obtained any Pol II enrichment on the miR-155 promoter region after IL-10 stimulation which regulates negatively miR-155 expression [80], that we used here as a negative control.

Consistent with the positive effect of IL-10 on the expression of miR-125a~99b~let-7e cluster, we validated by Chip the binding of the IL-10-dependent transcription factor STAT3 to a highly conserved site present in the miRNA cluster promoter (Fig. 7). ChIP data showed a STAT3 recruitment on this binding site only after short term exposure to IL-10 but not LPS (Fig. 8B). We also identified a binding site for SMAD3, a TGFβ- dependent transcription factor and Chip experiments showed its recruitment to miRNA cluster promoter 24h after TGFβ challenge, consistent with the miRNA kinetic data (Fig. 8C). Interestingly, ChIP experiments also showed that the NF-kB putative binding site predicted in the promoter region of the miR-125a~99b~let-7e cluster was engaged by the corresponding transcription factor after challenge with LPS but not IL-10 (Fig.8D).

Collectively, these data demonstrate that in monocytes the miR-125a~99b~let-7e cluster is transcriptional induced by anti-inflammatory stimuli (i.e. IL-10 and TGFb) and lately by TLR engagement.

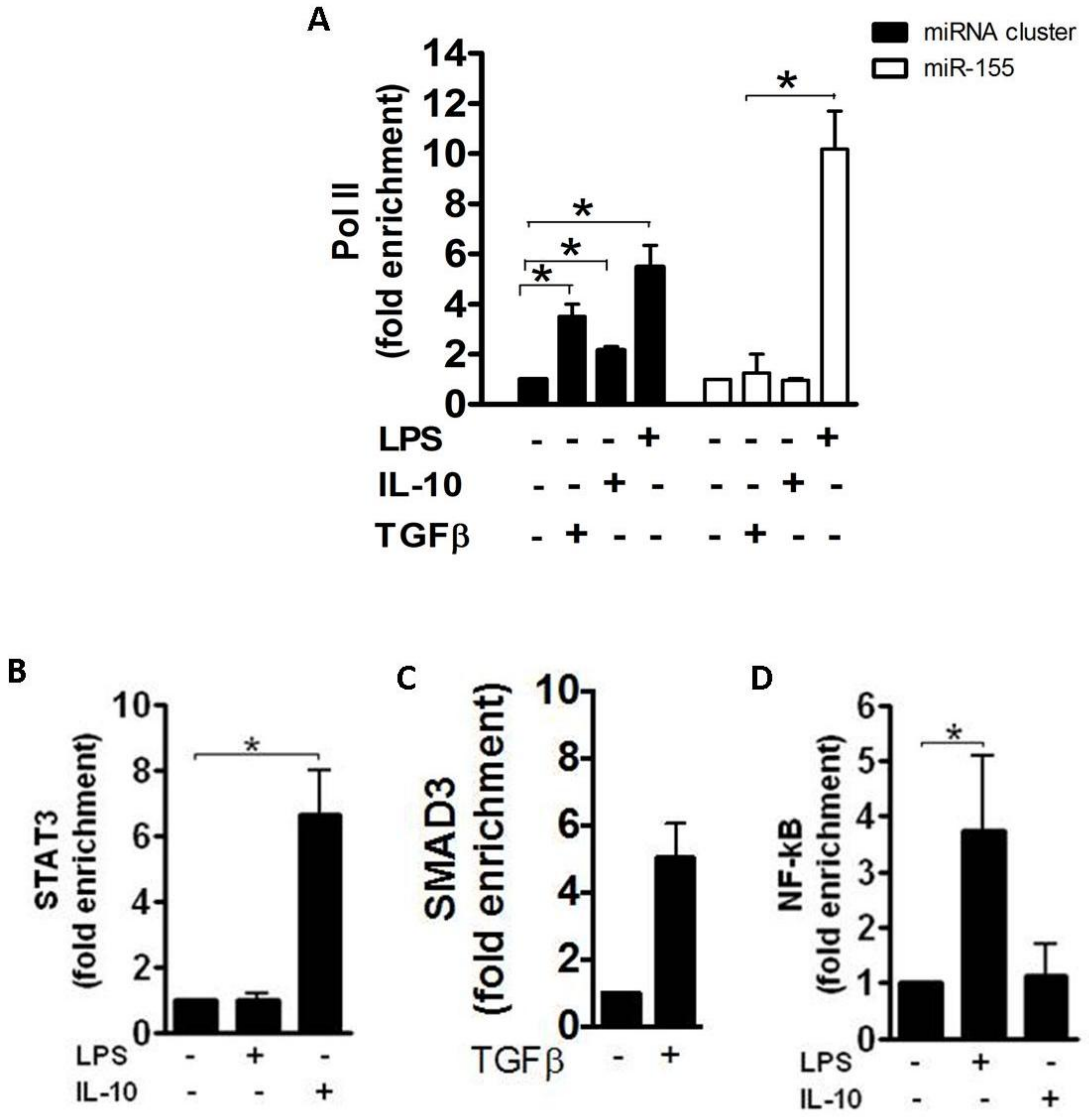

Figure 8: Transcriptional regulation of miR-125a~99b~let-7e cluster in human monocytes. ChIP assay was carried out on human monocytes stimulated or not for 2 h with 20 ng/ml of IL-10, 100ng/ml LPS or 50 ng/ml of TGFβ using anti-Pol II (A), anti-STAT3 (B), anti-SMAD3 (C) and anti-NFkB (D). Q-PCR was carried out using specific primers for the miR-125a~99b~let-7e promoter (black columns) or on miR-155 promoter (white column). Results are expressed as fold change over control (mean± SEM; n =3).

3.2.3 Genomic organization and bioinformatic analysis of miR-146b and miR-146a promoters.

MiR-146b is the second member of the miR-146 family and it is located in an intergenic region on human chromosome 10. According to published data [76], the miR-146b predicted transcription start site is located 700 bp upstream of the mature miR-146b sequence [76] (Fig. 9A). To identify putative *cis* regulatory elements critical for the transcriptional regulation of miR-146b, we analyzed 1000 bp upstream of the pre-miR-146b coding region with bioinformatic tools, as well the promoter of miR-146a [129]. Conserved putative binding sites for STAT3, the main transcription factor mediating the IL-10 anti-inflammatory action in monocytes [159], were predicted on both miR-146a and miR-146b promoter regions. NFkB binding sites were predicted on the promoter of miR-146a, as described by Taganov [76], and even on the promoter of miR-146b.

To study the transcriptional regulation of miR-146b in monocytes, we performed ChIP experiments. Stimulation of monocytes with LPS enriched the recruitment of Pol II onto the miR-146b promoter, as well as to the miR-146a and miR-155 promoters, known LPS-dependent miRNAs (Fig. 9B to D). Conversely, stimulation of monocytes with IL-10, resulted in Pol II recruitment only on the promoter region of miR-146b (Fig. 9C) and not on the promoter of miR-146a (Fig. 9B) or miR-155 (Fig. 9D), consistent with the selective IL-10-mediated upregulation of miR-146b expression.

To verify if the predicted STAT3 binding sites on both the promoters were functional, we performed ChIP analysis on monocytes stimulated with IL-10 and analyzed STAT3 recruitment. We demonstrated the recruitment of STAT3 protein exclusively on the miR-146b promoter region, while no STAT3 enrichment was found on the miR-146a promoter region (Fig. 9E).

MiR-146b could be even regulated by NF-kB because of the two putative NF-kB binding sites predicted on promoter region. We used two chemical inhibitors, CAPE (Caffeic acid phenethyl ester) [160] and PDTC (pyrrolidine dithiocarbamate) [161], to specifically impair NF-kB signaling. In LPS stimulated monocytes, blocking of NF-kB activity resulted in an impairment of miR-146a expression levels, consistent with previous reports of NF-kB driving the expression of miR-146a [76]; but blocking of NF-kB activity had no role on miR-146b induction by LPS (Fig. 9F).

These data indicate that miR-146a and miR-146b undergo a profound different regulation in monocytes exposed to pro- and anti-inflammatory stimuli and identify miR-146b, but not miR-146a, as an IL-10-dependent miRNA, suggesting that miR-146b may play a role in mediating the anti-inflammatory activity of IL-10.

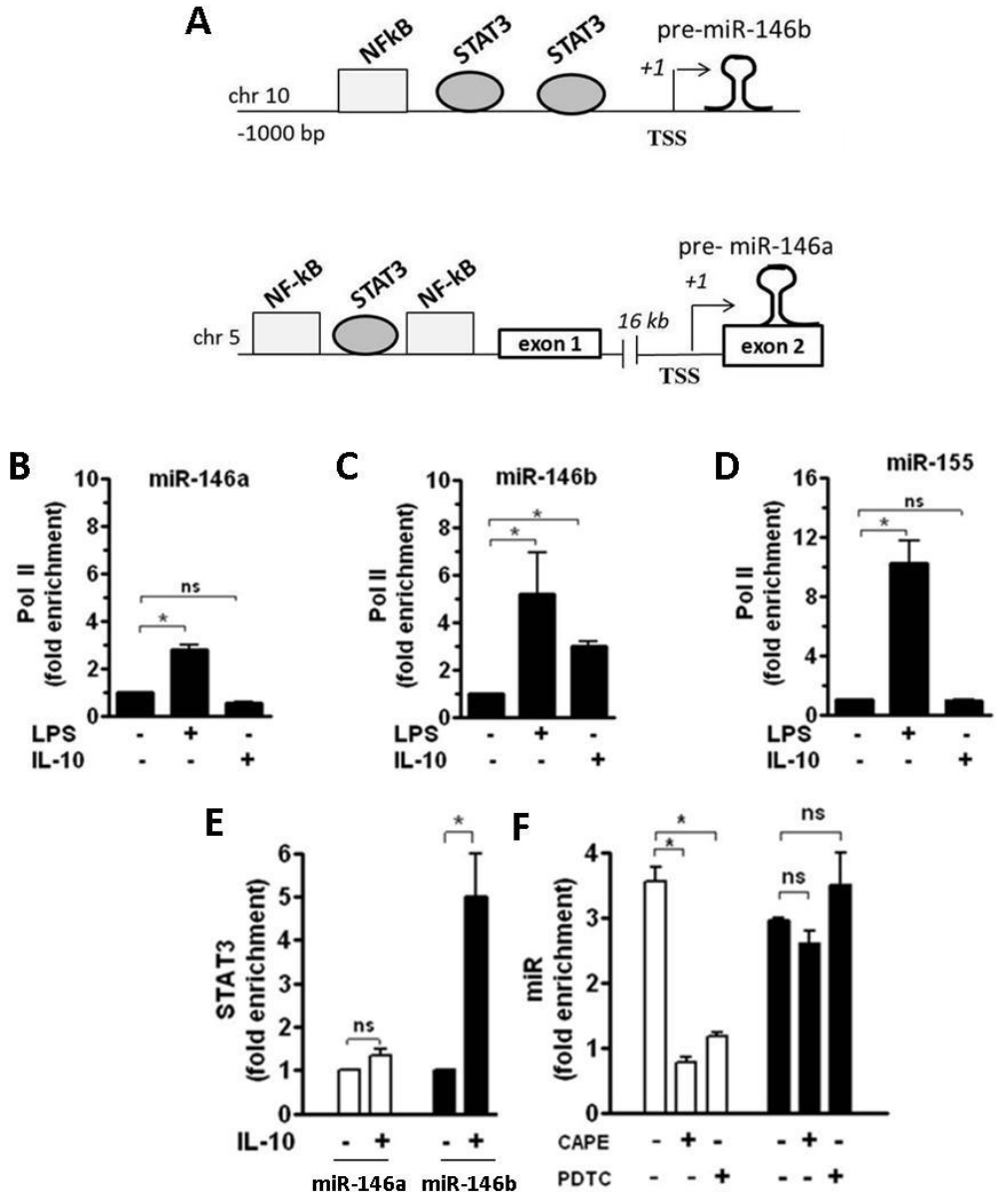

Figure 9: MiR-146b induction after LPS challenge is driven by IL-10. (A) Graphical representation of predicted promoter regions reporting binding sites of transcription factors of potential interest.(B to D) ChIP assays were carried out using anti-Pol II Ab and analysed by qPCR with specific primers binding to the miR-146b, miR-146a, and miR-155 promoters. Data from qPCR have been normalized to input DNA and displayed as fold change over untreated cells (mean ± SEM; n = 3 (E) Monocytes were stimulated or not for 4 h with 20 ng/ml IL-10. ChIP assays were carried out using anti-STAT3 Ab and analysed by qPCR with specific primers binding to miR-146a (white columns) and miR-146b (black columns) promoters. (F) Cells were pretreated for 1 h with the NF-kB inhibitors PDTC (1 μM) or CAPE (2 μM) and then stimulated for 12 h with 100 ng/ml LPS. MiR-146a (white columns) and miR-146b (black columns) expression levels were measured by qPCR in triplicate samples and results expressed as fold change over control (mean ± SEM; n = 3).

3.3 MiR-125a-5p, let-7e-5p and miR-146b directly target the TLR signaling pathway at multiple levels.

To gain insight into the functional role of miRNAs in the context of LPS-mediated inflammation, we chose an *in silico* approach to identify potential miR-125a~99b~let-7e cluster and miR-146b targets. We combined miRanda [150] target predictions with pathways analysis based on the Ingenuity Pathway Analysis database (available at www.ingenuity.com). The intersection between biological pathways and the predicted targets of each miRNA of the cluster indicated a significant enrichment of genes associated to the biological functions *Inflammatory response*, *Immune cell trafficking*, *Cell-mediated immune response*, and *Cell signaling* for both miR-125a-5p and let-7e-5p, while miR-99b-5p was not related to any of these functions (Table 2). In particular, the predicted target genes of miR-125a-5p and let-7e-5p generated an "inflammatory network" including a set of nodes with internal connectivity centered on the TLR pathway higher than the connectivity observed with the rest of the network, which included receptors (TLR4, CD14), signaling molecules (IRAK1), and inflammatory mediators (TNFα, IL-6, CCL3, CCL7, CXCL8) (Fig. 10).

For miR-146b, the targets analysis showed a significant enrichment in "TLR signaling", "NF-kB signaling", and "IL-1β signaling" pathways (Fig. 11A). Among the predicted targets there were the receptors TLR4 and TLR2, the signal transducers MYD88, TRAF6 and IRAK1 and the only effector molecules IL6 (Fig. 11B). From these results, we hypothesized a role for miR-125a~99b~let-7e cluster and miR-146b in fine tuning the inflammatory response induced in monocytes by TLR/ IL-1R activation.

Table 2.

Top biological functions	miR	p-value	Number of molecules
Cell death and survival	miR-125a-5p	6.98×10^{-5}	167
	let-7e-5p	1.97×10^{-5}	505
	miR-99b-5p	4.57×10^{-3}	31
Inflammatory response	miR-125a-5p	9.49×10^{-5}	140
	let-7e-5p	7.98×10^{-3}	34
	miR-99b-5p	ns	-
Immune cell trafficking	miR-125a-5p	3.37×10^{-4}	149
	let-7e-5p	8.07×10^{-3}	40
	miR-99b-5p	ns	-
Cell-mediated immune response	miR-125a-5p	2.48×10^{-3}	54
	let-7e-5p	ns	-
	miR-99b-5p	ns	-
Cell signalling	miR-125a-5p	2.49×10^{-3}	62
	let-7e-5p	1.48×10^{-3}	109
	miR-99b-5p	ns	-
Amino acid metabolism	miR-125a-5p	ns	-
	let-7e-5p	1.06×10^{-2}	44
	miR-99b-5p	ns	-
Cellular growth and proliferation	miR-125a-5p	ns	-
	let-7e-5p	ns	-
	miR-99b-5p	4.57×10^{-3}	179
Molecular transport	miR-125a-5p	ns	-
	let-7e-5p	ns	-
	miR-99b-5p	6.16×10^{-3}	30
Nucleic acid metabolism	miR-125a-5p	ns	-
	let-7e-5p	ns	-
	miR-99b-5p	4.57×10^{-3}	12
Cell cycle	miR-125a-5p	ns	-
	let-7e-5p	ns	-
	miR-99b-5p	4.57×10^{-3}	10

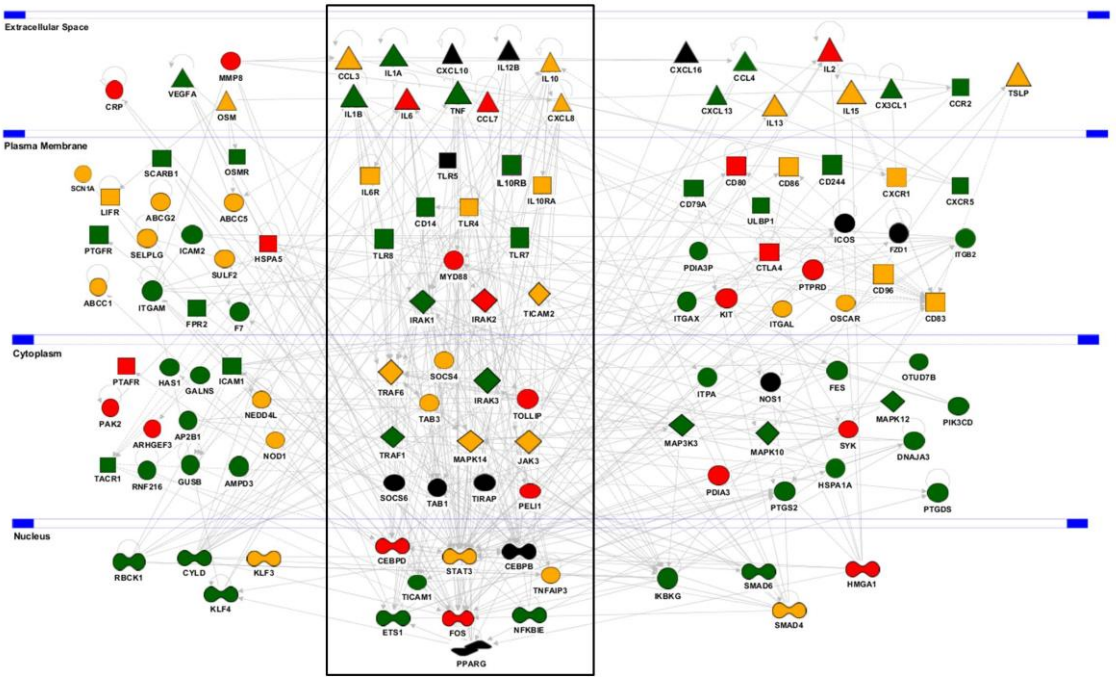

Figure 10: Predicted target genes of miR-125a-5p and let-7e-5p on the *Inflammatory response* molecular network. The *Inflammatory response* molecular network was extracted using the IPA analysis knowledge database and used to display functional relationships with predicted target genes of human miR-125a-5p (green), let-7e-5p (red), or both (yellow). Genes not predicted as targets are in black. The *Toll-Like Receptor pathway* (boxed) showed a significant enrichment of miR-125a~99b~let-7e cluster predicted target genes (*p* value = 1.42 x10^{-5}).

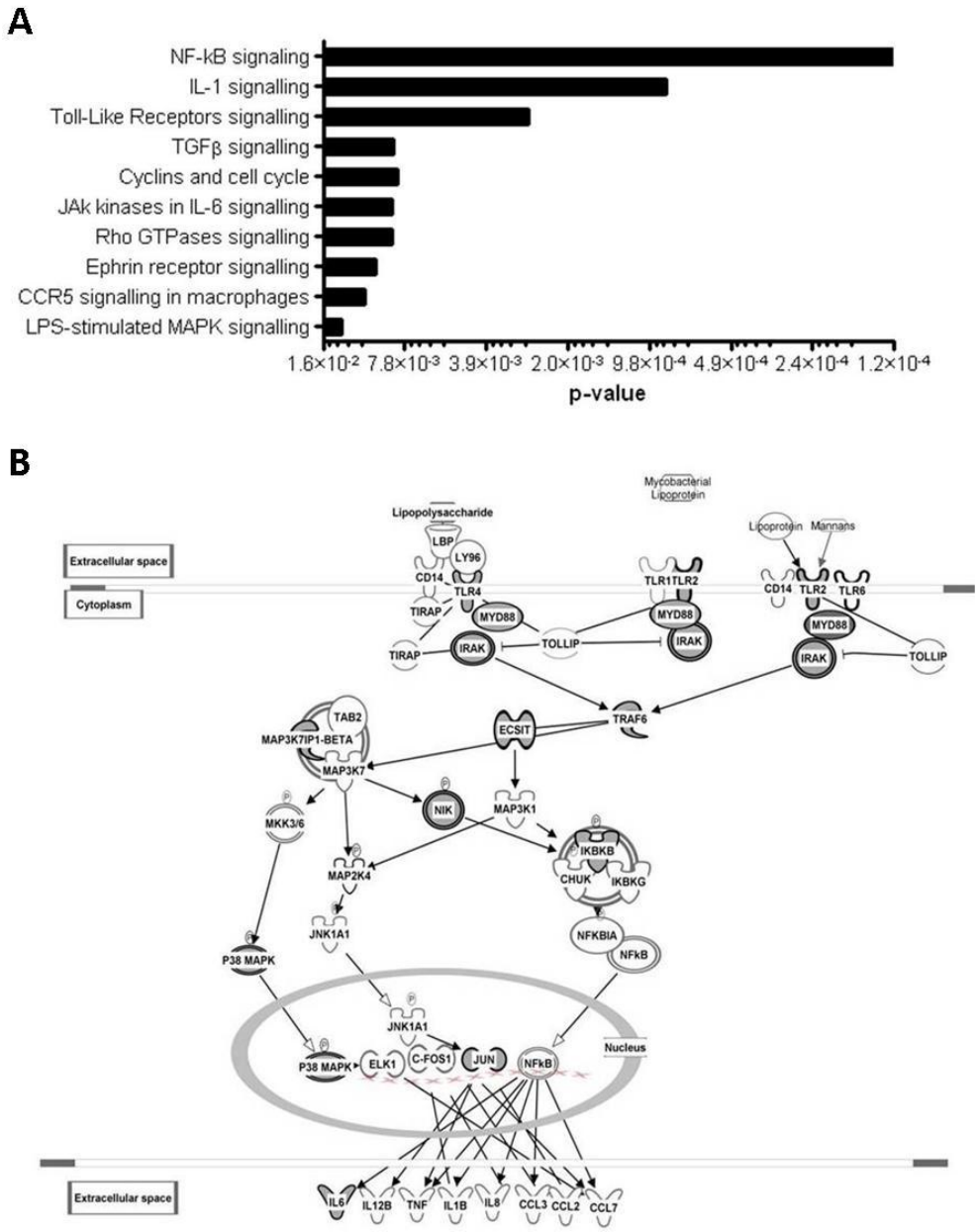

Figure 11 : miR-146b targets the TLR signaling pathway. (A) Canonical pathways significantly enriched for miR-146b predicted target genes as identified by the Ingenuity Pathways Analysis library [129]. (B) Predicted targets of miR-146b belonging to TLR signaling pathway

3.3.1 The targeting of the receptors: TLR4 is a direct target of miR-125a, let-7e and miR-146b

To validate bioinformatic predictions, we started to investigate the direct targeting at the receptors level of the TLR signaling pathway by miR-125a∼99b∼let-7e cluster and miR-146b.

We generated reporter constructs that contain the renilla luciferase gene fused to the 3′ UTRs mRNAs of putative miRNA cluster and miR-146b target genes. These reporter constructs were transiently transfected into 293T cells together with miRNA mimics, a chemically modified double-stranded RNAs that mimic endogenous miRNAs.

In 293T cells, over-expression of miR-125a-5p or let-7e-5p or miR-146b but not miR-99b-5p, significantly decreased the luciferase activity of the reporter construct containing the TLR4 3'UTR. 5 bp deletion in the miR-125a-5p or let-7e-5p or miR-146b miRNA-responsive element (MRE) fully restored luciferase levels, indicating miRNA specificity for their predicted target sites (Fig. 12A).

To confirm that TLR4 is a direct target of miR-125a-5p, let-7e and miR-146b, we generated miR/lentiviral-based expression vectors (pRRL-miR) over-expressing the individual miRNAs (pRRL-125a, pRRL-let7e and pRRL-miR146b) and we transduced them into the human monocytic cell line THP-1, a well-established model for *in vitro* studies of the TLR signaling [162]. We obtained a significant enrichment of the TRL4 transcript in the immunoprecipitated RISC of pRRL-125a, pRRL-let7e and pRRL-miR146b THP-1 cells, as compared to cells transduced with the control vector (pRRL-ct) (Fig. 12B).

In a complementary approach, cells transduced with lentiviral expression vectors expressing artificial mRNA targets to inhibit miR-125a-5p, let-7e-5p or miR-146b (miRT-125a-5p, miRT-let7e-5p and miRT-miR-146b, respectively) showed a significant decrease in the TLR4 transcript enrichment in the RISC after LPS stimulation as compared to cells transduced with the control vector (miRT-ct) (Fig. 12C).

Finally, when compared to control vector-transduced cells, TLR4 protein levels were significantly decreased in cells transduced with pRRL-125a, pRRL-let7e and pRRL-miR-146b and significantly increased in cells transduced with miRT-125a-5p, miRT-let7e-5p and miRT-miR-146b (Fig. 12D).

Taken together, these data validate the predicted direct targeting of TLR4 by miR-125a-5p, let7e-5p and miR-146b.

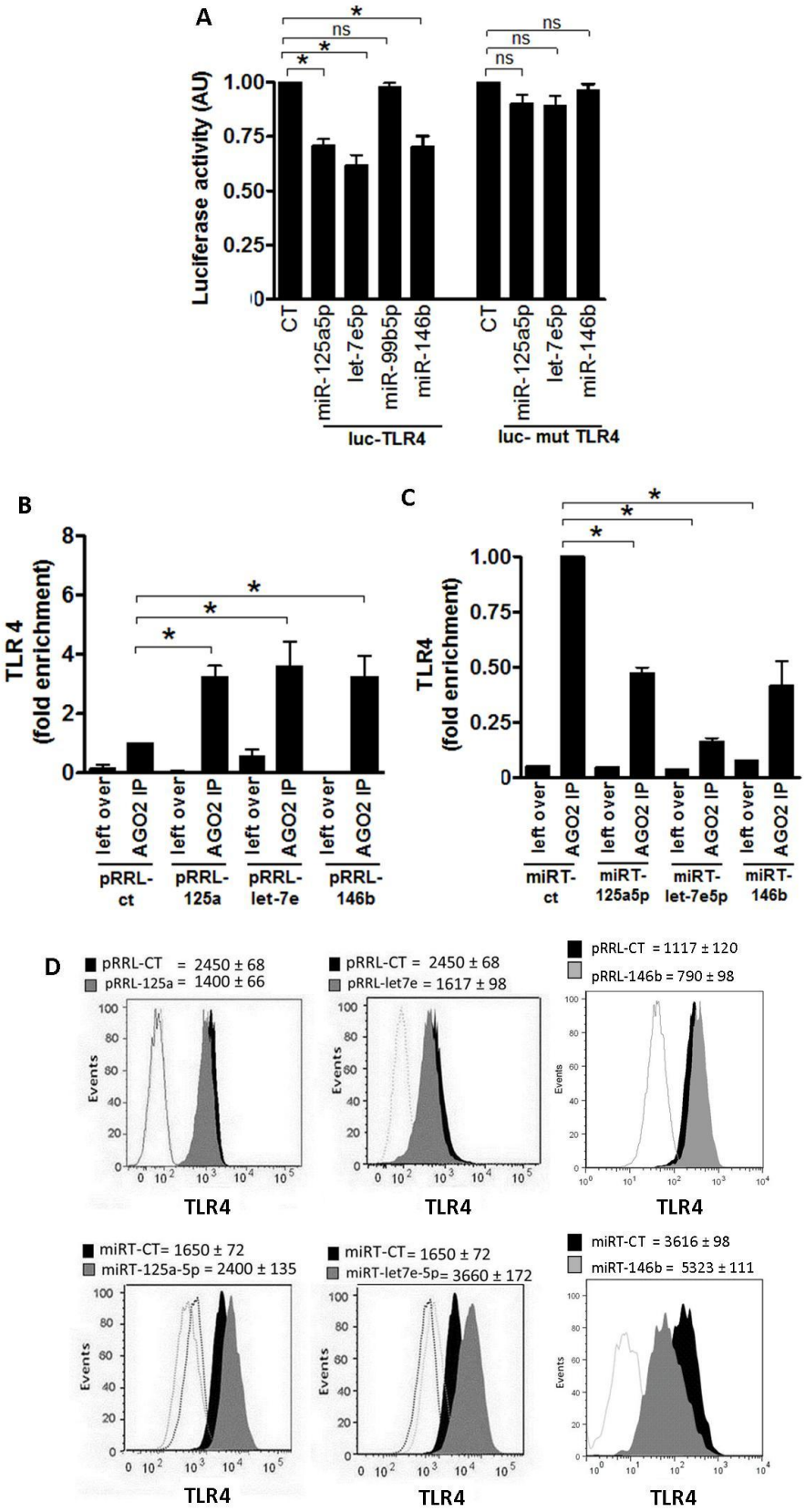
A
Luciferase activity (AU)
1.00
0.75
0.50
0.25
0
CT
miR-125a5p
let-7e5p
miR-99b5p
miR-146b
luc-TLR4
CT
miR-125a5p
let-7e5p
miR-146b
luc- mut TLR4
ns
B
TLR 4 (fold enrichment)
left over
AGO2 IP
pRRL-ct
pRRL-125a
pRRL-let-7e
pRRL-146b
C
TLR4 (fold enrichment)
miRT-ct
miRT-125a5p
miRT-let-7e5p
miRT-146b
D
pRRL-CT = 2450 ± 68
pRRL-125a = 1400 ± 66
pRRL-let7e = 1617 ± 98
pRRL-CT = 1117 ± 120
pRRL-146b = 790 ± 98
miRT-CT= 1650 ± 72
miRT-125a-5p = 2400 ± 135
miRT-let7e-5p= 3660 ± 172
miRT-CT = 3616 ± 98
miRT-146b = 5323 ± 111
Events
TLR4

Figure 12 : TLR4 is a direct target of miR-125a-5p, let-7e and miR-146b. (A) Luciferase assay was done in 293T cells cotransfecting TLR4 3'UTR (normal or mutated) with miR-125a-5p or let-7e-5p or miR-99b-5p or miR-146b mimic or a negative control (CT). Results are expressed as mean (% variation ± SEM; n = 3) of the ratio between *renilla* luciferase and *firefly* control luciferase activities. Cell extracts from THP-1 cells transduced with pRRL-125a or pRRL-let-7e or pRRL-146b and the control vector pRRL-ct (B) or with miRT-125a-5p or miRT-let-7e-5p or miRT-146b and the control vector miRT-ct (C) were subjected to RIP assay using anti-Ago2 or IgG control Abs. Levels of TLR4 transcript was assayed in triplicate by qPCR and expressed as normalized fold enrichment. TLR4 protein level was measured by flow cytometry in pRRL-125A or pRRL-let-7e or pRRL-146b THP-1 cells (D, upper panels, grey histograms) or miRT-125a-5p or miRT-let-7e-5p (D, lower panels, grey histograms) or their corresponding control vectors (CT; black histograms). Isotype control staining are shown in dotted histograms. Results from one representative experiment are shown. Mean Fluorescence Intensity values (± SEM) from 5 independent experiments are reported.

3.3.2 The targeting of the receptors: TLR2 is not a direct target of miR-146b

Among the predicted targets of miR-146b, that are components of the TLR pathway, we also identified TLR2. Despite it is a predicted target of miR-146b, miR-146b over-expression did not induce any impairment of the luciferase activity (Fig. 13A) , did not cause any enrichment of TLR2 mRNA in the RISC complex (Fig. 13B) and did not reduce TLR2 protein expression (Fig. 13D). In complementary experiments, THP-1 cells transduced with miRT-146b and stimulated with LPS did not show any increase of the TLR2 transcript in the RISC complex (Fig. 13C) nor a decrease in TLR2 protein expression as compared to miRT-ct THP-1 cells (Fig. 13E). Taken together, these results indicate that, contrary to predictions, TLR2 is not a direct target of miR-146b.

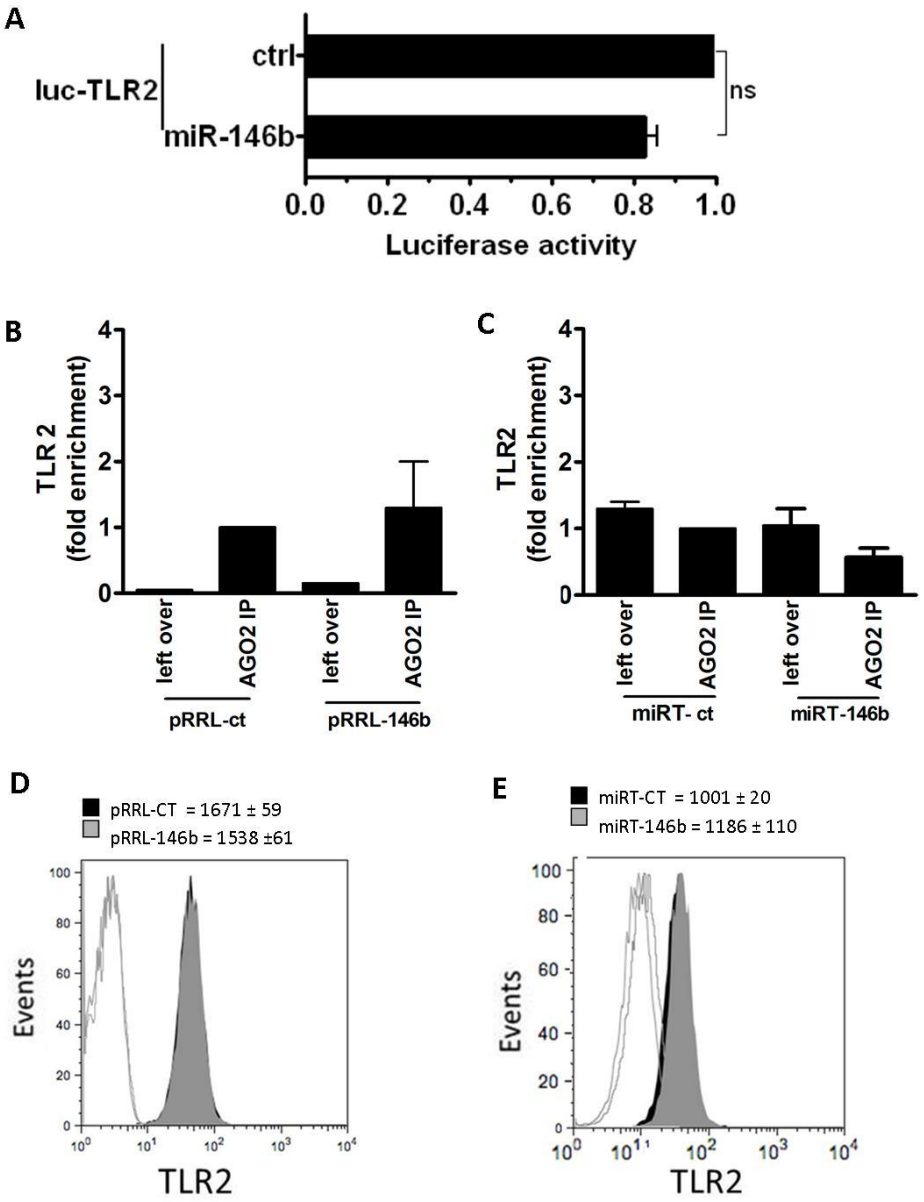

Figure 13: TLR2 is not a direct target of miR-146b. Luciferase constructs based on the 3'UTR of TLR2 was cotransfected in 293T cells with miR-146b mimic or a negative control (CT). Results are expressed as mean (% variation ± SEM; n = 3) of the ratio between *renilla* luciferase and *firefly* control luciferase activities. Cell extracts from THP-1 cells transduced with pRRL-146b and the control vector pRRL-ct (B) or with miRT-146b and the control vector miRT-ct (C) were subjected to RIP assay using anti-Ago2 or IgG control Abs. Levels of TLR2 transcript was assayed in triplicate by qPCR and expressed as normalized fold enrichment. TLR2 protein level was measured by flow cytometry in cells transduced with pRRL-146b or miRT-146b vectors (D and E, grey histograms) or their corresponding control vectors (CT; black histograms). Isotype control staining are shown in dotted histograms. Results from one representative experiment are shown. Mean Fluorescence Intensity values (± SEM) from 5 independent experiments are reported.

3.3.3 The targeting of the receptors: CD14 is a direct target of miR-125a-5p

Another important member for the TLR signaling is CD14, a co-receptor of TLR4 for the detection of bacterial LPS [163]. CD14 is predicted to be a direct target of miR-125a-5p by the bioinformatic analysis. Indeed we obtained a reduction in luciferase activity only in 293T cells transfected with CD14 3'UTR reporter construct together with miR-125a-5p mimic and not with let-7e and miR-99b-5p mimic. This targeting is specific because the mutation of miR-125a-5p MRE abrogated the downregulation of the luciferase activity (Fig. 14A). As expected we obtained an enrichment of CD14 mRNA in the RISC complex only in pRRL- 125a THP1 cells (Fig. 14B), whereas the inhibition of miR-125a-5p, in miRT- 125a-5p THP1 cells, caused a decrease of CD14 mRNA content in the Ago2-immunoprecipitated fraction (Fig. 14C). At the protein level, only the over-expression or the inhibition of miR-125a-5p modulated the CD14 expression on cell surface, in comparison of let-7e (Fig. 14D and E) . We can conclude that CD14 is a specific and direct target of miR-125a-5p.

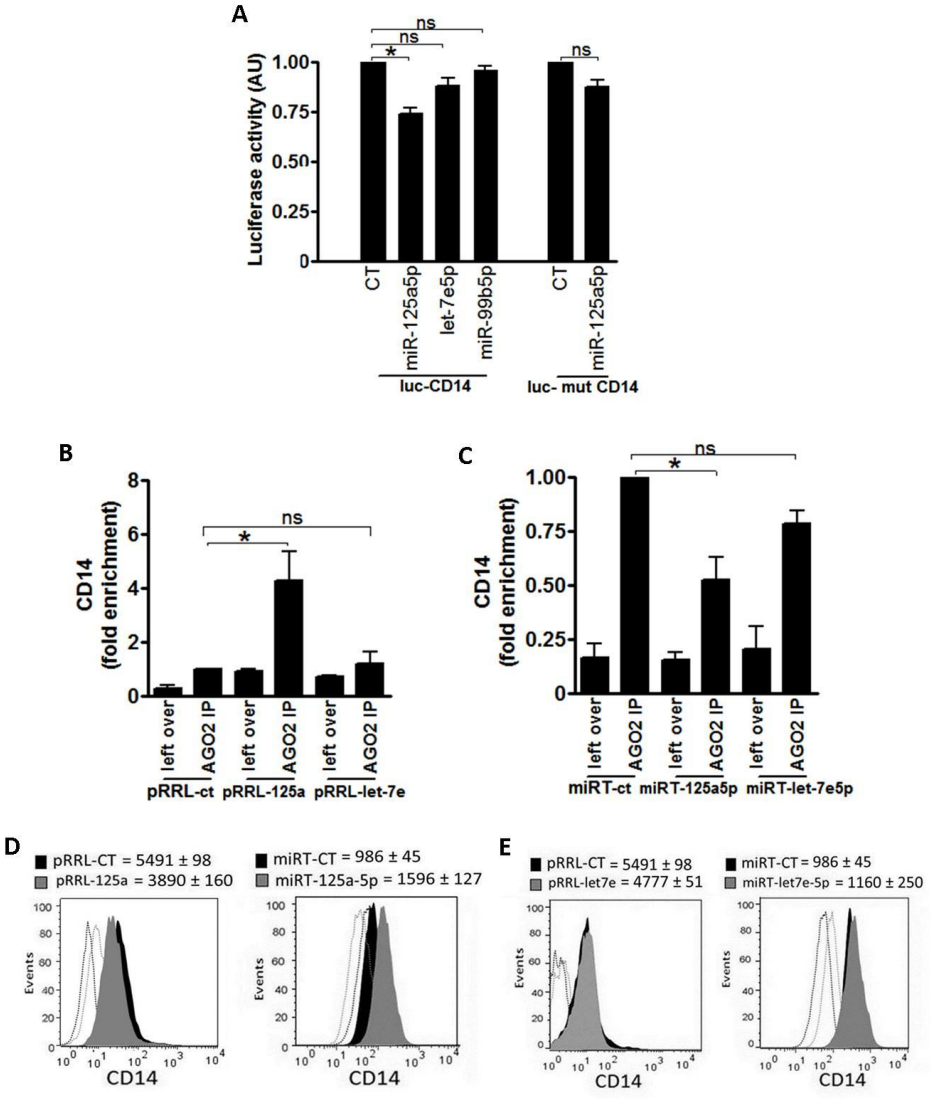

Figure 14: CD14 is a direct target of miR-125a-5p. (A) Luciferase assay was done in 293T cells cotransfecting CD14 3'UTR (normal or mutated) with miR-125a-5p or let-7e-5p or miR-99b-5p mimic or a negative control (CT). Results are expressed as mean (% variation ± SEM; n = 3) of the ratio between *renilla* luciferase and *firefly* control luciferase activities. Cell extracts from THP-1 cells transduced with pRRL-125a or pRRL-let-7e and the control vector pRRL-ct (B) or with miRT-125a-5p or miRT-let-7e-5p and the control vector miRT-ct (C) were subjected to RIP assay using anti-Ago2 or IgG control Abs. Levels of CD14 transcript was assayed in triplicate by qPCR and expressed as normalized fold enrichment. CD14 protein level was measured by flow cytometry in pRRL-125A or pRR-let-7e THP-1 cells (D and E, grey histograms, left graphs) or miRT-125a-5p or miRT-let-7e-5p (D and E, grey histograms, right graphs) or their corresponding control vectors (CT; black histograms). Isotype control staining are shown in dotted histograms. Results from one representative experiment are shown. Mean Fluorescence Intensity values (± SEM) from 5 independent experiments are reported.

3.3.4 The targeting of the adaptors: IRAK-1, MyD88 and TRAF6

According to the bioinformatics prediction, together with the receptors, also other component of TLR signaling pathway are putative targets of these miRNAs. Therefore, we investigated the miRNAs role in regulating the signaling adaptors involved in this pathway. Luciferase assays validated IRAK-1 as direct target of miR-125a-5p and miR-146b (Fig. 15A), MyD88 as direct target of let-7e-5p and miR-146b (Fig. 16A), and TRAF6 (Fig. 17A) as direct target of miR-146b. In all cases, abrogation of miR-125a-5p, let-7e and miR-146b effects by mutagenesis of their seed match regions in targets 3'UTR demonstrated the specificity of their action. Consistent with this, RIP analysis revealed a significant enrichment of IRAK-1 (Fig. 15B), MyD88 (Fig. 16B), and TRAF6 (Fig. 17B) transcripts in the corresponding pRRL-125a, pRRL-let-7e, pRRL-146b transduced THP-1 cells and a reduction in THP-1 cells transduced with miRT-125a, miRT-let-7e and miRT-146b compared to miRT-ct (Fig. 15C, 16C, and 17C). Western blot analysis confirmed that protein levels of IRAK-1 are reduced when miR-125a or miR-146b are over-expressed (Fig. 15D and E, left panels); instead the inhibition of miR-125a-5p (Fig. 15D, right panel) or miR-146b (Fig. 15E, right panel) increased its expression. Western blot of Myd88 confirmed its targeting by let-7e and miR-146b (Fig. 16D and E), whereas TRAF6 protein level is modulated by miR-146b (Fig. 17D and E).

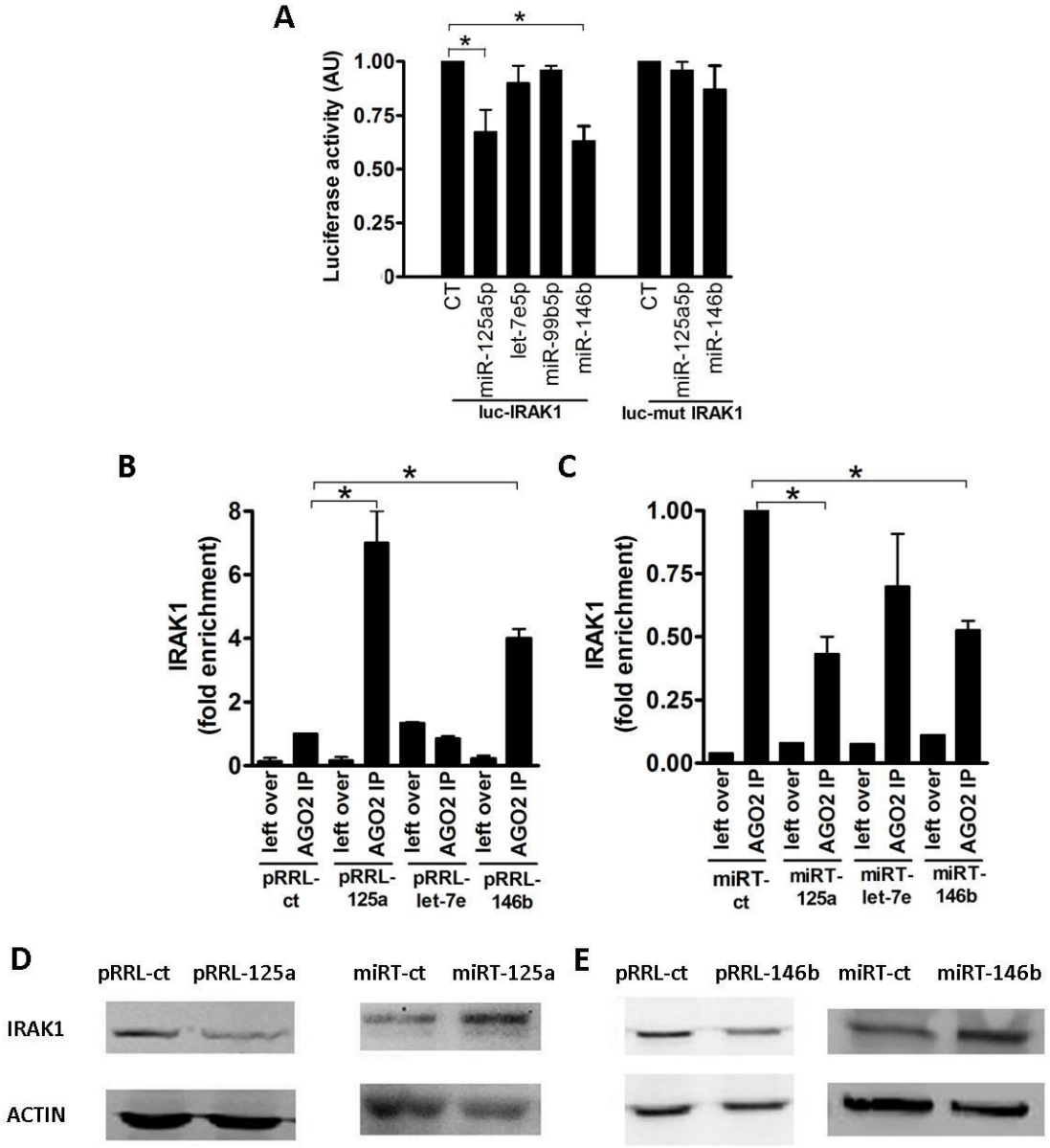

Figure 15: IRAK1 is a direct target of miR-125a-5p and miR-146b. (A) Luciferase assay was done in 293T cells cotransfecting IRAK1 3'UTR (normal or mutated) with miR-125a-5p or let-7e-5p or miR-99b-5p or miR.146b mimic or a negative control (CT). Results are expressed as mean (% variation ± SEM; n = 3) of the ratio between *renilla* luciferase and *firefly* control luciferase activities. Cell extracts from THP-1 cells transduced with pRRL-125a or pRRL-let-7e or pRRL-146b and the control vector pRRL-ct (B) or with miRT-125a-5p or miRT-let-7e-5p or miRT-146b and the control vector miRT-ct (C) were subjected to RIP assay using anti-Ago2 or IgG control Abs. Levels of IRAK1 transcript was assayed in triplicate by qPCR and expressed as normalized fold enrichment. Protein levels of IRAK1(D and E) were evaluated on immunoblots using specific Ab followed by incubation with goat anti-rabbit Ab. Normalization was performed on actin levels (D and E, lower panels) evaluated on the same blot. Results from one representative experiment of 3 performed are shown.

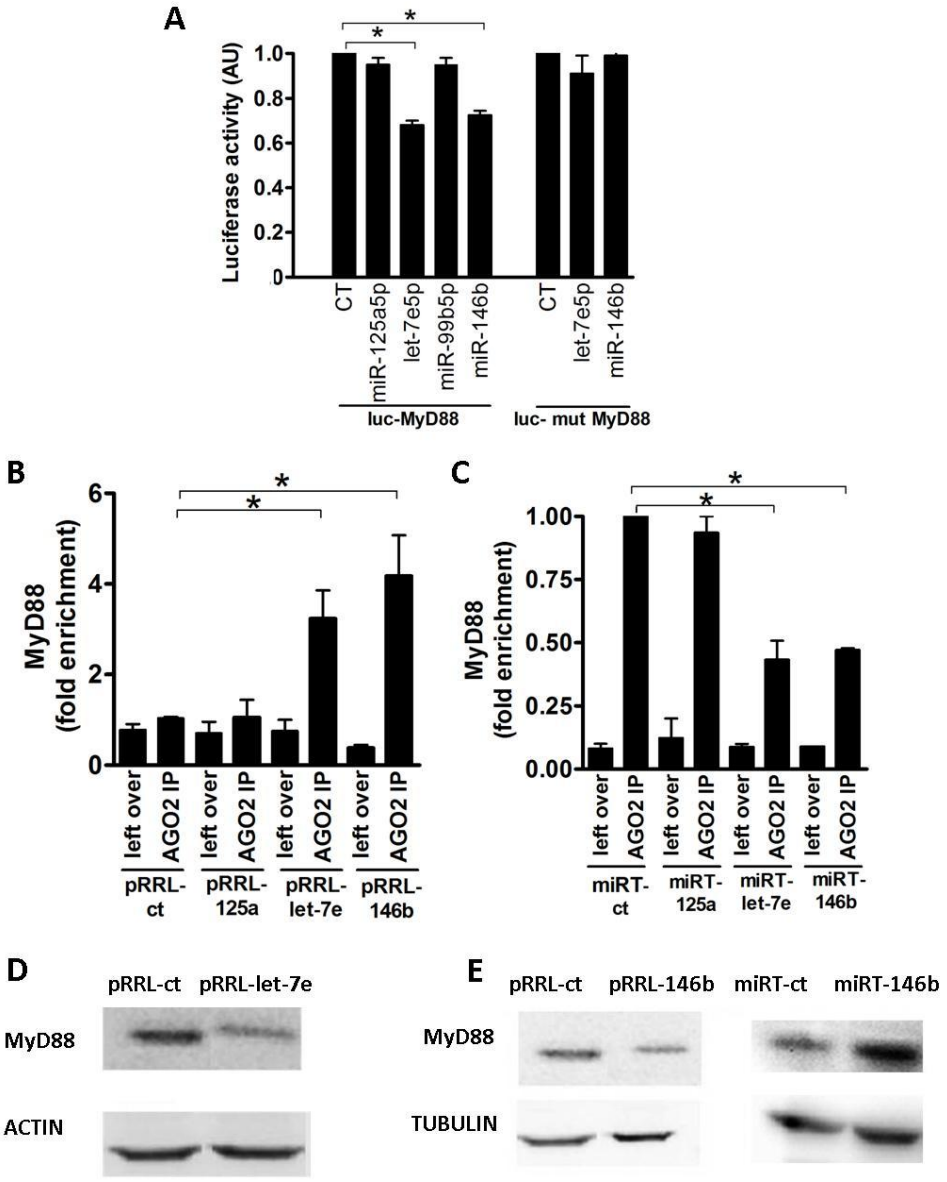

Figure 16: MyD88 is a direct target of let-7e-5p and miR-146b. (A) Luciferase assay was done in 293T cells cotransfecting MyD88 3'UTR (normal or mutated) with miR-125a-5p or let-7e-5p or miR-99b-5p or miR.146b mimic or a negative control (CT). Results are expressed as mean (% variation ± SEM; n = 3) of the ratio between *renilla* luciferase and *firefly* control luciferase activities. Cell extracts from THP-1 cells transduced with pRRL-125a or pRRL-let-7e or pRRL-146b and the control vector pRRL-ct (B) or with miRT-125a-5p or miRT-let-7e-5p or miRT-146b and the control vector miRT-ct (C) were subjected to RIP assay using anti-Ago2 or IgG control Abs. MyD88 transcript was quantified in triplicate by qPCR and expressed as normalized fold enrichment. Protein levels of MyD88 (D and E) were evaluated by Western Blot using anti-Myd88 Ab. Normalization was performed on actin or tubulin expression (D and E, lower panels) evaluated on the same blot. Results are representative of 3 independent experiments.

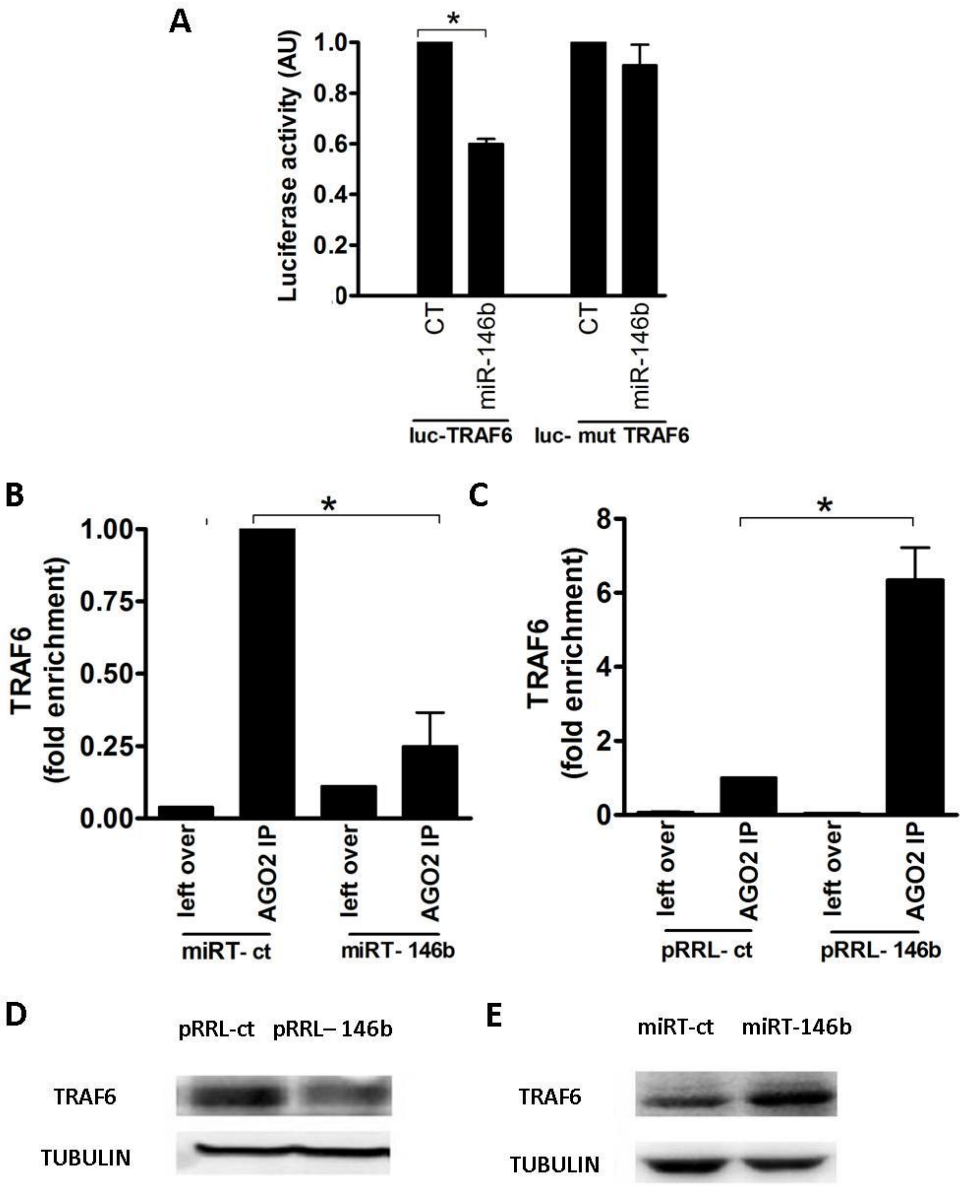

Figure 17: TRAF6 is a direct target of miR-146b. (A) Luciferase assay was done in 293T cells cotransfecting TRAF6 3'UTR (normal or mutated) with miR.146b mimic or a negative control (CT). Results are expressed as mean (% variation ± SEM; n = 3) of the ratio between *renilla* luciferase and *firefly* control luciferase activities. Cell extracts from THP-1 cells transduced with pRRL-146b and the control vector pRRL-ct (B) or with miRT-146b and the control vector miRT-ct (C) were subjected to RIP assay using anti-Ago2 or IgG control Abs. TRAF6 transcript was quantified in triplicate by qPCR and expressed as normalized fold enrichment. Protein levels of TRAF6 (D and E) were evaluated by Western Blot using anti-TRAF6 Ab. Normalization was performed on tubulin expression (D and E, lower panels) evaluated on the same blot. Results are representative of 3 independent experiments.

3.3.5 Direct targeting of pro-inflammatory cytokines by miR-125a, let-7e and miR-146b

Bioinformatic analysis also predicted a significant number of LPS-dependent pro-inflammatory cytokines as potential targets of miR-125a-5p or let-7e-5p (Fig. 10). Luciferase assays confirmed that miR-125a-5p negatively regulates TNFα, and mutations at the corresponding MRE abolished miR125a-5p-mediated suppression (Fig. 18A). Consistent with this, RIP analysis revealed a significant enrichment of the TNFα transcript in miR-125a transduced THP-1 cells (Fig. 18B) and a parallel decrease of their loading in the RISC when miR-125a-5p was inhibited (Fig. 18C). Similar approaches confirmed targeting by let-7e-5p of IL-6 and CCL7 (Fig. 18D to F and Fig. 18G to I, respectively), while CCL3 and CXCL8 were shown to be targeted by both miR-125a-5p and let-7e-5p (Fig. 18J to L and Fig. 18M to O, respectively). Conversely, though IL-6 was also predicted as a direct target of miR-146b, luciferase assay on the IL-6 3'UTR and RIP assay did not confirm this prediction (Fig. 19).

Over-expression of miR-125a-5p and let-7e-5p caused a significant reduction of most but not all their direct target transcripts, suggesting that, depending on the specific target, either mRNA destabilization or transduction inhibition could be involved in their inhibitory effect (Fig. 20A). For miR-146b, its targeting affects stability of MyD88 and TRAF6 but not IRAK1 transcript; instead the over-expression of miR-146a destabilizes IRAK1 and TRAF6 and not MyD88 mRNA (Fig. 20B). Even if the two miR-146 isoforms share most of all the targets, they can adopt different mechanism to regulate the same pathway.

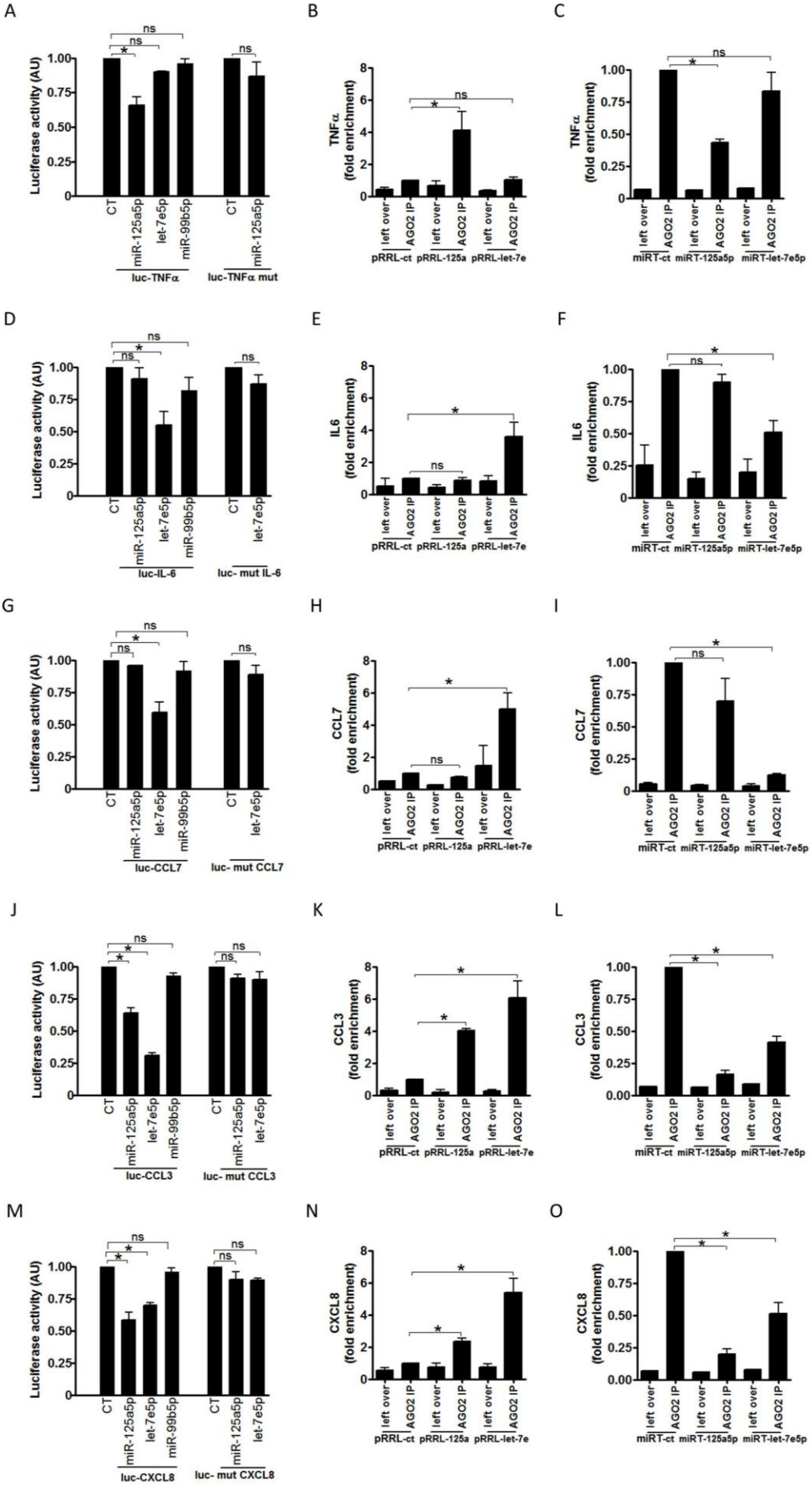
A
B
C
D
E
F
G
H
I
J
K
L
M
N
O
Luciferase activity (AU)
TNFα (fold enrichment)
IL6 (fold enrichment)
CCL7 (fold enrichment)
CCL3 (fold enrichment)
CXCL8 (fold enrichment)
ns
*
CT
miR-125a5p
let-7e5p
miR-99b5p
luc-TNFα
luc-TNFα mut
luc-IL-6
luc- mut IL-6
luc-CCL7
luc- mut CCL7
luc-CCL3
luc- mut CCL3
luc-CXCL8
luc- mut CXCL8
left over
AGO2 IP
pRRL-ct
pRRL-125a
pRRL-let-7e
miRT-ct
miRT-125a5p
miRT-let-7e5p

Figure 18: Direct targeting of pro-inflammatory cytokines by miR-125a-5p and let-7e-5p. Luciferase constructs with the 3'UTR of TNFα (A), IL-6 (D), CCL7 (G), CCL3 (J), and CXCL8 (M) were cotransfected in 293T cells with miR-125a-5p, let-7e-5p, miR-99b-5p mimics or with a negative control mimic (CT). Results are expressed as mean (% variation ± SEM; n = 3) of the ratio between *renilla* luciferase and *firefly* control luciferase activities. Cell extracts from THP-1 cells transduced with pRRL-125a, pRRL-let-7e, and the control vector pRRL-ct (panels B, E, H, K, N) or with miRT-125a-5p, miRT-let-7e-5p, and the control vector miRT-ct (panels C, F, I, L, O) were subjected to RIP assay using anti-Ago2 or IgG Abs and levels of TNFα (panels B and C), IL-6 (panels E and F), CCL7 (panels H and I), CCL3 (panels K and L), and CXCL8 (panels N and O) mRNAs were assayed in triplicate by Q-PCR and expressed as normalized fold enrichment.

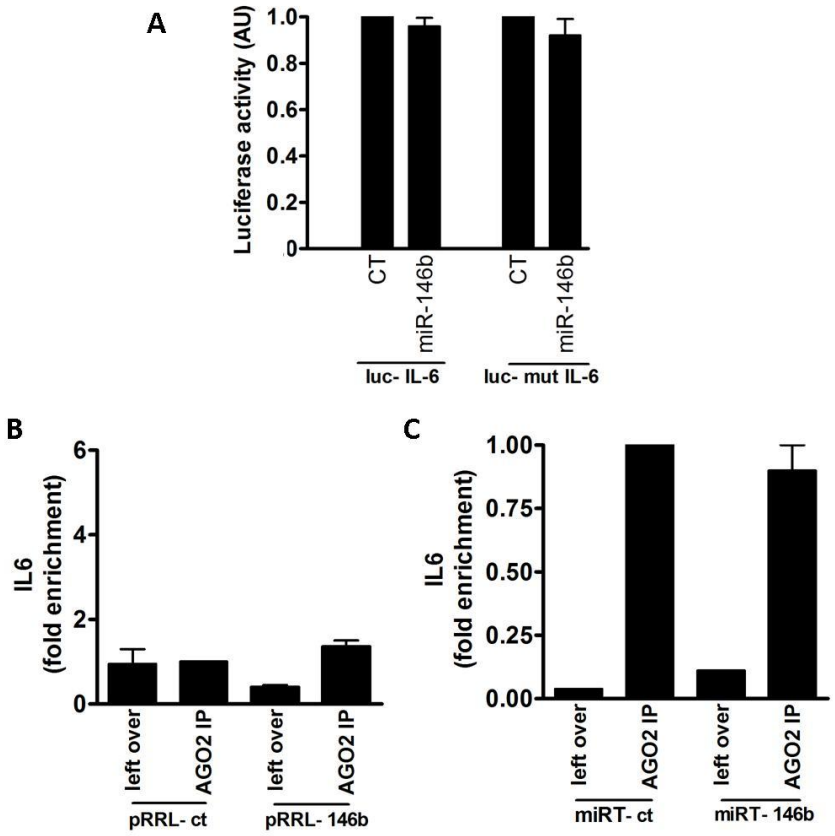

Figure 19: IL-6 is not a direct target of miR-146b. Luciferase construct with the 3'UTR of IL-6(A) (normal or mutated) was cotransfected in 293T cells with miR-146b mimic or with a negative control mimic (CT). Results are expressed as mean (% variation ± SEM; n = 3) of the ratio between *renilla* luciferase and *firefly* control luciferase activities. Cell extracts from THP-1 cells transduced with pRRL-146b and the control vector pRRL-ct (B) or with miRT-146b and the control vector miRT-ct (C) were subjected to RIP assay using anti-Ago2 or anti-IgG. Abs and levels of IL-6 mRNA were assayed in triplicate by qPCR and expressed as normalized fold enrichment.

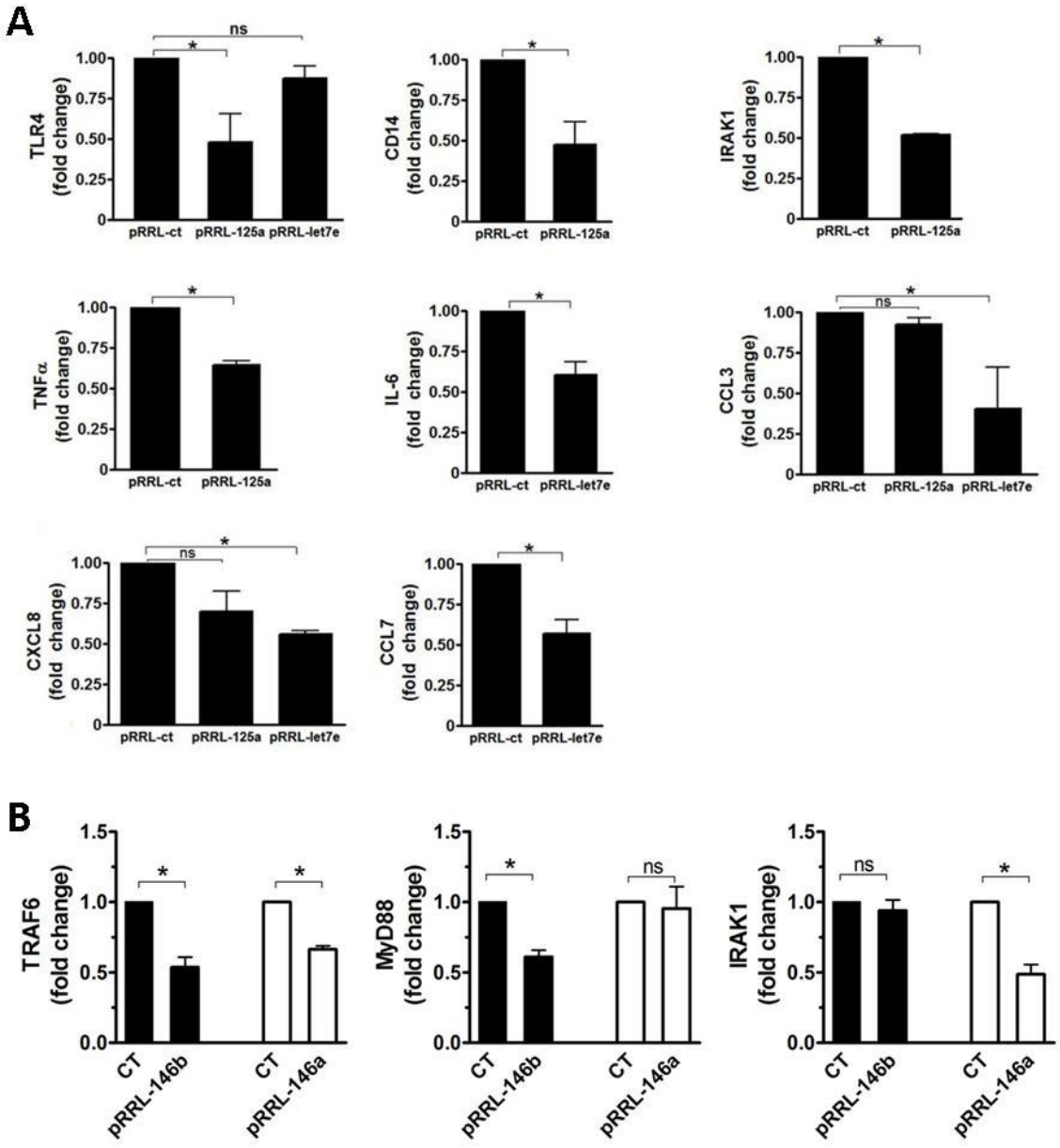

Figure 20: Effect of miR-125a-5p, let-7e-5p and miR-146b on transcripts of their direct target genes. (A) Levels of transcripts encoding TLR4, CD14, IRAK1, TNFα, IL-6, CCL3, CXCL8 and CCL7 were measured by Q-PCR in pRRL-ct, pRRL-125a, and pRRL-let7e THP-1 cells stimulated for 4 h with 100ng/mL LPS and normalized to GAPDH. (B) Levels of transcripts encoding TRAF6, MyD88, and IRAK1 were measured by qPCR in pRRL-ct, pRRL-146b and pRRL-146a THP-1 cells stimulated for 4 h with 100ng/mL LPS and normalized to GAPDH. Results are shown as fold change over non stimulated control (mean ± SEM; n = 3).

3.4 MiR-125a-5p, let-7e-5p and miR-146b regulate LPS-dependent production of inflammatory cytokines

As we demonstrated a direct targeting of multiple components involved in the TLR4 signaling pathway by cluster miR-125a~99b~let-7e and by miR-146b, we investigated their biological impact on TLR4 activity evaluating the production of inflammatory cytokines after LPS exposure. As compared to pRRL-ct THP-1 cells, pRRL-125a (Fig. 21A to G, left panels), pRRL-let7e (Fig. 22A to G, left panels) and pRRL-146b (Fig. 23A to G, left panels) THP-1 cells showed a significant reduction of LPS-dependent production of several inflammatory cytokines, including IL-6, TNFα, CXCL8, CCL2, CCL3, CCL7 and IL-12p40. Conversely, a significant increase of these pro-inflammatory cytokines was observed when miR-125a-5p (Fig. 21A to G, right panels) or let-7e-5p (Fig. 22A to G, right panels) or miR-146b (Fig. 23A to G, right panels) were inhibited using corresponding miRT vectors. Of note, miR-125a-5p and let-7e-5p showed a significant effect on both cytokines identified as direct targets (TNFα, IL-6, CCL3, CCL7, CXCL8; see Fig.18) as well as others known to be not direct targets (IL-12p40, CCL2), indicating a global effect of these miRNAs on the TLR4 signaling pathway.

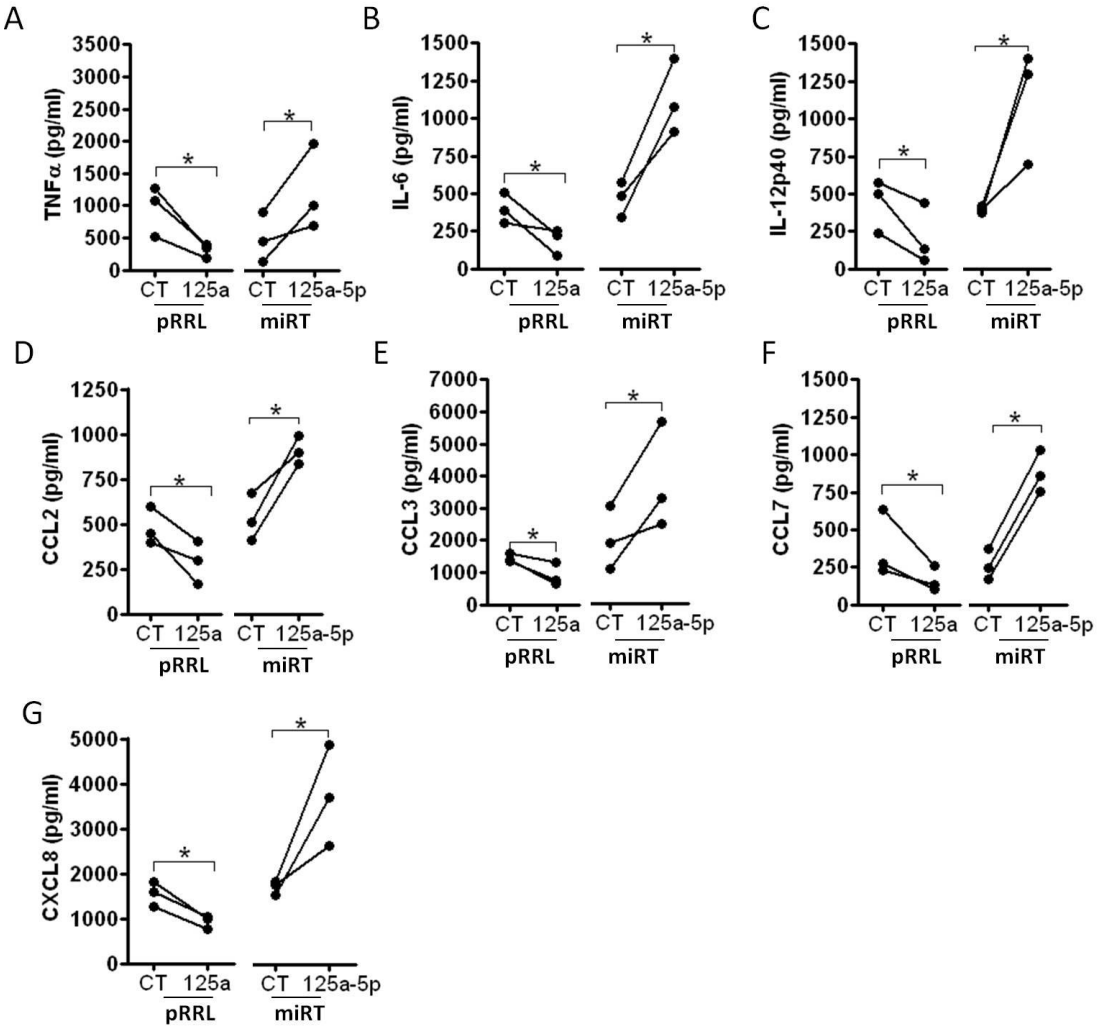

Figure 21: MiR-125a-5p down-regulates the production of pro-inflammatory cytokines. Levels of pro-inflammatory cytokines measured by ELISA in cell-free supernatants of THP-1 cells transduced with pRRL-ct and pRRL-125a or with miRT-ct and miRT-125a-5p after stimulation with 1 µg/mL LPS for 8 h for TNFα (A), CCL3 (E), and CXCL8 (G), or 24 h for IL-6 (B), IL-12p40 (C), CCL7 (F), CCL2 (D). Results of three independent experiments are shown.

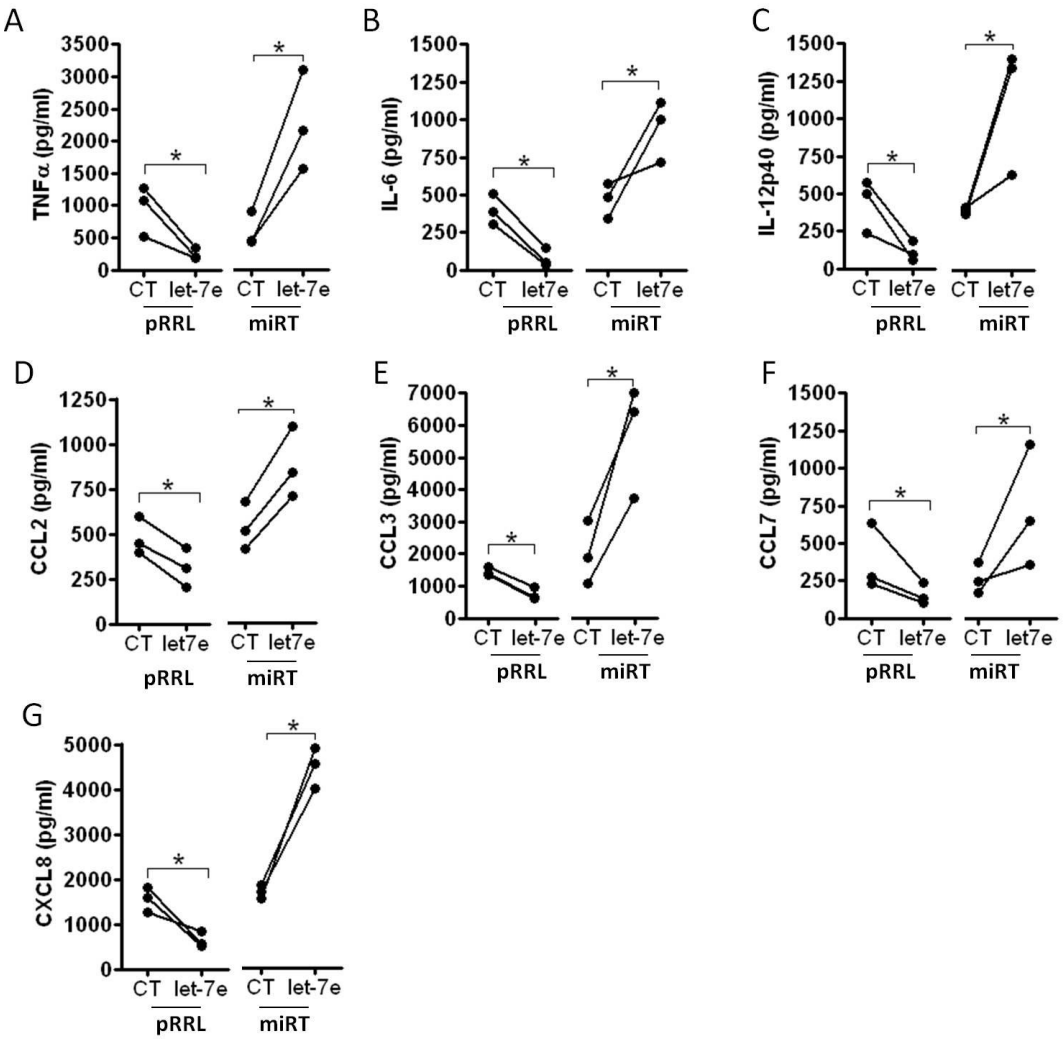

Figure 22: let-7e-5p down-regulates the production of pro-inflammatory cytokines. Levels of pro-inflammatory cytokines measured by ELISA in cell-free supernatants of THP-1 cells transduced with pRRL-ct and pRRL-let-7e or with miRT-ct and miRT-let-7e after stimulation with 1 µg/mL LPS for 8 h for TNFα (A), CCL3 (E), and CXCL8 (G), or 24 h for IL-6 (B), IL-12p40 (C), CCL7 (F), CCL2 (D). Results of three independent experiments are shown.

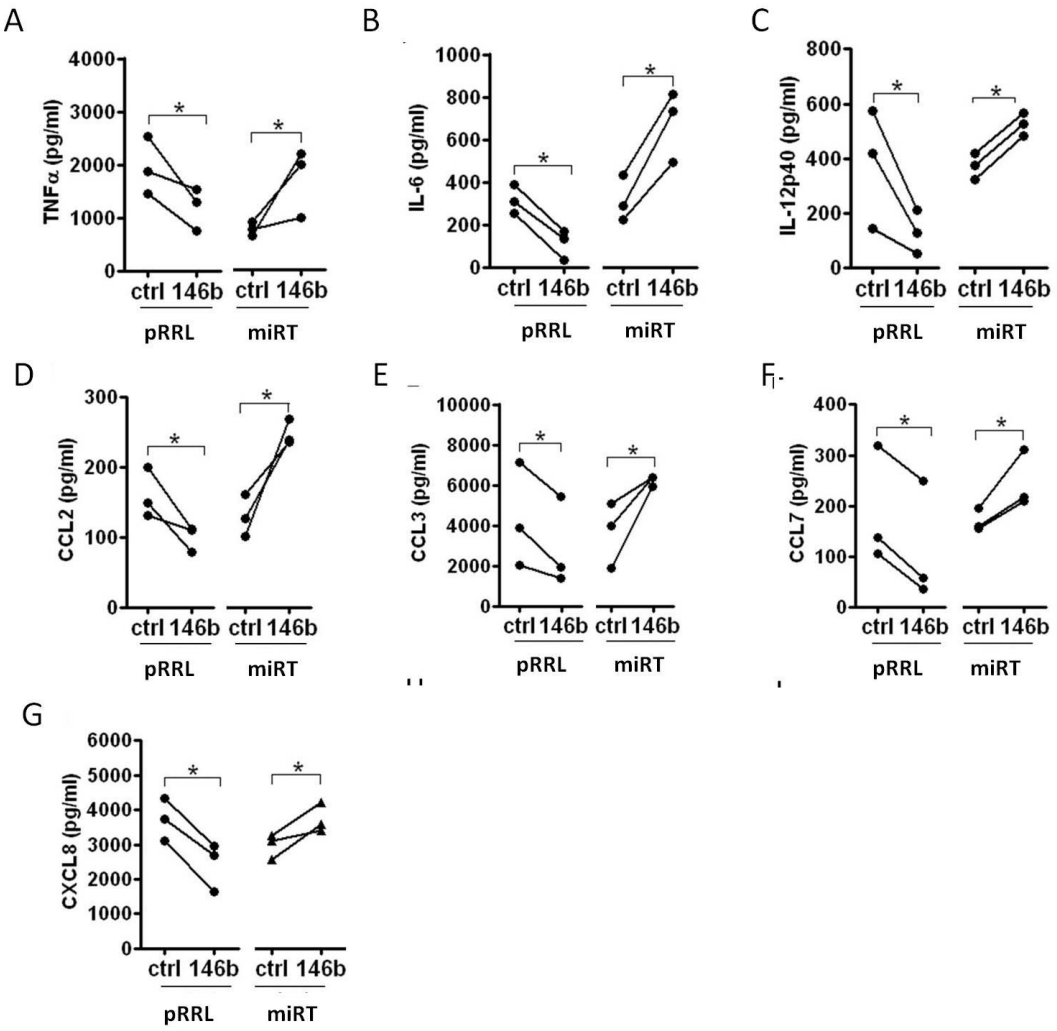

Figure 23: miR-146b down-regulates the production of pro-inflammatory cytokines. Levels of pro-inflammatory cytokines measured by ELISA in cell-free supernatants of THP-1 cells transduced with pRRL-ct and pRRL-146b or with miRT-ct and miRT-146b after stimulation with 1 µg/mL LPS for 8 h for TNFα (A), CCL3 (E), and CXCL8 (G), or 24 h for IL-6 (B), IL-12p40 (C), CCL7 (F), CCL2 (D). Results of three independent experiments are shown.

3.4.1 miR-125a-5p, let-7e-5p and miR-146b target specifically TLR4 signaling pathway

To confirm the specific targeting of TLR4 signaling pathway, we measured the effect of cluster miR-125a~99b~let-7e and miR-146b on the production of the IFN-inducible gene CXCL10. CXCL10 can be induced by LPS, mainly as a secondary effect of TRIF-dependent IFNβ production, or by IFNγ, which operates through the activation of a MyD88/IRAK-1-independent STAT1-dependent pathway [164]. The expression level of CXCL10 were significantly inhibited in pRRL-125a, pRRL-let-7e and pRRL-146b THP-1 cells (Fig. 24A to C, left panels) and increased in miRT-125a-5p, miRT-let-7e-5p and miRT-146b THP-1 cells after stimulation with LPS (Fig. 24A to C, right panels). While no expression change was observed when CXCL10 was induced by IFNγ in THP1 cells that over-express or inhibit the miRNAs (Fig. 24D to F), confirming that the effects of the miRNAs were mediated by their specific targeting of the TLR4 signaling pathway.

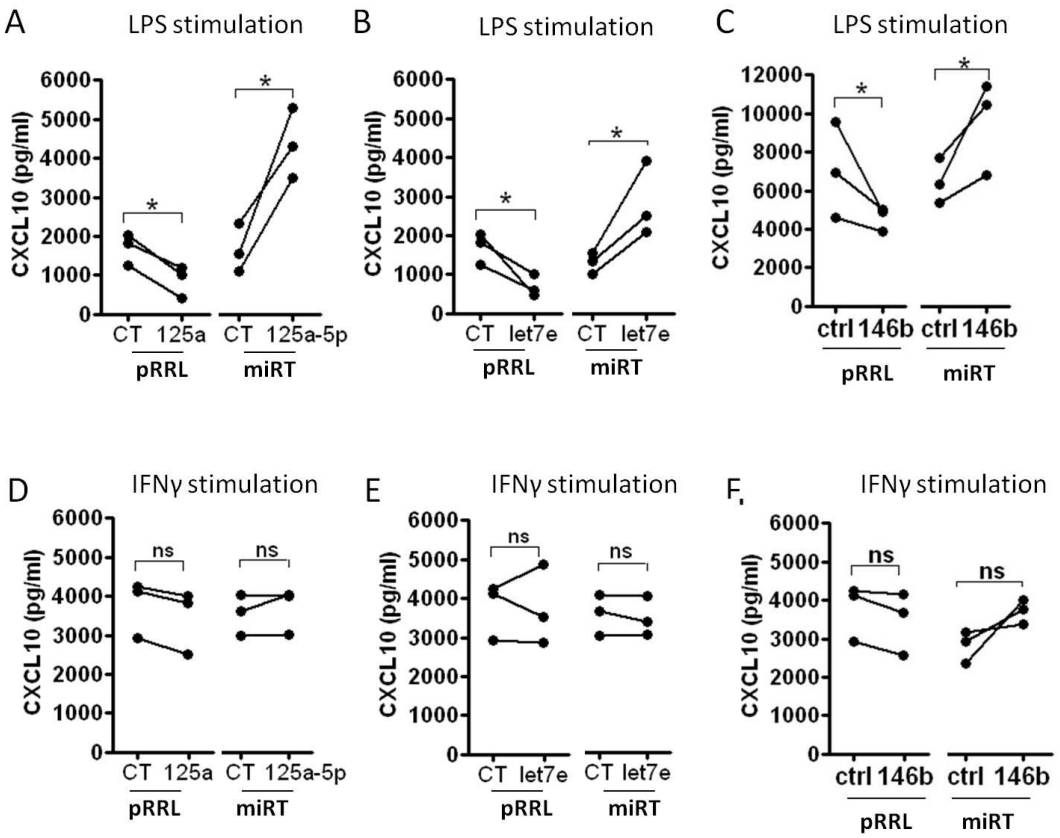

Figure 24: miR-125a-5p, let-7e-5p and miR-146b targeting are TLR4-dependent. (A to C) Levels of CXCL10 cytokine measured by ELISA in cell-free supernatants of THP-1 cells transduced with pRRL-ct, pRRL-125a, pRRL-let-7e and pRRL-146b or with miRT-ct, miRT-125a-5p, miRT-let-7e and miRT-146b after stimulation with 1 µg/mL LPS 24h. (D to F) Levels of CXCL10 cytokine measured by ELISA in cell-free supernatants of transduced THP-1 cells stimulated with 10 ng/ml of IFNγ for 24h. Results of three independent experiments are shown.

3.5 The miR-125a-5p and miR-146b mediates LPS tolerance

3.5.1 miR-125a-5p, miR-99b-5p and miR-146b are induced in endotoxin tolerized human monocytes

As we demonstrated that miR-125a-5p, let-7e-5p and miR-146b represent effective negative regulators of TLR signaling, we asked whether they were involved in the induction of LPS tolerance, the phenomenon of reduced sensitivity to subsequent challenge of LPS. Human monocytes were primed with different doses of LPS for 18 hours followed by wash with PBS and challenged with a second dose of LPS. After 24 hours of incubation with challenged LPS, we measured TNFα and miRNAs expression. TNFα is considered the most reliable marker of endotoxin tolerance because it is downregulated in all tolerized samples compared to untolerized control, as we shown here and as expected from previous studies (Fig. 25 and [165]). Given that during our life we are usually exposed to different doses of LPS and since it is also known that low doses of priming LPS can induced endotoxin tolerance [166], we wanted to recapitulate that in vitro, by using different priming conditions.

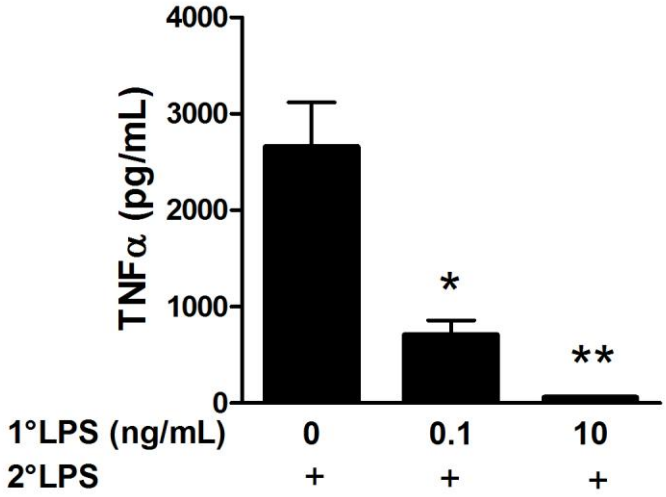

Figure 25: Human monocytes pretreated with different doses of LPS reduce TNFα expression. Human monocytes were primed with 0, 0.1 or 10 ng/ml LPS continuously for 18 h, washed twice with PBS, and challenged with 10 ng/ml LPS. Supernatants and cell pellets were collected 24 h later. Results are expressed as mean ± SEM of three donors. * $p < 0.05$.

To understand the role of miRNAs in LPS tolerance, we analyzed miRNAs expression in the tolerized monocytes in relation to untolerized control. As expected, miR-146a (Fig. 26E) showed significantly higher expression in primed and challenged monocytes, as described in Nahid et al. [93]. Even miR-125a-5p, miR-99b-5p and miR-146b resulted up-regulated in tolerized monocytes in relation to untolerized control (Fig. 26A, B and C). In the case of let-7e-5p we did not measured any increment in its expression after the subsequent challenge of LPS (Fig. 26C). Consequently, miR-125a-5p and miR-146b may play an important role in LPS tolerance, targeting fundamental components of TLR pathway. Even if miR-99b-5p is up-regulated in tolerized monocytes we did not find any functional role of it in inflammatory pathways. Conversely, for let-7e-5p we have demonstrated its role in targeting of TLR pathway but we did not observed its induction in the tolerance process. [167]

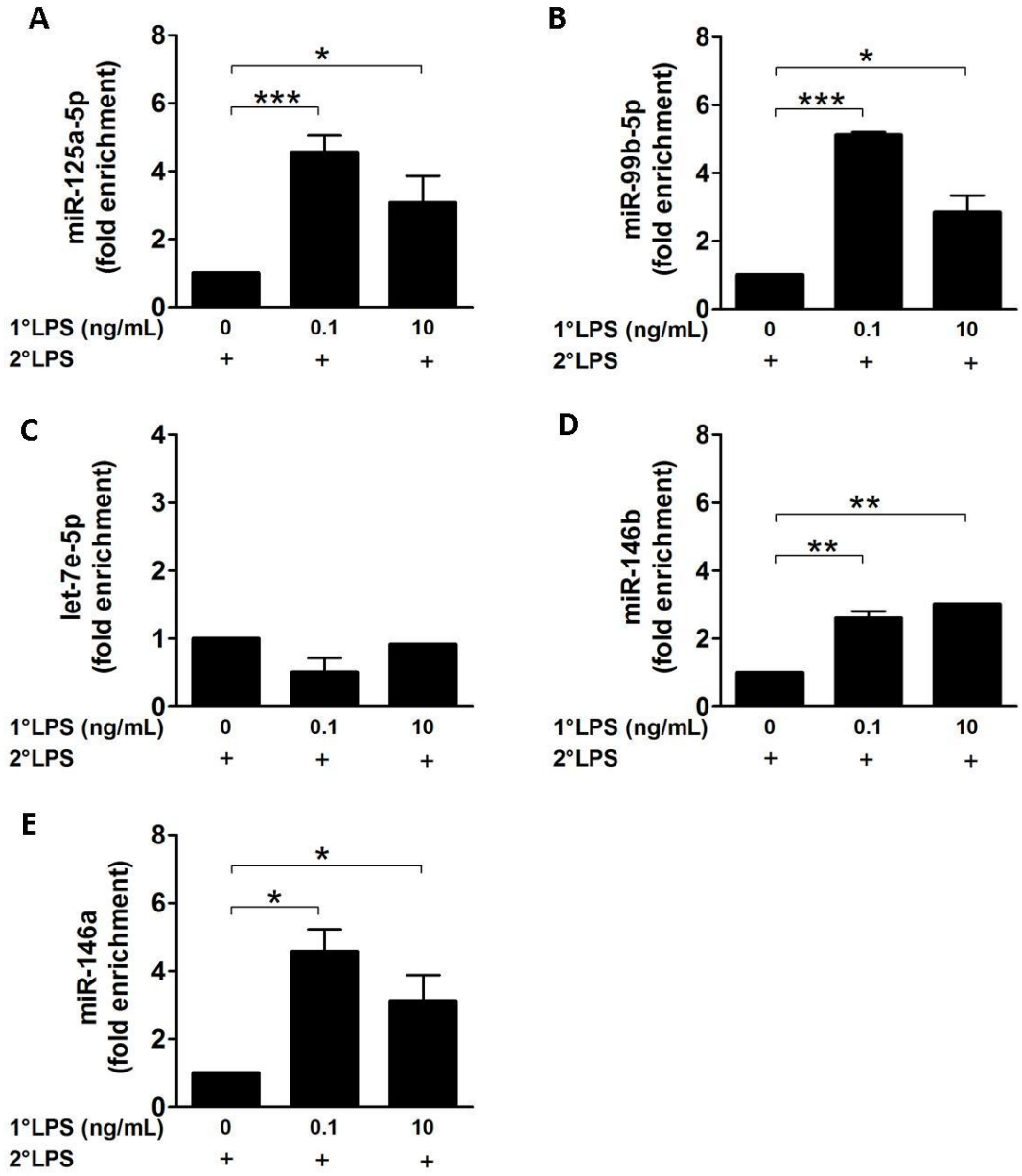

Figure 26: miR-125a-5p, miR-99b-5p and miR-146b are induced in endotoxin tolerized human monocytes. Human monocytes were primed with 0, 0.1 or 10 ng/ml LPS continuously for 18 h, washed twice with PBS, and challenged with 10 ng/ml LPS. Supernatants and cell pellets were collected 24 h later. Results are expressed as mean ± SEM of three donors. * $p < 0.05$.

3.5.2 IFNγ blocks the upregulation of miR-125a-5p, miR-99b-5p and miR-146b during endotoxin tolerance

IFNγ has activating effect on monocytes and it has been demonstrated that IFNγ can revert LPS tolerance in human [168] and mice [169]. In addition, in experimental model of endotoxin tolerance in mice, IFNγ production was reduced by T/NK cells, major producer of this cytokine [170]. These results suggest IFNγ as a key regulator of this process even if its LPS tolerance reversal is not well understood. We have shown that IFNγ was able to abolished miRNA cluster and miR-146b induction due to LPS stimulation (Fig.6) so we hypothesized that these miRNAs inhibition can have a role in LPS tolerance impairment. Human monocytes were pretreated with IFNγ and then subjected to LPS tolerance model. After 24h of incubation with challenged LPS, we measured TNFα and miRNAs expression.

In our endotoxin model, TNFα was down-regulated by subsequent LPS stimulation as we have shown in Fig. 24, but IFNγ pre-treatment was able to restore the diminished TNFα production of tolerized monocytes as the expression levels of monocytes pre-treated with IFNγ but not tolerized (Fig. 27). For miRNAs expression, LPS tolerance induced the up-regulation of miR-125a-5p, miR-99b-5p and miR-146b as shown in Fig. 26. If monocytes were pre-treated with IFNγ and than challenged two times with LPS, the same miRNAs could not be up-regulated anymore, as in monocytes that are pre-treated with IFNγ and stimulated only once with LPS (Fig. 28A,B and D). For let-7e-5p expression, we did not observed any variation in expression even after IFNγ stimulation (Fig. 28C). Differently is for miR-146a, because IFNγ did not abolished its expression in tolerized monocytes but rather IFNγ increased its expression after LPS stimulation (Fig. 28E). These results demonstrate the ability of IFNγ to block miRNAs expression even during LPS tolerance induction.

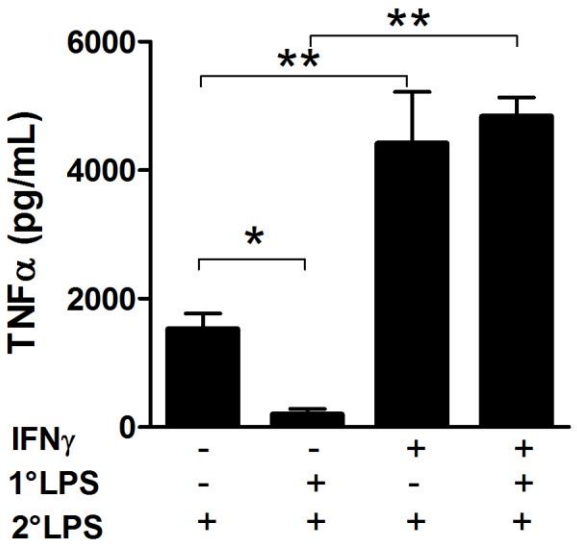

Figure 27: IFNγ pre-treatment restores the diminished TNFα production of tolerized monocytes. Human monocytes were pre-treated with 10 ng/ml IFNγ and primed with 0.1 ng/ml LPS continuously for 18 h, washed twice with PBS, and challenged with 10 ng/ml LPS. Supernatants and cell pellets were collected 24 h later. Results are expressed as mean ± SEM of three donors. * p< 0.05.

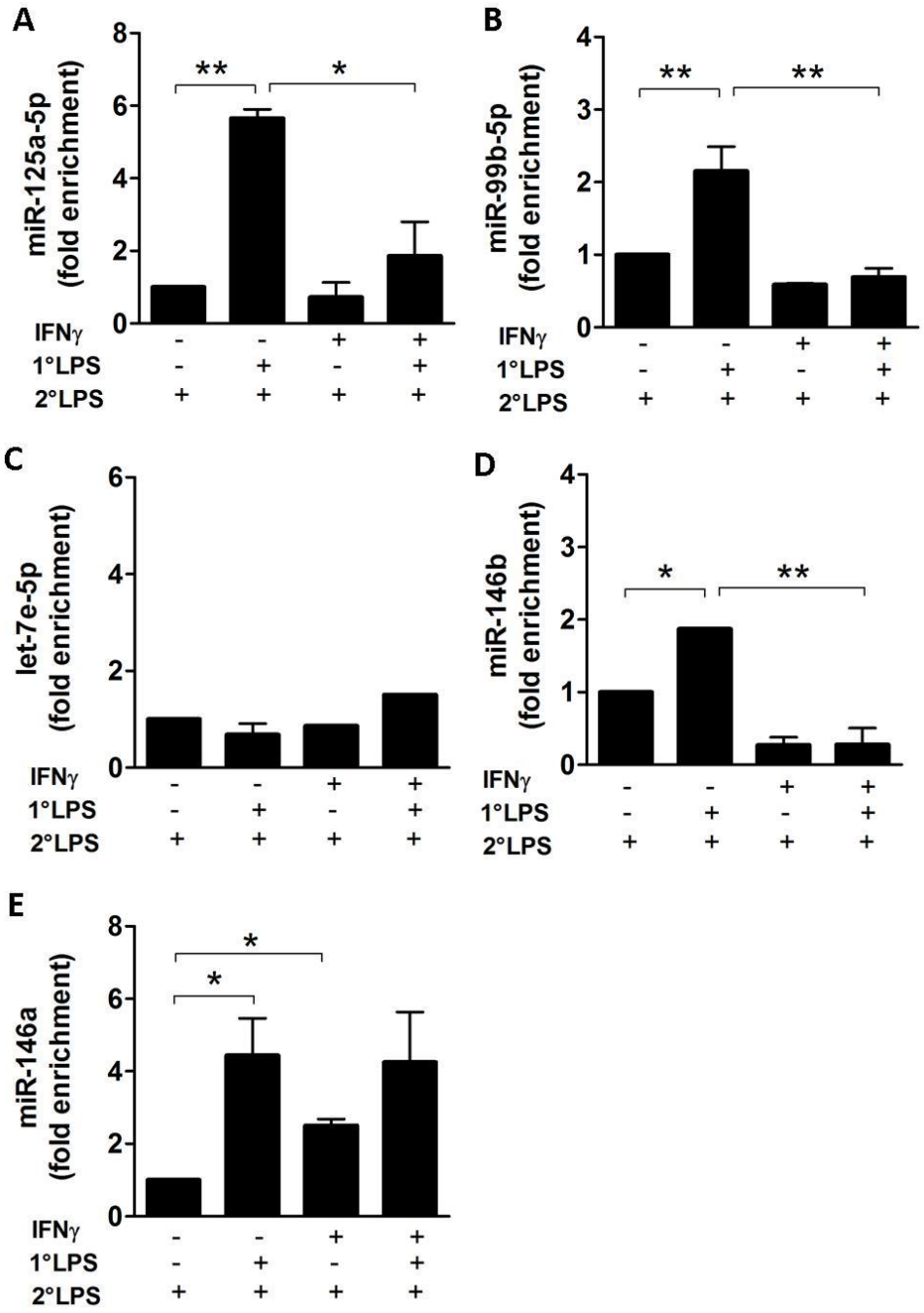

Figure 28: IFNγ pre-treatment blocks up-regulation of miRNA cluster and miR-146b in tolerized monocytes. Human monocytes were pre-treated with 10 ng/ml IFNγ and primed with 0.1 ng/ml LPS continuously for 18 h, washed twice with PBS, and challenged with 10 ng/ml LPS. Supernatants and cell pellets were collected 24 h later. Results are expressed as mean ± SEM of three donors. * $p < 0.05$.

3.5.3 Up-regulation of miR-125a-5p and miR-146b mimic LPS priming to induce endotoxin tolerance.

It has been shown that the anti-inflammatory IL-10 and TGFβ are involved in the process of LPS desensitization [171]. Furthermore, IL-10 and TGFβ can directly induce a state of LPS hyporesponsiveness [171]. Exposure of human monocytes to TGFβ and IL-10 for 2 hours induced their hyporesponsiveness to LPS challenge with respect the production of inflammatory cytokines (Fig. 29). As previously reported [171, 172], IFNγ pre-treatment strongly enhanced LPS-dependent production of inflammatory cytokines and significantly impaired the LPS- (Fig. 27), TGFβ- and IL-10-dependent tolerization effect (Fig. 29A and B).

Considering that LPS, IL-10 and TGFβ can induce the expression of miRNA cluster and miR-146b and they target the principal molecules of TLR signaling, we investigated whether the up-regulation of miRNA cluster and miR-146b was involved in the induction of LPS hyporesponsiveness. In particular we only focused on miR-125a-5p and miR-146b because let-7e-5p did not appear to be induced during LPS tolerance and miR-99b-5p has not target correlated to immune functions.

To determine the functional role of these miRNAs in the process of endotoxin tolerance, THP1 cells were primed and challenged with LPS. THP1 cells that over-express miR-125a-5p or miR-146b and stimulated only once with LPS produced significantly lower levels of TNFα in comparison of pRRL-control cells, inducing a state of tolerization (as shown even in fig. 21A and 23A). Furthermore, the ability of pRRL-125a-5p and pRRL-146b THP1 cells to cause tolerization was almost similar to the tolerance induced in pRRL-ct with subsequent LPS stimulation (Fig. 30). These data demonstrate the ability of miR-125a-5p and miR-146b to induce LPS tolerance in our *in vitro* model.

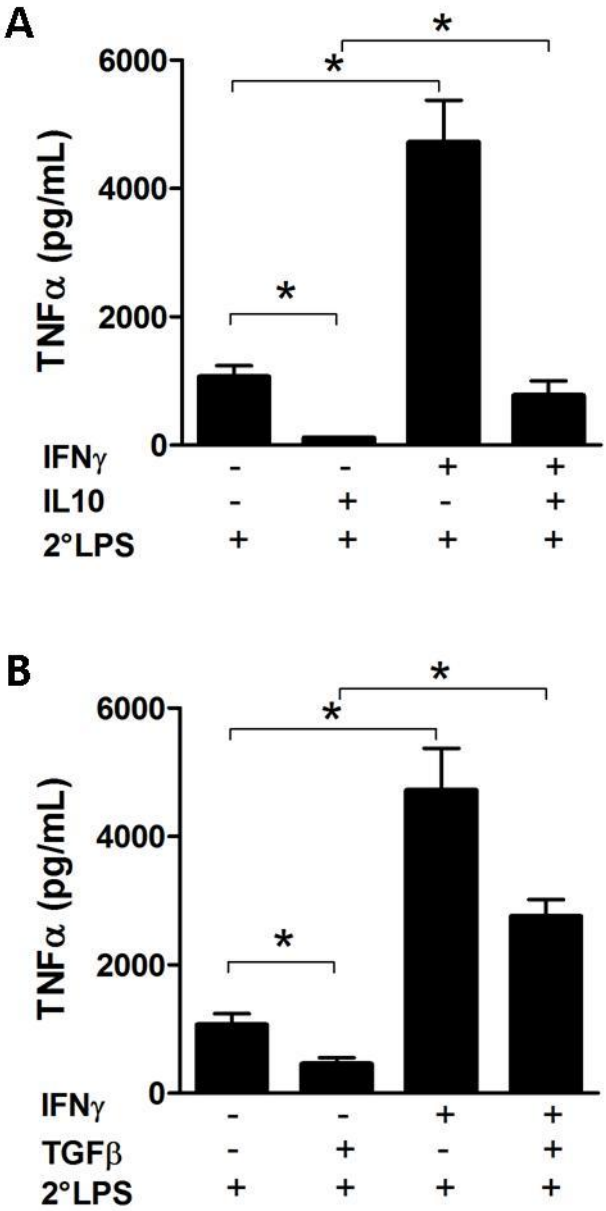

Figure 29: IL-10 and TGFβ induce a state of LPS hyporesponsiveness in monocytes but IFNγ pre-treatment impairs it. Human monocytes were pre-treated or not with 10 ng/ml IFNγ over-night and primed or not with 20 ng/ml IL-10 (A) or 50 ng/ml TGFβ (B) for 2 h and challenged with 10 ng/ml LPS for 48 h. Levels of TNFα were measured by ELISA in cell free supernatants. Results are expressed as mean ± SEM of at least three donors. * $p < 0.05$.

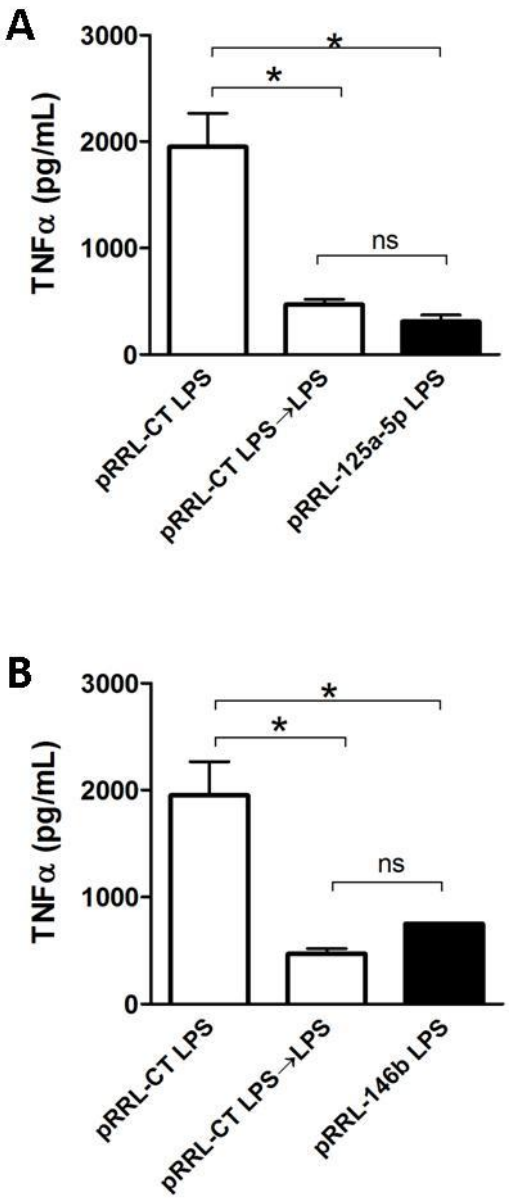

Figure 30: Up-regulation of miR-125a-5p and miR-146b mimic LPS priming to induce endotoxin tolerance. TNFα levels were measured by ELISA in cell free supernatants of pRRL-ct and pRRL-125a (A)or pRRL-146b (B) THP1 cells stimulated with 1000 ng/ml LPS for 24 h. To induce tolerance, pRRL-ct THP1 cells were stimulated over-night with 100 ng/ml, washed twice with PBS, and challenged with 1000 ng/ml LPS for 24 h. Results are expressed as mean ± SEM of three independent experiments. * $p < 0.05$.

3.5.4 Inhibition of miR-125a-5p and miR-146b expression reduce LPS-, IL-10-, TGFβ- tolerance.

To corroborate the role of mR-125a-5p and miR-146b on tolerance, miRT-ct, miRT-125a-5p and miRT-146b THP-1cells were subjected to LPS-, IL-10-, and TGFβ- tolerance. Blocking miR-125a-5p or miR-146b expression resulted in a increased TNFα expression upon LPS stimulation respect to ct cells; the induction of a tolerized state by pre-treating cells with IL10, LPS or TGFb, as also described in the literature, causes a decrease of TNFα expression that was partially or fully restored when the miRT-125a-5p or miRT-146b THP1 cells were used in tolerizing conditions (Fig. 31A and B). These implies that miRNA inhibition is important but not sufficient to completely revert the tolerant phenotype in THP1 cells and that the different priming stimulus induced a different degree of tolerization.

Taken together, our results strongly suggest that miR-125a-5p and miR-146b represents a molecular effector of LPS, IL-10 and TGFβ pathways to negatively regulate the LPS inflammatory signal.

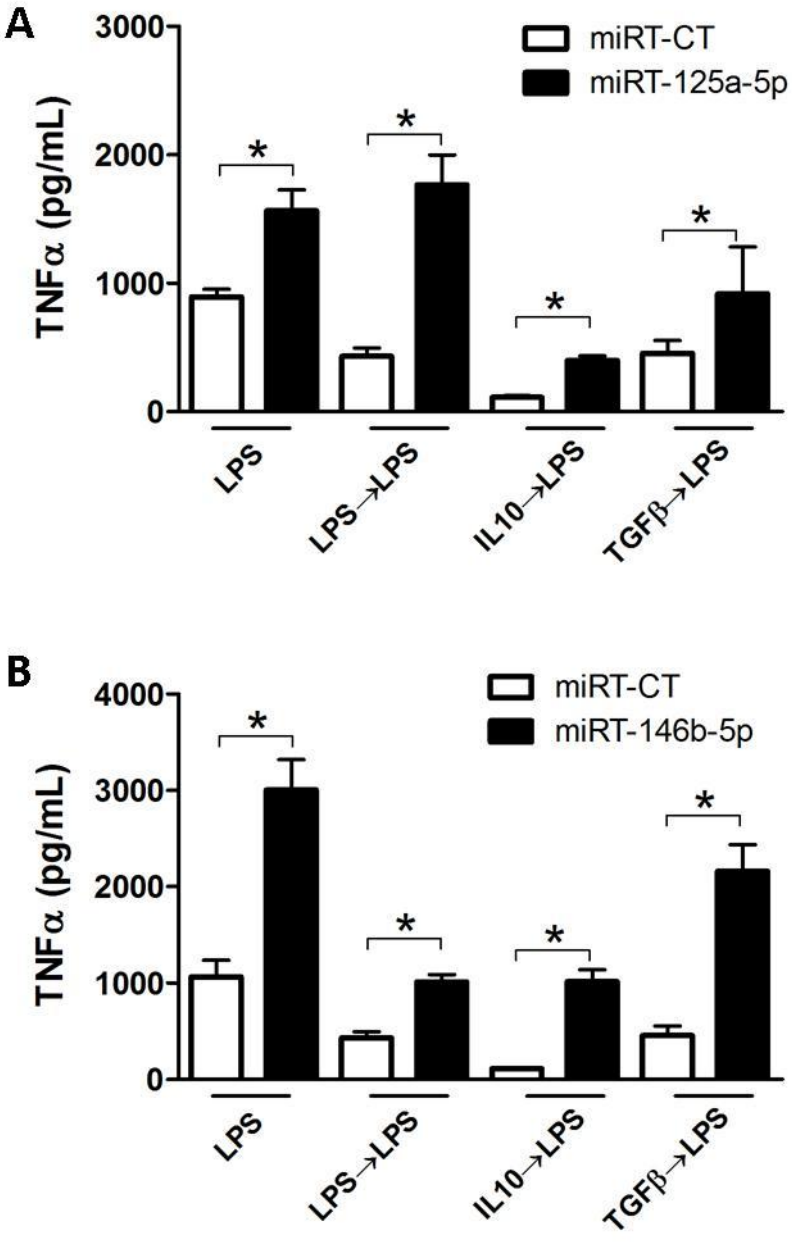

Figure 31: Inhibition of miR-125a-5p and miR-146b expression reduce LPS-, IL-10-, TGFβ-tolerance. TNFα levels were measured by ELISA in cell free supernatants of miRT-ct and miRT-125a (A) or miRT-146b (B) THP1 cells stimulated with 1000 ng/ml LPS for 48 h. To induce tolerance, miRT-THP1 cells were stimulated with100 ng/ml LPS, 20 ng/ml IL-10 or 50 ng/ml TGFβ for 2 h and challenged with 1000 ng/ml LPS for 48 h. Results are expressed as mean ± SEM of independent experiments. * $p < 0.05$.

3.6 Role of miRNA cluster and miR-146b in resolution of inflammation

3.6.1 miRNA cluster and miR-146b expression in BMdM of WT and IL-10 KO mice

As shown in fig.7 miRNA cluster is well conserved between human and mice both at the level of its promoter region both in their pre- and mature sequences. This is also true for miR-146b. To assess our miRNAs induction in mice, we performed a kinetic experiments on bone marrow derived macrophages (BMdM) from WT and IL-10 KO mice, stimulated with LPS or LPS plus IL-10 for 2, 4, 8, 24 hours. Mir-125a-5p, miR-99b-5p, let-7e-5p and miR-146b were induced in response to LPS in WT BMdM with a delay kinetic as in human monocytes. In IL-10 KO BMdM, LPS could not induce miRNA expression as in WT BMdM (Fig. 32A, C, E and G). Addition of exogenous IL-10 up-regulated and accelerated miRNAs induction over non stimulated-control in comparison of stimulation with LPS alone in WT and IL-10 KO macrophages (Fig. 32B, D, F and H). Furthermore, IL-10 rescued the gap of miR-125a-5p and miR-146b expression between WT and IL-10 KO BMdM (Fig. 32B and H). The fold changes after LPS stimulation were not as in human experiments because for human we used monocytes instead for mouse we used bone marrow differentiated- macrophages. We also measured miR-146a as a positive control for LPS responsiveness and we observed significant induction to LPS but no difference between WT and IL-10 KO BMdM (Fig. 32I). Even the presence of exogenous IL-10 did not change miR-146a expression in both WT and IL-10 KO BMdM (Fig. 32L).

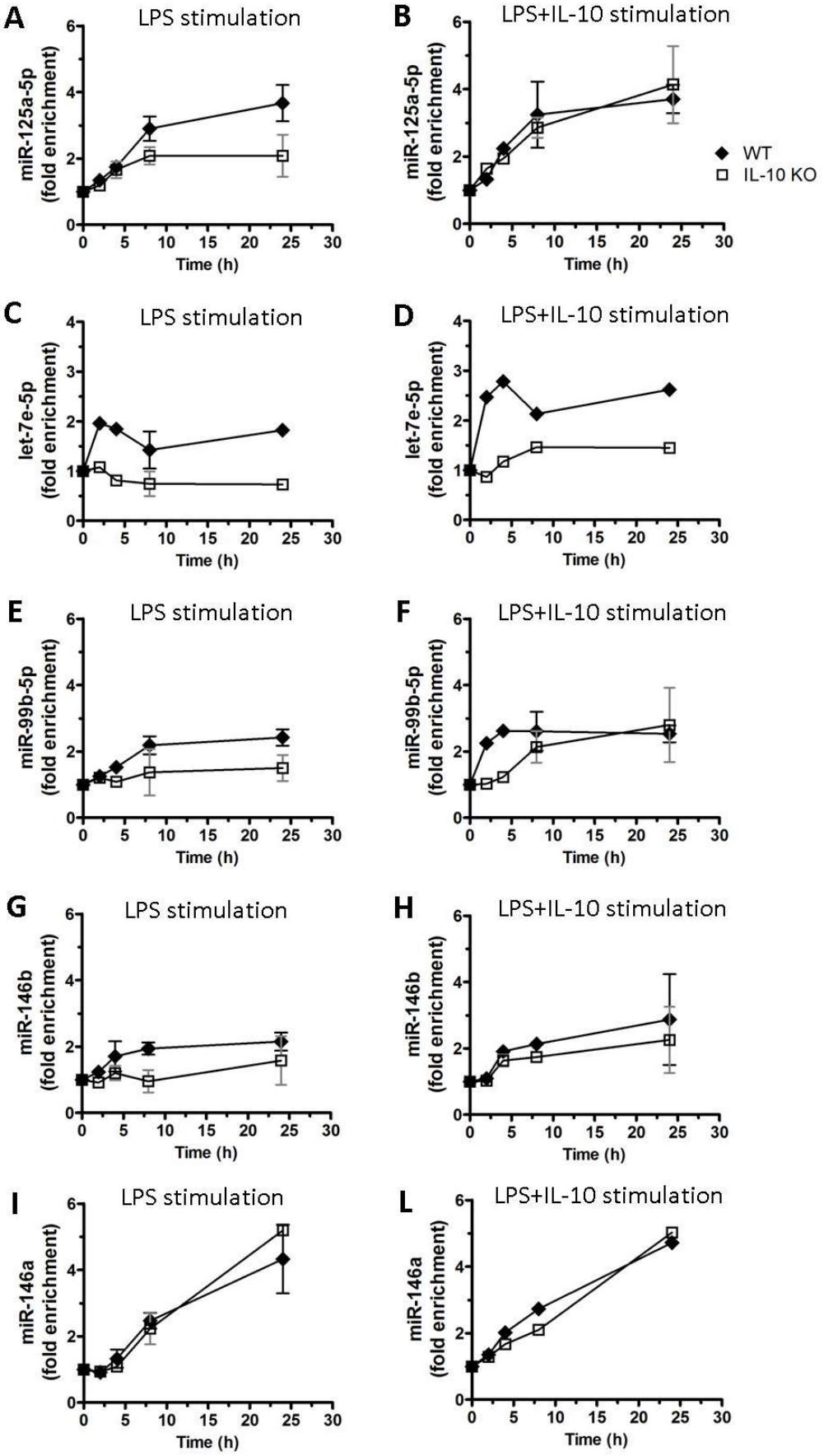
A
LPS stimulation
miR-125a-5p (fold enrichment)
Time (h)
B
LPS+IL-10 stimulation
miR-125a-5p (fold enrichment)
Time (h)
WT
IL-10 KO
C
LPS stimulation
let-7e-5p (fold enrichment)
Time (h)
D
LPS+IL-10 stimulation
let-7e-5p (fold enrichment)
Time (h)
E
LPS stimulation
miR-99b-5p (fold enrichment)
Time (h)
F
LPS+IL-10 stimulation
miR-99b-5p (fold enrichment)
Time (h)
G
LPS stimulation
miR-146b (fold enrichment)
Time (h)
H
LPS+IL-10 stimulation
miR-146b (fold enrichment)
Time (h)
I
LPS stimulation
miR-146a (fold enrichment)
Time (h)
L
LPS+IL-10 stimulation
miR-146a (fold enrichment)
Time (h)

Figure 32: miRNA cluster and miR-146b induction in WT and IL-10 KO BMdM. Primary BMdM of WT (black symbol) or IL-10 KO (white symbol) mice were stimulated with 100 ng/ml LPS (A, C, E, G) or 100 ng/ml plus 20 ng/ml IL-10(B, D, F, H) for 2, 4, 8 and 24 hours or left unstimulated prior to cell lysis. MiRNAs levels were measured by qPCR. Results were expressed as fold change over unstimulated control (mean ± SEM; n = 3; * $p < 0.05$).

3.6.2 miRNA cluster and miR-146b expression in peritoneal macrophages after LPS- induced peritonitis

To further investigate the induction of miRNA cluster and miR-146b in an *in vivo* setting, an intra-peritoneal (i.p) injection of LPS or PBS was administered in WT mice and miRNAs expression levels measured in peritoneal macrophages at different time points. In agreement with fig. 32, fig. 33 reveals induction of expression of miR-125a-5p, let-7e-5p, miR-99b-5p and miR-146b in response of LPS *in vivo,* with the peak at later time points. For miR-155 we observed the major increment at earlier time point because it is known to be potently induced in response of TLR4 activation [75] (Fig. 33F). Mir-146a increment also indicates LPS responsiveness of the peritoneal macrophages (Fig. 33E). Analysis of the cell populations at different time points after LPS injections, revealed a decreasing macrophages percentage on all the leukocytes immediately after the infection, and an increased neutrophil cell compositions (Fig. 34). The peak of miRNA induction in macrophages at 48 hours correspond to decreasing neutrophils. Together these data suggest a role for miR-125a-5p, let-7e-5p, miR-99b-5p and miR-146b in macrophages to shutdown the inflammatory process.

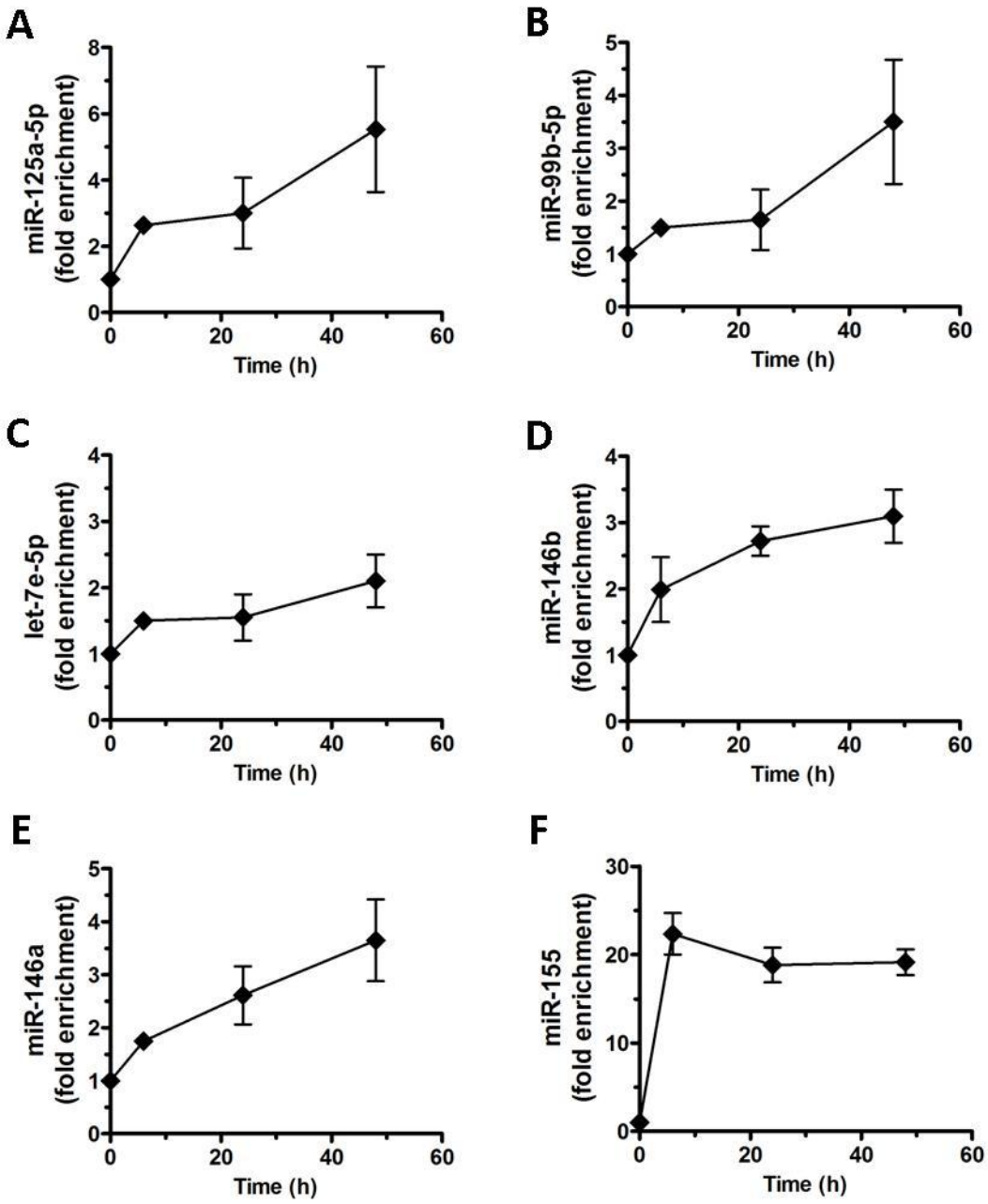

Figure 33: miRNA cluster and miR-146b induction in WT peritoneal macrophages. C57BL/6 mice were administered an intra-peritoneal injection of LPS (2.5 mg/kg) or PBS. Exudates were collected at 0, 6, 24 and 48 hours and macrophages were isolated with MACS cell separations. MiRNAs levels were measured by qPCR and results were expressed as fold change over non treated mice. The data were the mean of 2 independent experiments with 4 mice per condition ± SEM.

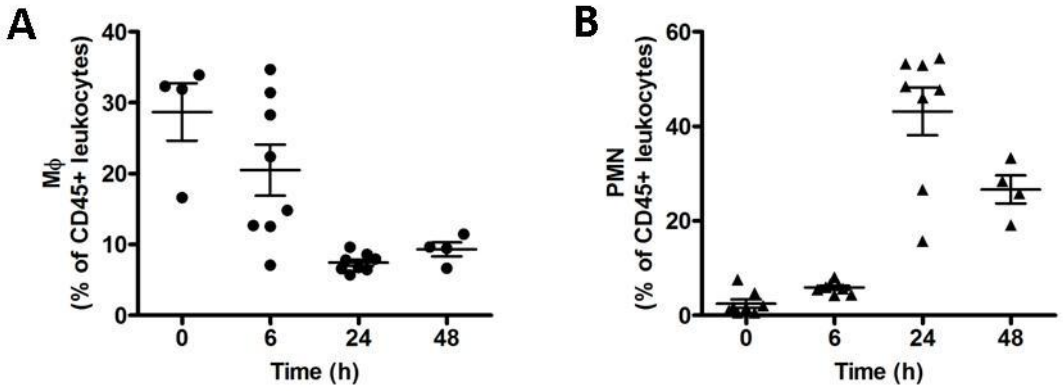

Figure 34: analysis of peritoneal cell populations after LPS injections. C57BL/6 mice were administered an intra-peritoneal injection of LPS (2.5 mg/kg) or PBS. Exudates were collected at 0, 6, 24 and 48 hours and analyzed by flow cytometry. (A) Macrophages were characterized as F4/80+ and CD11b+; (B) neutrophils as LY6G+, CD11b+ among CD45+ cells. Results are the mean of 4-8 mice per condition ± SEM.

3.6.3 miRNA cluster and miR-146b expression in peritoneal macrophages after zymosan-induced peritonitis

Since miRNA cluster and miR-146b have emerged as fine tuners of inflammatory signaling induced especially by anti-inflammatory IL-10, it was of interest to investigate whether they played roles in resolution. To identify a miRNA kinetic of expression during resolution in an acute inflammatory response, we used the zymosan-induced peritonitis model that has been widely used as a self-resolving model of acute inflammation. Since KO mice of our miRNAs of interest were not available, we applied the resolving model on WT and IL-10 KO mice that express less miR-125a-5p, miR-99b-5p, let-7e-5p and miR-146b. Zymosan A particles from S. cerevisiae, a Toll-like receptor 2 and 4 ligand, were injected i.p. in WT and IL-10 KO mice and peritoneal exudates were collected to monitor temporal changes in leukocyte composition and macrophage miRNAs expression. After zymosan injection, leukocytes infiltrated the peritoneal cavity during the onset phase of acute inflammation reaching a maximum at ~12 hours (data not shown) and declined at later hours [101]. In IL-10 KO mice we observed an increased number of peritoneal cells at 72 hours comparing to WT (Fig. 35A). Flow cytometry analysis confirmed that the majority of leukocytes in WT and IL-10 KO exudates were PMN (Ly-6G high/CD11b+). In WT mice, PMN declined during the resolution phase from 24 to 72 hours after initiation of peritonitis. Instead in IL-10 KO mice, there were a delay in PMN reduction that starts at 48 hours compared to WT. At 72 hours after zymosan injection we observed more PMN in IL-10 KO exudates than in WT (Fig. 35B). Resident peritoneal macrophages (F4/80+/ CD11b+ cells), which represent the main leukocyte population in naive mice peritonea [173], were slightly detected in exudates at 6 hours, with no significantly difference in WT and IL-10 exudates (Fig. 35C). Conversely to PMN, macrophages gradually increased during the resolution phase in WT mice, but not in IL-10 KO mice, where they were significantly less abundant at 24 and 72 hours (Fig. 35C). Altogether these data demonstrate that the absence of IL-10 results in increased neutrophil infiltrations and reduced recruitment of resolving macrophages, thus

furtherly confirming that IL-10 is an important anti-inflammatory mediator having a role in the resolution of inflammation.

To identify if miR-125a-5p, miR-99b-5p, let-7e-5p and miR-146b were temporally regulated during acute inflammation and the self-limited resolution, we monitored miRNA expression in exudates of WT and IL-10 KO mice. At 6 hours, most likely representing the PMN content of these exudates, miR-125a-5p, miR-99b-5p, let-7e-5p and miR-146a did not increase (Fig. 36A, B, C and E). Instead, miR-146b and miR-155 were up-regulated at 6 hours respect to basal and for miR-146b the absence of IL-10 did not increase its expression, suggesting an IL-10 dependent expression even in PMN (Fig. 36D and F). Afterward, miR-125a-5p, miR-99b-5p and let-7e-5p increased gradually at later intervals (24-72 hours) in the resolution phase. In IL-10 KO exudates, we obtained a reduced miR-125a-5p, miR-99b-5p and let-7e-5p expression, confirming an IL-10 dependency (Fig. 36A, B and C). The absence of IL-10 had no impact on miR-146a expression, instead augmented miR-155 induction, consistent with the known IL-10 inhibition on its expression [80] (Fig. 36E and F).

To further address the miRNA induction in specific cells during resolution, we quantified miRNA expression in sorted macrophages from basal, 48 and 72 hours after zymosan injection. In WT resolving macrophages, we obtained an higher induction of all miRNAs analyzed compared to the resident macrophages (Fig. 37). The lack of IL-10 significantly influenced the expression of miR-125a-5p at both 48 and 72 hours (Fig. 37A) and the expression of miR-99b-5p only at 72 hours (Fig. 37B). For let-7e-5p there was a difference in the expression between WT and IL-10 KO cells even if it is not statistically significant (Fig. 37C). miR-146b and miR-146a showed an equal increased in resolving macrophages of WT and IL-10 KO mice (Fig. 37D and E). Consistent with previous data, miR-155 was highly expressed in IL-10 KO mice (Fig. 37F). Together, these data indicate that miR-125a-5p, miR-99b-5p, let-7e-5p and miR-146b are temporally and differentially regulated during self-limited resolution and IL-10 has an important role on their induction.

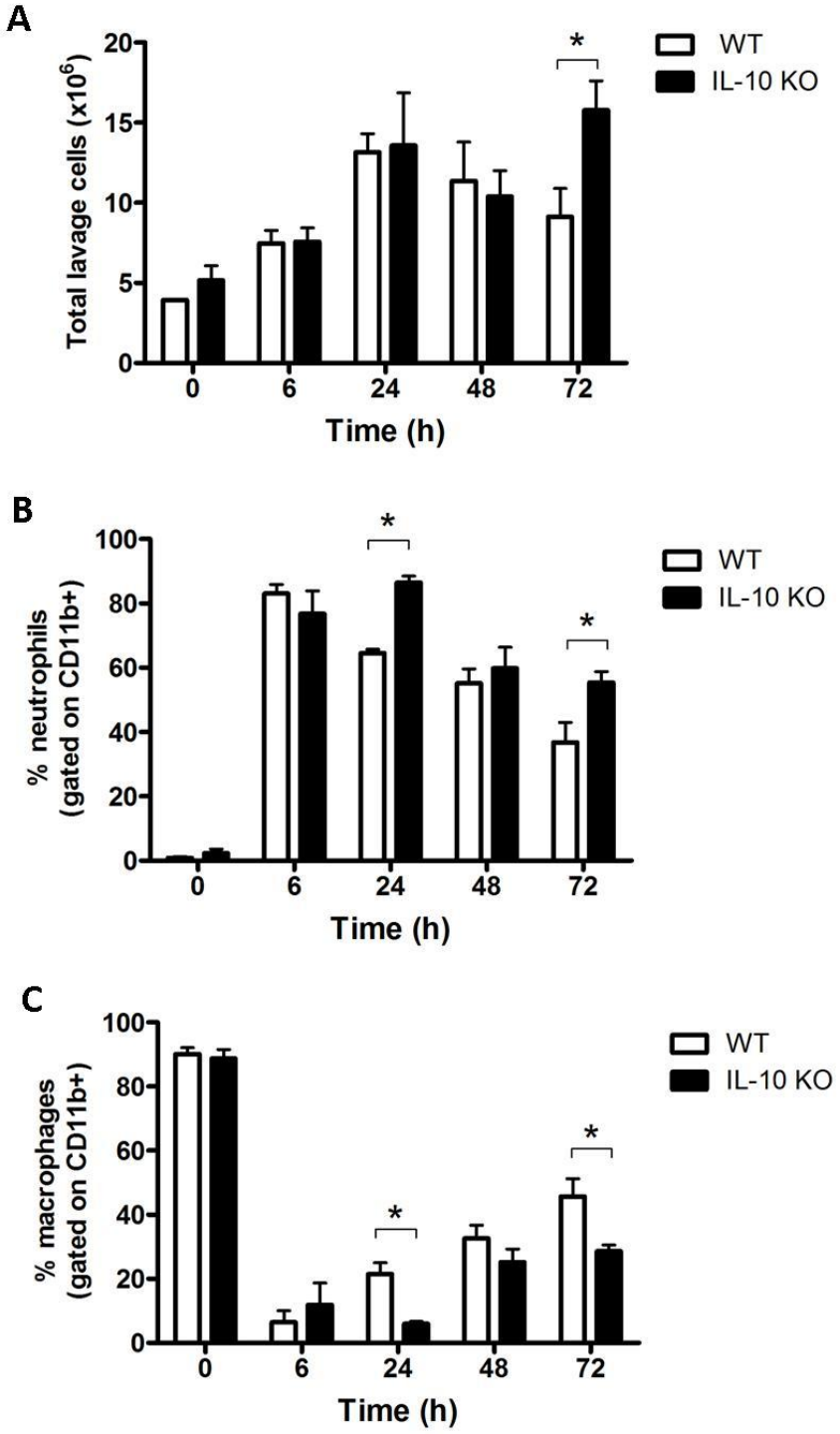

Figure 35: increased neutrophil infiltrations and reduced recruitment of resolving macrophages in IL-10 KO mice. WT and IL-10 KO mice were administered an intra-peritoneal injection of Zymosan-A (1 mg/mouse) or PBS. Exudates were collected at 0, 6, 24, 48 and 72 hours, counted (A) and analyzed by flow cytometry. (B) Neutrophils were gated as LY6G+/CD11b+ (C) Macrophages were gated as F4/80+/CD11b+. Results are the mean of 3-4 mice per condition ± SEM. * $p < 0.05$.

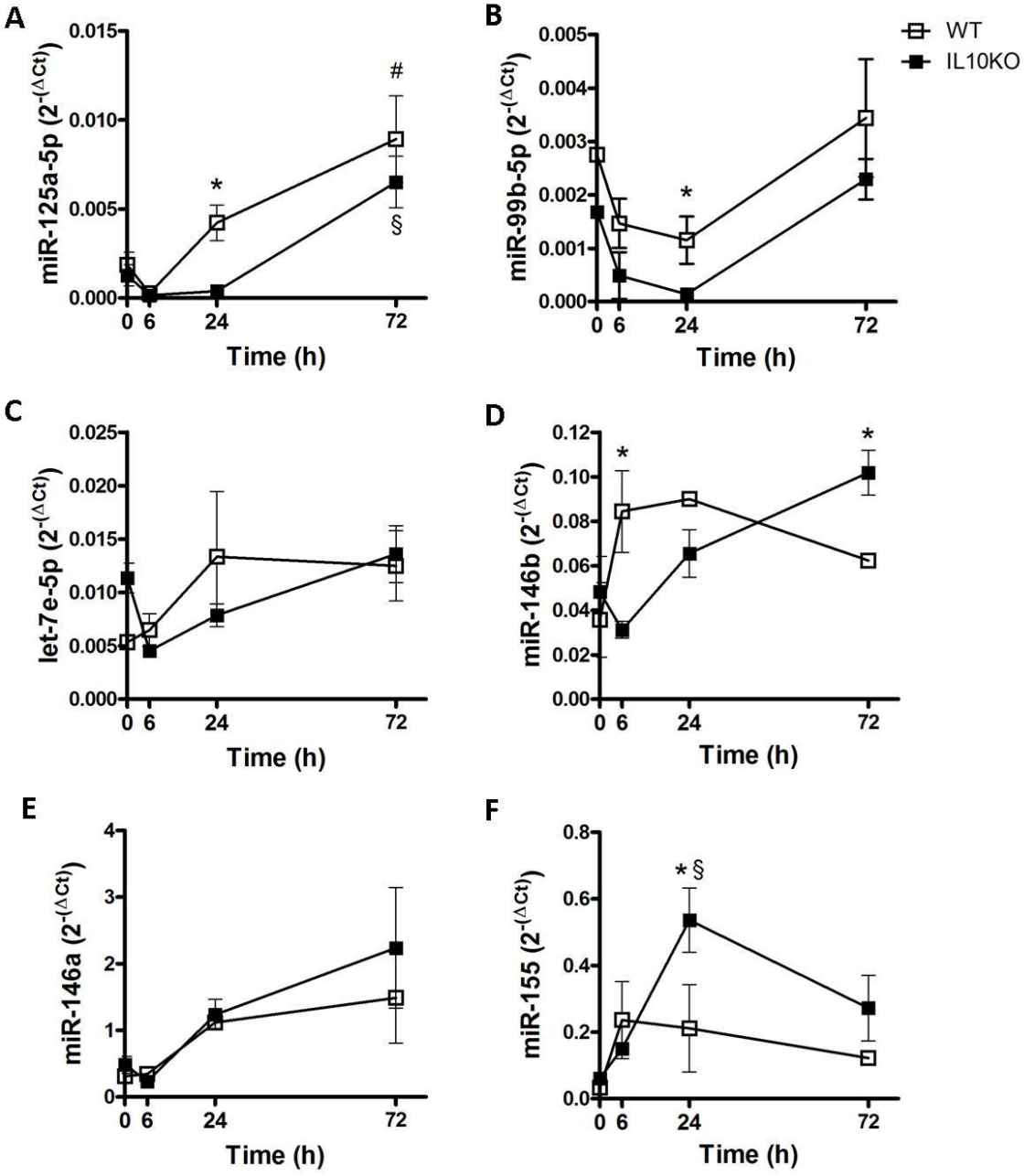

Figure 36: miRNA cluster and miR-146b are temporally regulated in peritoneal inflammatory exudates. WT and IL-10 KO mice were administered an intra-peritoneal injection of Zymosan-A (1 mg/mouse) or PBS. Exudates were collected at 0, 6, 24 and 72 hours. MiRNAs levels were measured by qPCR and results were expressed as $2^{-\Delta Ct}$. Results are the mean of 3-4 mice per condition ± SEM. * $p < 0.05$ IL-10 KO vs WT group; # $p < 0.05$ vs basal WT; § $p < 0.05$ vs basal IL-10 KO.

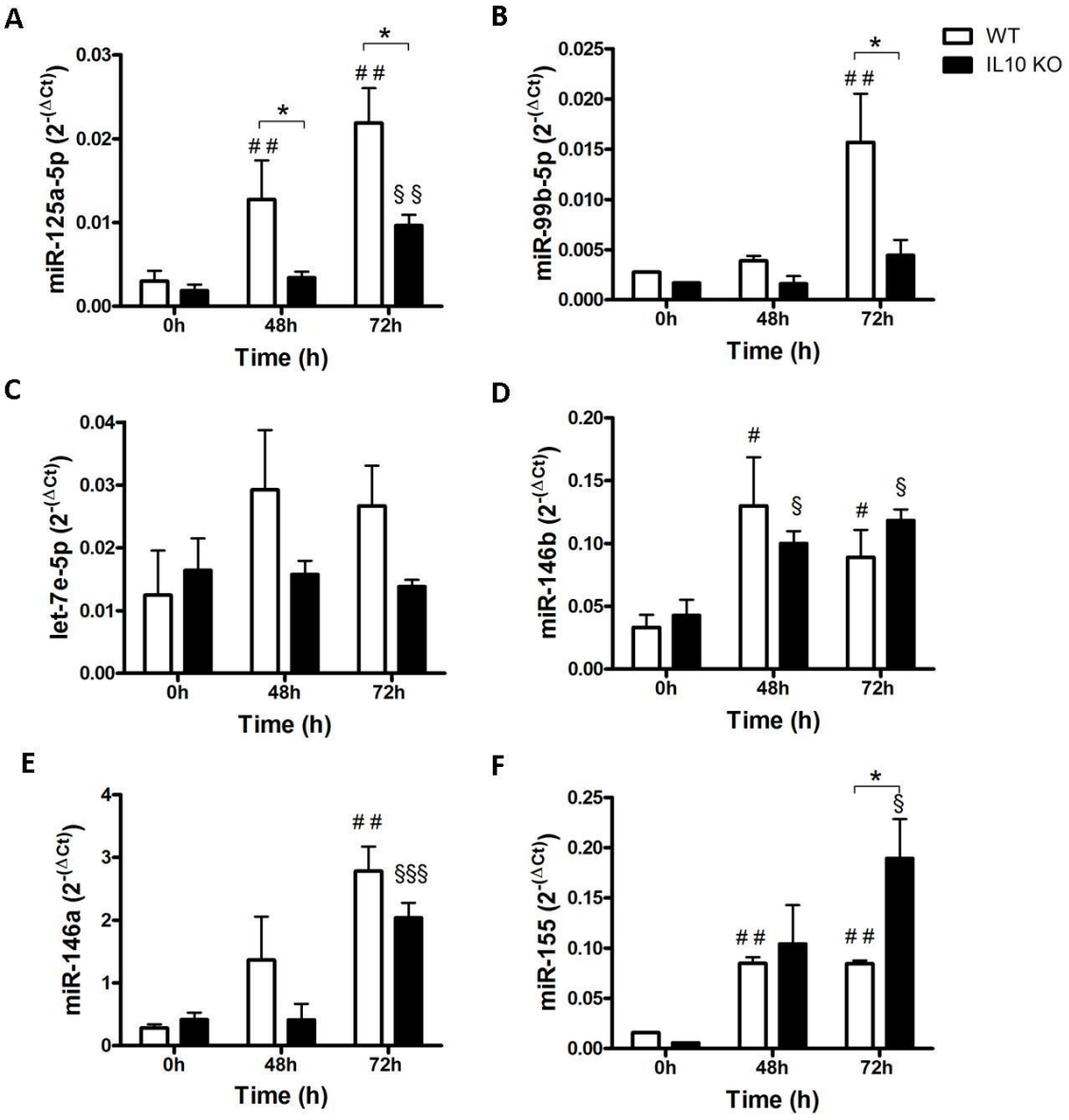

Figure 37: miRNA cluster and miR-146b expression in resolving macrophages. WT and IL-10 KO mice were administered an intra-peritoneal injection of Zymosan-A (1 mg/mouse) or PBS. Exudates were collected at 0, 48 and 72 hours. MiRNAs levels were measured by qPCR and results were expressed as $2^{-\Delta Ct}$. Results are the mean of 3-4 mice per condition ± SEM. * $p< 0.05$ IL-10 KO vs WT group; # $p< 0.05$ vs basal WT; § $p< 0.05$ vs basal IL-10 KO.

4. DISCUSSION

Inflammation is a protective physiological process that must be tightly regulated to prevent development of diseases such as autoimmunity. Several regulatory mechanisms have evolved to control the magnitude and duration of inflammation. Among such negative regulators, IL-10 and TGFβ are important inhibitors of TLR signaling pathway and act primarily by inhibiting the production of pro-inflammatory cytokines at both transcriptional [153] and post-transcriptional levels [124]. MiRNAs are now emerging as additional negative feedback mechanism operating in innate immune system. By investigating the potential role of miRNAs in the post-transcriptional mechanisms dampening innate immune cell activation, we identified the evolutionary conserved miR-125a~99b~let-7e cluster and the miR-146b as late-induced genes after LPS stimulation in human monocytes and murine macrophages.

Our study demonstrate that the LPS-late induction of miRNAs expression is due to the action of the anti-inflammatory cytokines IL-10 and TGFβ.

Through bioinformatics tools, we characterized the core promoter region of the miRNA cluster and we experimentally confirmed a direct transcriptional role for IL-10, TGFβ and LPS stimulation on miRNA cluster expression.

MiR-146b belongs to the miR-146 family, composed also by miR-146a and the two isoforms differ only by 2 nt at the 3' end in their mature sequence. Despite their sequence similarity, we provide evidence that they are differentially regulated at a transcriptional level. By performing chromatin immunoprecipitation we showed that miR-146b induction depends on the activity of IL-10, whereas IL-10 does not influence miR-146a expression.

These findings uncover new direct targets of IL-10 and TGFβ and suggest that miRNA cluster and miR-146b could mediate their anti-inflammatory mechanism of action.

To date, the biological role of this miRNAs in the context of the innate immune response is still poorly understood. Let-7e-5p and miR-125a-5p have been

associated with the development of the immune system [82] and miR-125a-5p has been proposed to suppress classical activation and promote the anti-inflammatory alternative activation of macrophages [174]. Instead, miR-146b functional role is mostly associated with tumor biology and it has been found less expressed in many human solid tumors compared with normal tissues[97, 98]. To investigate the functional role of miRNA cluster and miR-146b in the regulation of the inflammatory response in macrophages we adopted a computational method based on IPA analysis to identify potential targets. As clustered miRNAs are usually co-regulated, it is conceivable that members within the same cluster could function in a cooperative manner, acting coordinately to control a biological process. The *in silico* analysis revealed that predicted targets of miR-125a-5p and let-7e-5p were significantly enriched in the *Inflammatory response* (97/124 and 52/124 genes, respectively) and more specifically in the *TLR signaling pathway* (27/43 and 22/43 genes, respectively), with multiple key genes being predicted as targets for both miRNAs. Even for miR-146b, the target analysis showed a significant enrichment in "TLR signaling", "NF-kB signaling", and "IL-1β signaling" pathways. Bioinformatic predictions were experimentally confirmed by luciferase and RIP assays, as well as by the quantification of protein levels in monocytes over-expressing or inhibiting the specific miRNA. Notably, miR-99b-5p, which has an overall significantly reduced number of predicted targets when compared to miR-125a-5p and let-7e-5p (1364, 7089, and 5595 target genes, respectively), was not actively involved in the modulation of these pathways, suggesting that its expression could represent the consequence of evolutionary constrains imposed by the other cluster members.

Among the predicted targets of miR-125a-5p, let-7e-5p and miR-146b, belonging to the TLR pathway we have validated the receptor TLR4, the co-receptor CD14, the adaptors IRAK-1, MyD88 and TRAF6, and the pro-inflammatory cytokines TNFα, IL-6, CCL7, CCL3 and CXCL8. Most but not all the transcripts of these direct targets are reduced because either mRNA destabilization or transduction inhibition could be involved in their inhibitory effects. These findings indicate that miR-125a-5p, let-7e-5p and miR-146b cooperatively regulate key genes at different steps of TLR signaling pathway, through the subtle individual

regulation of multiple genes rather than operating a strong repression of isolated targets [175, 176].

We demonstrate that the expression modulation of the individual miRNA influences the monocytes inflammatory response triggered by LPS stimulations. In particular, enforced expression of miR-125a-5p, let-7e-5p and miR-146b resulted in a significant reduction in LPS-dependent production of several inflammatory cytokines. Conversely, inhibition of 125a-5p or let-7e-5p or miR-146b significantly increase these pro-inflammatory cytokines release.

Due to the aberrant inflammatory response associated with abnormal expression of miR-125a-5p, let-7e-5p and miR-146b, it is of outmost importance that these miRNAs are carefully regulated.

It has been shown that the anti-inflammatory IL-10 and TGFβ are involved in the process of LPS desensitization in monocytes and they can directly induce a state of LPS hyporesponsiveness [171]. This hyporesponsiveness state is characterized by a significant reduction in the inflammatory capacity of monocytes/macrophages to a subsequent endotoxin challenge. Trancriptome analysis on murine and human macrophages have shown that the tolerization process not only down-regulate a large number of pro-inflammatory genes, but also up-regulate some anti-inflamamtory genes [167]. In keeping with these previously studies, we demonstrate the up-regulation of miR-125a-5p, miR-99b-5p and miR-146b in tolerized human monocytes induced by LPS, IL-10 or TGFβ priming. More interestingly, we demonstrate that miR-125a-5p and miR-146b over-expression or inhibition impact on the outcome of the tolerant state.

Another important molecule in the endotoxin tolerance is IFNγ, which has the ability to amplify the pro-inflammatory response in macrophages but it is down-regulated in experimental models of tolerance [170]. Specifically, in LPS-tolerant mice model the suppression of IFNγ production is due to the dysfunction of tolerant macrophages which have impaired ability to induce IFNγ by T and NK cells. IL-10 is an inhibitor of IFNγ production and its expression is sustained after

the induction of LPS tolerance[170]. It has been shown that IFNγ can revert LPS tolerance in human [168] and mice [169] but its mechanism of action is not well understood. We demonstrate that IFNγ can inhibit miRNA cluster and miR-146b expression in human monocytes stimulated with LPS. Moreover, we show that IFNγ blocks miRNAs expression even during LPS tolerance induction.

Altogether these evidences suggest that during the initial phase of inflammation, LPS stimulation of monocytes leads to the production of pro-inflammatory cytokines which act on T/NK cells to induce IFNγ production. IFNγ amplifies the monocytes immune response even by blocking the anti-inflammatory miRNA cluster and miR-146b expression. At late phase of inflammation the production of TGFβ and IL-10, which inhibits IFNγ, induce the up-regulation of the miRNAs that act as a negative feedback loop inhibiting the TLR pathways and thus promoting tolerance.

Another model in which we provide evidence of a role of miRNA cluster and miR-146b as anti-inflammatory molecules, is the *in vivo* self-limited resolution of inflammation. The acute inflammatory response is a protective process unless it is uncontrolled because it is now recognized that persistent inflammation plays a central role in many diseases, as arthritis, asthma, cancers, and cardiovascular diseases [102]. In self-limited inflammation, neutrophils immediately infiltrate the inflamed tissue sites and, usually, the starting point of resolution is defined as the time when neutrophils number decreased. Contemporary, activated tissue-resident macrophages go to the lymph nodes and are substitute by monocytes-derived macrophages that can acquire different phenotypes, from pro-inflammatory to alternatively activated, depending on the microenvironment. In time course experiments, miRNA cluster and miR-146b expression kinetics were measured in different murine *in vivo* models of acute inflammation (LPS- and zymosan- induced peritonitis). Interestingly, we found a gradually increased expression of the anti-inflammatory miRNA cluster and miR-146b in macrophages. This suggests a miRNA role in the dampening of inflammation, that is an important step through which immune cells switch to an anti-inflammatory phenotype.

Published studies have analyzed the macrophage phenotype isolated from a resolving peritonitis elicited by zymosan [177]. They described this resolving macrophages with typically M2 markers, as they express mannose receptor, IL-10, TGFβ, and arginase 1 but also express markers typical of M1 macrophages (e.g. COX 2 and iNOS). Transcriptomic analysis of resolving macrophages revealed that, comparing to pro-inflammatory macrophages, they up-regulate genes necessary for antigen uptake, cell proliferation and chemoattraction and priming of T/B cells and to a lesser extent, immune function [178]. These phenotypic characteristics are consistent with a role of miRNA cluster and miR-146b that we observed up-regulated in sorted macrophages of resolving peritonitis (48-72h after zymosan injection).

Moreover, we confirmed the key role of IL-10 for the resolution of inflammation. In particular we showed a delay in the neutrophil clearance and in the macrophages recruitment at the site of infection in IL-10 KO mice injected with zymosan respect to WT mice. In addition, IL-10 KO resolving macrophages showed an impaired induction of miR-125a-5p, miR-99b-5p and let-7e-5p that results in a augmented production of inflammatory cytokines (data not shown).

It is likely that the anti-inflammatory IL-10 and TGFβ that are produced during the acute inflammation, can induce the production of miRNA cluster and miR-146b, that act to dampening the inflammatory characteristic of macrophages to acquire a resolving phenotype.

Overall, in this project we have identify miR-125a-5p, let-7e-5p and miR-146b as a new set of anti-inflammatory miRNAs. They are actively involved in the feedback regulatory mechanism of TLR4-inflammatory pathway by a multiple targeting mechanism, directed to the receptors, the adaptor proteins and the downstream effectors. The demonstration that miR-125a-5p and miR-146b mediate the LPS desensitization supports the hypothesis that miRNA action represents an important homeostatic layer of regulation, buffering the duration and intensity of inflammatory responses. For clinical relevance, this state of LPS

hyporesponsiveness is observed in sepsis, trauma and high-risk surgery patients, in which an excessive pro-inflammatory reaction is often followed by a compensatory anti-inflammatory response syndrome, called immunoparalysis. If this immunoparalysis is long-lasting, it may therefore lead to a fatal outcome in critically ill patients due to opportunistic infections [179]. It will be interesting to speculate that modulating the level of miR-125a-5p and miR-146b can be used in therapeutic intervention for inflammation diseases.

5. REFERENCES

1. Janeway, C.A., Jr. and R. Medzhitov, *Innate immune recognition.* Annu Rev Immunol, 2002. **20**: p. 197-216.
2. Borregaard, N., *Neutrophils, from marrow to microbes.* Immunity, 2010. **33**(5): p. 657-70.
3. Brinkmann, V., et al., *Neutrophil extracellular traps kill bacteria.* Science, 2004. **303**(5663): p. 1532-5.
4. Hayashi, F., T.K. Means, and A.D. Luster, *Toll-like receptors stimulate human neutrophil function.* Blood, 2003. **102**(7): p. 2660-9.
5. Pillay, J., et al., *In vivo labeling with 2H2O reveals a human neutrophil lifespan of 5.4 days.* Blood, 2010. **116**(4): p. 625-7.
6. Tili, E., et al., *Modulation of miR-155 and miR-125b levels following lipopolysaccharide/TNF-alpha stimulation and their possible roles in regulating the response to endotoxin shock.* J Immunol, 2007. **179**(8): p. 5082-9.
7. Yona, S., et al., *Fate mapping reveals origins and dynamics of monocytes and tissue macrophages under homeostasis.* Immunity, 2013. **38**(1): p. 79-91.
8. Woollard, K.J. and F. Geissmann, *Monocytes in atherosclerosis: subsets and functions.* Nat Rev Cardiol, 2010. **7**(2): p. 77-86.
9. van Furth, R. and W. Sluiter, *Distribution of blood monocytes between a marginating and a circulating pool.* J Exp Med, 1986. **163**(2): p. 474-9.
10. Swirski, F.K., et al., *Identification of splenic reservoir monocytes and their deployment to inflammatory sites.* Science, 2009. **325**(5940): p. 612-6.
11. Hettinger, J., et al., *Origin of monocytes and macrophages in a committed progenitor.* Nat Immunol, 2013. **14**(8): p. 821-30.
12. Ginhoux, F. and S. Jung, *Monocytes and macrophages: developmental pathways and tissue homeostasis.* Nat Rev Immunol, 2014. **14**(6): p. 392-404.
13. Martinez, F.O., L. Helming, and S. Gordon, *Alternative activation of macrophages: an immunologic functional perspective.* Annu Rev Immunol, 2009. **27**: p. 451-83.

14. Gordon, S. and P.R. Taylor, *Monocyte and macrophage heterogeneity.* Nat Rev Immunol, 2005. **5**(12): p. 953-64.

15. Schulz, C., et al., *A lineage of myeloid cells independent of Myb and hematopoietic stem cells.* Science, 2012. **336**(6077): p. 86-90.

16. Gordon, S., *Alternative activation of macrophages.* Nat Rev Immunol, 2003. **3**(1): p. 23-35.

17. Hazlett, L.D., et al., *IL-33 shifts macrophage polarization, promoting resistance against Pseudomonas aeruginosa keratitis.* Invest Ophthalmol Vis Sci, 2010. **51**(3): p. 1524-32.

18. Pesce, J., et al., *The IL-21 receptor augments Th2 effector function and alternative macrophage activation.* J Clin Invest, 2006. **116**(7): p. 2044-55.

19. Bergenfelz, C., et al., *Wnt5a induces a tolerogenic phenotype of macrophages in sepsis and breast cancer patients.* J Immunol, 2012. **188**(11): p. 5448-58.

20. Mantovani, A., et al., *The chemokine system in diverse forms of macrophage activation and polarization.* Trends Immunol, 2004. **25**(12): p. 677-86.

21. Mantovani, A., et al., *Macrophage plasticity and polarization in tissue repair and remodelling.* J Pathol, 2013. **229**(2): p. 176-85.

22. Medzhitov, R. and C.A. Janeway, Jr., *Innate immunity: impact on the adaptive immune response.* Curr Opin Immunol, 1997. **9**(1): p. 4-9.

23. Gewurz, H., et al., *C-reactive protein and the acute phase response.* Adv Intern Med, 1982. **27**: p. 345-72.

24. Holmskov, U.L., *Collectins and collectin receptors in innate immunity.* APMIS Suppl, 2000. **100**: p. 1-59.

25. Garlanda, C., et al., *Pentraxins at the crossroads between innate immunity, inflammation, matrix deposition, and female fertility.* Annu Rev Immunol, 2005. **23**: p. 337-66.

26. Fraser, I.P., H. Koziel, and R.A. Ezekowitz, *The serum mannose-binding protein and the macrophage mannose receptor are pattern recognition molecules that link innate and adaptive immunity.* Semin Immunol, 1998. **10**(5): p. 363-72.

27. Peiser, L., S. Mukhopadhyay, and S. Gordon, *Scavenger receptors in innate immunity.* Curr Opin Immunol, 2002. **14**(1): p. 123-8.

28. Elomaa, O., et al., *Cloning of a novel bacteria-binding receptor structurally related to scavenger receptors and expressed in a subset of macrophages.* Cell, 1995. **80**(4): p. 603-9.

29. Franchi, L., et al., *Function of Nod-like receptors in microbial recognition and host defense.* Immunol Rev, 2009. **227**(1): p. 106-28.

30. Schlee, M., *Master sensors of pathogenic RNA - RIG-I like receptors.* Immunobiology, 2013. **218**(11): p. 1322-35.

31. Akira, S., S. Uematsu, and O. Takeuchi, *Pathogen recognition and innate immunity.* Cell, 2006. **124**(4): p. 783-801.

32. Kawai, T. and S. Akira, *The role of pattern-recognition receptors in innate immunity: update on Toll-like receptors.* Nat Immunol, 2010. **11**(5): p. 373-84.

33. Medzhitov, R., P. Preston-Hurlburt, and C.A. Janeway, Jr., *A human homologue of the Drosophila Toll protein signals activation of adaptive immunity.* Nature, 1997. **388**(6640): p. 394-7.

34. Serhan, C.N., N. Chiang, and T.E. Van Dyke, *Resolving inflammation: dual anti-inflammatory and pro-resolution lipid mediators.* Nat Rev Immunol, 2008. **8**(5): p. 349-61.

35. Akashi-Takamura, S. and K. Miyake, *TLR accessory molecules.* Curr Opin Immunol, 2008. **20**(4): p. 420-5.

36. Vabulas, R.M., et al., *Endocytosed HSP60s use toll-like receptor 2 (TLR2) and TLR4 to activate the toll/interleukin-1 receptor signaling pathway in innate immune cells.* J Biol Chem, 2001. **276**(33): p. 31332-9.

37. Kurt-Jones, E.A., et al., *Pattern recognition receptors TLR4 and CD14 mediate response to respiratory syncytial virus.* Nat Immunol, 2000. **1**(5): p. 398-401.

38. Underhill, D.M., et al., *The Toll-like receptor 2 is recruited to macrophage phagosomes and discriminates between pathogens.* Nature, 1999. **401**(6755): p. 811-5.

39. Ozinsky, A., et al., *The repertoire for pattern recognition of pathogens by the innate immune system is defined by cooperation between toll-like receptors.* Proc Natl Acad Sci U S A, 2000. **97**(25): p. 13766-71.

40. Goodridge, H.S. and D.M. Underhill, *Fungal Recognition by TLR2 and Dectin-1.* Handb Exp Pharmacol, 2008(183): p. 87-109.

41. Uematsu, S., et al., *Regulation of humoral and cellular gut immunity by lamina propria dendritic cells expressing Toll-like receptor 5.* Nat Immunol, 2008. **9**(7): p. 769-76.

42. Zhang, D., et al., *A toll-like receptor that prevents infection by uropathogenic bacteria.* Science, 2004. **303**(5663): p. 1522-6.

43. Hornung, V., et al., *Sequence-specific potent induction of IFN-alpha by short interfering RNA in plasmacytoid dendritic cells through TLR7.* Nat Med, 2005. **11**(3): p. 263-70.

44. Hemmi, H., et al., *A Toll-like receptor recognizes bacterial DNA.* Nature, 2000. **408**(6813): p. 740-5.

45. Kim, Y.M., et al., *UNC93B1 delivers nucleotide-sensing toll-like receptors to endolysosomes.* Nature, 2008. **452**(7184): p. 234-8.

46. Kaufmann, S.H., *The contribution of immunology to the rational design of novel antibacterial vaccines.* Nat Rev Microbiol, 2007. **5**(7): p. 491-504.

47. Deng, L., et al., *Activation of the IkappaB kinase complex by TRAF6 requires a dimeric ubiquitin-conjugating enzyme complex and a unique polyubiquitin chain.* Cell, 2000. **103**(2): p. 351-61.

48. Wang, C., et al., *TAK1 is a ubiquitin-dependent kinase of MKK and IKK.* Nature, 2001. **412**(6844): p. 346-51.

49. Takaoka, A., et al., *Integral role of IRF-5 in the gene induction programme activated by Toll-like receptors.* Nature, 2005. **434**(7030): p. 243-9.

50. Yamamoto, M., et al., *Regulation of Toll/IL-1-receptor-mediated gene expression by the inducible nuclear protein IkappaBzeta.* Nature, 2004. **430**(6996): p. 218-22.

51. Litvak, V., et al., *Function of C/EBPdelta in a regulatory circuit that discriminates between transient and persistent TLR4-induced signals.* Nat Immunol, 2009. **10**(4): p. 437-43.

52. Hacker, H., et al., *Specificity in Toll-like receptor signalling through distinct effector functions of TRAF3 and TRAF6.* Nature, 2006. **439**(7073): p. 204-7.

53. Kagan, J.C., et al., *TRAM couples endocytosis of Toll-like receptor 4 to the induction of interferon-beta.* Nat Immunol, 2008. **9**(4): p. 361-8.

54. O'Neill, L.A., D. Golenbock, and A.G. Bowie, *The history of Toll-like receptors - redefining innate immunity.* Nat Rev Immunol, 2013. **13**(6): p. 453-60.

55. Mercer, T.R., M.E. Dinger, and J.S. Mattick, *Long non-coding RNAs: insights into functions.* Nat Rev Genet, 2009. **10**(3): p. 155-9.

56. Bartel, D.P., *MicroRNAs: genomics, biogenesis, mechanism, and function.* Cell, 2004. **116**(2): p. 281-97.

57. Lee, R.C., R.L. Feinbaum, and V. Ambros, *The C. elegans heterochronic gene lin-4 encodes small RNAs with antisense complementarity to lin-14.* Cell, 1993. **75**(5): p. 843-54.

58. Eis, P.S., et al., *Accumulation of miR-155 and BIC RNA in human B cell lymphomas.* Proc Natl Acad Sci U S A, 2005. **102**(10): p. 3627-32.

59. Tanzer, A. and P.F. Stadler, *Molecular evolution of a microRNA cluster.* J Mol Biol, 2004. **339**(2): p. 327-35.

60. Lee, Y., et al., *MicroRNA genes are transcribed by RNA polymerase II.* EMBO J, 2004. **23**(20): p. 4051-60.

61. Gregory, R.I., T.P. Chendrimada, and R. Shiekhattar, *MicroRNA biogenesis: isolation and characterization of the microprocessor complex.* Methods Mol Biol, 2006. **342**: p. 33-47.

62. Berezikov, E., et al., *Mammalian mirtron genes.* Mol Cell, 2007. **28**(2): p. 328-36.

63. Murchison, E.P. and G.J. Hannon, *miRNAs on the move: miRNA biogenesis and the RNAi machinery.* Curr Opin Cell Biol, 2004. **16**(3): p. 223-9.

64. Lund, E. and J.E. Dahlberg, *Substrate selectivity of exportin 5 and Dicer in the biogenesis of microRNAs.* Cold Spring Harb Symp Quant Biol, 2006. **71**: p. 59-66.

65. Krol, J., et al., *Structural features of microRNA (miRNA) precursors and their relevance to miRNA biogenesis and small interfering RNA/short hairpin RNA design.* J Biol Chem, 2004. **279**(40): p. 42230-9.

66. Guo, L. and Z. Lu, *The fate of miRNA* strand through evolutionary analysis: implication for degradation as merely carrier strand or potential regulatory molecule?* PLoS One, 2010. **5**(6): p. e11387.

67. Wang, X.J., et al., *Prediction and identification of Arabidopsis thaliana microRNAs and their mRNA targets.* Genome Biol, 2004. **5**(9): p. R65.

68. Lewis, B.P., C.B. Burge, and D.P. Bartel, *Conserved seed pairing, often flanked by adenosines, indicates that thousands of human genes are microRNA targets.* Cell, 2005. **120**(1): p. 15-20.

69. Janas, M.M., et al., *Alternative RISC assembly: binding and repression of microRNA-mRNA duplexes by human Ago proteins.* RNA, 2012. **18**(11): p. 2041-55.

70. Kiriakidou, M., et al., *An mRNA m7G cap binding-like motif within human Ago2 represses translation.* Cell, 2007. **129**(6): p. 1141-51.

71. Chendrimada, T.P., et al., *MicroRNA silencing through RISC recruitment of eIF6.* Nature, 2007. **447**(7146): p. 823-8.

72. Maroney, P.A., et al., *Evidence that microRNAs are associated with translating messenger RNAs in human cells.* Nat Struct Mol Biol, 2006. **13**(12): p. 1102-7.

73. Parker, R. and U. Sheth, *P bodies and the control of mRNA translation and degradation.* Mol Cell, 2007. **25**(5): p. 635-46.

74. Winter, J., et al., *Many roads to maturity: microRNA biogenesis pathways and their regulation.* Nat Cell Biol, 2009. **11**(3): p. 228-34.

75. O'Connell, R.M., et al., *MicroRNA-155 is induced during the macrophage inflammatory response.* Proc Natl Acad Sci U S A, 2007. **104**(5): p. 1604-9.

76. Taganov, K.D., et al., *NF-kappaB-dependent induction of microRNA miR-146, an inhibitor targeted to signaling proteins of innate immune responses.* Proc Natl Acad Sci U S A, 2006. **103**(33): p. 12481-6.

77. Bazzoni, F., et al., *Induction and regulatory function of miR-9 in human monocytes and neutrophils exposed to proinflammatory signals.* Proc Natl Acad Sci U S A, 2009. **106**(13): p. 5282-7.

78. Chen, X.M., et al., *A cellular micro-RNA, let-7i, regulates Toll-like receptor 4 expression and contributes to cholangiocyte immune responses against Cryptosporidium parvum infection.* J Biol Chem, 2007. **282**(39): p. 28929-38.

79. Calin, G.A. and C.M. Croce, *MicroRNA signatures in human cancers.* Nat Rev Cancer, 2006. **6**(11): p. 857-66.

80. McCoy, C.E., et al., *IL-10 inhibits miR-155 induction by toll-like receptors.* J Biol Chem, 2010. **285**(27): p. 20492-8.

81. Salmena, L., et al., *A ceRNA hypothesis: the Rosetta Stone of a hidden RNA language?* Cell, 2011. **146**(3): p. 353-8.

82. Gerrits, A., et al., *Genetic screen identifies microRNA cluster 99b/let-7e/125a as a regulator of primitive hematopoietic cells.* Blood, 2012. **119**(2): p. 377-87.

83. Guo, S., et al., *MicroRNA miR-125a controls hematopoietic stem cell number.* Proc Natl Acad Sci U S A, 2010. **107**(32): p. 14229-34.

84. Scott, G.K., et al., *Coordinate suppression of ERBB2 and ERBB3 by enforced expression of micro-RNA miR-125a or miR-125b.* J Biol Chem, 2007. **282**(2): p. 1479-86.

85. Bi, Q., et al., *Ectopic expression of MiR-125a inhibits the proliferation and metastasis of hepatocellular carcinoma by targeting MMP11 and VEGF.* PLoS One, 2012. **7**(6): p. e40169.

86. Zhao, X., et al., *MicroRNA-125a contributes to elevated inflammatory chemokine RANTES levels via targeting KLF13 in systemic lupus erythematosus.* Arthritis Rheum, 2010. **62**(11): p. 3425-35.

87. Chen, T., et al., *MicroRNA-125a-5p partly regulates the inflammatory response, lipid uptake, and ORP9 expression in oxLDL-stimulated monocyte/macrophages.* Cardiovasc Res, 2009. **83**(1): p. 131-9.

88. Boyerinas, B., et al., *The role of let-7 in cell differentiation and cancer.* Endocr Relat Cancer, 2010. **17**(1): p. F19-36.

89. Androulidaki, A., et al., *The kinase Akt1 controls macrophage response to lipopolysaccharide by regulating microRNAs.* Immunity, 2009. **31**(2): p. 220-31.

90. Sun, D., et al., *miR-99 family of MicroRNAs suppresses the expression of prostate-specific antigen and prostate cancer cell proliferation.* Cancer Res, 2011. **71**(4): p. 1313-24.

91. Turcatel, G., et al., *MIR-99a and MIR-99b modulate TGF-beta induced epithelial to mesenchymal plasticity in normal murine mammary gland cells.* PLoS One, 2012. **7**(1): p. e31032.

92. Boldin, M.P., et al., *miR-146a is a significant brake on autoimmunity, myeloproliferation, and cancer in mice.* J Exp Med, 2011. **208**(6): p. 1189-201.

93. Nahid, M.A., et al., *miR-146a is critical for endotoxin-induced tolerance: IMPLICATION IN INNATE IMMUNITY.* J Biol Chem, 2009. **284**(50): p. 34590-9.

94. Hou, J., et al., *MicroRNA-146a feedback inhibits RIG-I-dependent Type I IFN production in macrophages by targeting TRAF6, IRAK1, and IRAK2.* J Immunol, 2009. **183**(3): p. 2150-8.

95. Tang, Y., et al., *MicroRNA-146A contributes to abnormal activation of the type I interferon pathway in human lupus by targeting the key signaling proteins.* Arthritis Rheum, 2009. **60**(4): p. 1065-75.

96. Zhai, P.F., et al., *The Regulatory Roles of MicroRNA-146b-5p and Its Target Platelet-derived Growth Factor Receptor alpha (PDGFRA) in Erythropoiesis and Megakaryocytopoiesis.* J Biol Chem, 2014. **289**(33): p. 22600-13.

97. Garcia, A.I., et al., *Down-regulation of BRCA1 expression by miR-146a and miR-146b-5p in triple negative sporadic breast cancers.* EMBO Mol Med, 2011. **3**(5): p. 279-90.

98. Raponi, M., et al., *MicroRNA classifiers for predicting prognosis of squamous cell lung cancer.* Cancer Res, 2009. **69**(14): p. 5776-83.

99. Jukic, D.M., et al., *Microrna profiling analysis of differences between the melanoma of young adults and older adults.* J Transl Med, 2010. **8**: p. 27.

100. Kanaan, Z., et al., *Differential microRNA expression tracks neoplastic progression in inflammatory bowel disease-associated colorectal cancer.* Hum Mutat, 2012. **33**(3): p. 551-60.

101. Recchiuti, A., et al., *MicroRNAs in resolution of acute inflammation: identification of novel resolvin D1-miRNA circuits.* FASEB J, 2011. **25**(2): p. 544-60.

102. Nathan, C. and A. Ding, *Nonresolving inflammation.* Cell, 2010. **140**(6): p. 871-82.

103. Recchiuti, A. and C.N. Serhan, *Pro-Resolving Lipid Mediators (SPMs) and Their Actions in Regulating miRNA in Novel Resolution Circuits in Inflammation.* Front Immunol, 2012. **3**: p. 298.

104. Clark, A.R., *Anti-inflammatory functions of glucocorticoid-induced genes.* Mol Cell Endocrinol, 2007. **275**(1-2): p. 79-97.

105. Deng, J., et al., *Protective role of reactive oxygen species in endotoxin-induced lung inflammation through modulation of IL-10 expression.* J Immunol, 2012. **188**(11): p. 5734-40.

106. Pestka, S., et al., *Interleukin-10 and related cytokines and receptors.* Annu Rev Immunol, 2004. **22**: p. 929-79.

107. Moore, K.W., et al., *Interleukin-10 and the interleukin-10 receptor.* Annu Rev Immunol, 2001. **19**: p. 683-765.

108. Weber-Nordt, R.M., et al., *Stat3 recruitment by two distinct ligand-induced, tyrosine-phosphorylated docking sites in the interleukin-10 receptor intracellular domain.* J Biol Chem, 1996. **271**(44): p. 27954-61.

109. Murray, P.J., *Understanding and exploiting the endogenous interleukin-10/STAT3-mediated anti-inflammatory response.* Curr Opin Pharmacol, 2006. **6**(4): p. 379-86.

110. Takeda, K., et al., *Enhanced Th1 activity and development of chronic enterocolitis in mice devoid of Stat3 in macrophages and neutrophils.* Immunity, 1999. **10**(1): p. 39-49.

111. Croker, B.A., et al., *SOCS3 negatively regulates IL-6 signaling in vivo.* Nat Immunol, 2003. **4**(6): p. 540-5.

112. Lang, R., et al., *Shaping gene expression in activated and resting primary macrophages by IL-10.* J Immunol, 2002. **169**(5): p. 2253-63.

113. El Kasmi, K.C., et al., *Cutting edge: A transcriptional repressor and corepressor induced by the STAT3-regulated anti-inflammatory signaling pathway.* J Immunol, 2007. **179**(11): p. 7215-9.

114. Antoniv, T.T. and L.B. Ivashkiv, *Interleukin-10-induced gene expression and suppressive function are selectively modulated by the PI3K-Akt-GSK3 pathway.* Immunology, 2011. **132**(4): p. 567-77.

115. Koppelman, B., et al., *Interleukin-10 down-regulates MHC class II alphabeta peptide complexes at the plasma membrane of monocytes by affecting arrival and recycling.* Immunity, 1997. **7**(6): p. 861-71.

116. Alessandri, A.L., et al., *Resolution of inflammation: mechanisms and opportunity for drug development.* Pharmacol Ther, 2013. **139**(2): p. 189-212.

117. Kuhn, R., et al., *Interleukin-10-deficient mice develop chronic enterocolitis.* Cell, 1993. **75**(2): p. 263-74.

118. Gupta, M., et al., *Elevated serum IL-10 levels in diffuse large B-cell lymphoma: a mechanism of aberrant JAK2 activation.* Blood, 2012. **119**(12): p. 2844-53.

119. Moore, K.W., et al., *Homology of cytokine synthesis inhibitory factor (IL-10) to the Epstein-Barr virus gene BCRFI.* Science, 1990. **248**(4960): p. 1230-4.

120. Chang, E.Y., et al., *Cutting edge: involvement of the type I IFN production and signaling pathway in lipopolysaccharide-induced IL-10 production.* J Immunol, 2007. **178**(11): p. 6705-9.

121. Ma, W., et al., *The p38 mitogen-activated kinase pathway regulates the human interleukin-10 promoter via the activation of Sp1 transcription factor in*

lipopolysaccharide-stimulated human macrophages. J Biol Chem, 2001. **276**(17): p. 13664-74.

122. Hu, X., et al., *IFN-gamma suppresses IL-10 production and synergizes with TLR2 by regulating GSK3 and CREB/AP-1 proteins.* Immunity, 2006. **24**(5): p. 563-74.

123. Saraiva, M. and A. O'Garra, *The regulation of IL-10 production by immune cells.* Nat Rev Immunol, 2010. **10**(3): p. 170-81.

124. Quinn, S.R. and L.A. O'Neill, *The role of microRNAs in the control and mechanism of action of IL-10.* Curr Top Microbiol Immunol, 2014. **380**: p. 145-55.

125. Sharma, A., et al., *Antagonism of mmu-mir-106a attenuates asthma features in allergic murine model.* J Appl Physiol (1985), 2012. **113**(3): p. 459-64.

126. Ma, F., et al., *MicroRNA-466l upregulates IL-10 expression in TLR-triggered macrophages by antagonizing RNA-binding protein tristetraprolin-mediated IL-10 mRNA degradation.* J Immunol, 2010. **184**(11): p. 6053-9.

127. Sheedy, F.J., et al., *Negative regulation of TLR4 via targeting of the proinflammatory tumor suppressor PDCD4 by the microRNA miR-21.* Nat Immunol, 2010. **11**(2): p. 141-7.

128. Rossato, M., et al., *IL-10-induced microRNA-187 negatively regulates TNF-alpha, IL-6, and IL-12p40 production in TLR4-stimulated monocytes.* Proc Natl Acad Sci U S A, 2012. **109**(45): p. E3101-10.

129. Curtale, G., et al., *Negative regulation of Toll-like receptor 4 signaling by IL-10-dependent microRNA-146b.* Proc Natl Acad Sci U S A, 2013. **110**(28): p. 11499-504.

130. Blobe, G.C., W.P. Schiemann, and H.F. Lodish, *Role of transforming growth factor beta in human disease.* N Engl J Med, 2000. **342**(18): p. 1350-8.

131. Gordon, K.J. and G.C. Blobe, *Role of transforming growth factor-beta superfamily signaling pathways in human disease.* Biochim Biophys Acta, 2008. **1782**(4): p. 197-228.

132. Govinden, R. and K.D. Bhoola, *Genealogy, expression, and cellular function of transforming growth factor-beta.* Pharmacol Ther, 2003. **98**(2): p. 257-65.

133. Roberts, A.B. and M.B. Sporn, *Differential expression of the TGF-beta isoforms in embryogenesis suggests specific roles in developing and adult tissues.* Mol Reprod Dev, 1992. **32**(2): p. 91-8.

134. Annes, J.P., J.S. Munger, and D.B. Rifkin, *Making sense of latent TGFbeta activation.* J Cell Sci, 2003. **116**(Pt 2): p. 217-24.

135. Massague, J. and D. Wotton, *Transcriptional control by the TGF-beta/Smad signaling system.* EMBO J, 2000. **19**(8): p. 1745-54.

136. Sirard, C., et al., *Targeted disruption in murine cells reveals variable requirement for Smad4 in transforming growth factor beta-related signaling.* J Biol Chem, 2000. **275**(3): p. 2063-70.

137. Shi, Y. and J. Massague, *Mechanisms of TGF-beta signaling from cell membrane to the nucleus.* Cell, 2003. **113**(6): p. 685-700.

138. Li, M.O., et al., *Transforming growth factor-beta regulation of immune responses.* Annu Rev Immunol, 2006. **24**: p. 99-146.

139. Ikushima, H. and K. Miyazono, *TGFbeta signalling: a complex web in cancer progression.* Nat Rev Cancer, 2010. **10**(6): p. 415-24.

140. Kulkarni, A.B., et al., *Transforming growth factor beta 1 null mutation in mice causes excessive inflammatory response and early death.* Proc Natl Acad Sci U S A, 1993. **90**(2): p. 770-4.

141. Shull, M.M., et al., *Targeted disruption of the mouse transforming growth factor-beta 1 gene results in multifocal inflammatory disease.* Nature, 1992. **359**(6397): p. 693-9.

142. Gorelik, L. and R.A. Flavell, *Transforming growth factor-beta in T-cell biology.* Nat Rev Immunol, 2002. **2**(1): p. 46-53.

143. Wahl, S.M., et al., *Transforming growth factor type beta induces monocyte chemotaxis and growth factor production.* Proc Natl Acad Sci U S A, 1987. **84**(16): p. 5788-92.

144. Naiki, Y., et al., *Transforming growth factor-beta differentially inhibits MyD88-dependent, but not TRAM- and TRIF-dependent, lipopolysaccharide-induced TLR4 signaling.* J Biol Chem, 2005. **280**(7): p. 5491-5.

145. Werner, F., et al., *Transforming growth factor-beta 1 inhibition of macrophage activation is mediated via Smad3.* J Biol Chem, 2000. **275**(47): p. 36653-8.

146. Takeuchi, M., P. Alard, and J.W. Streilein, *TGF-beta promotes immune deviation by altering accessory signals of antigen-presenting cells.* J Immunol, 1998. **160**(4): p. 1589-97.

147. Zhong, H., et al., *Targeting Smad4 links microRNA-146a to the TGF-beta pathway during retinoid acid induction in acute promyelocytic leukemia cell line.* Int J Hematol, 2010. **92**(1): p. 129-35.

148. Tzur, G., et al., *Comprehensive gene and microRNA expression profiling reveals a role for microRNAs in human liver development.* PLoS One, 2009. **4**(10): p. e7511.

149. Gregory, P.A., et al., *The miR-200 family and miR-205 regulate epithelial to mesenchymal transition by targeting ZEB1 and SIP1.* Nat Cell Biol, 2008. **10**(5): p. 593-601.

150. Betel, D., et al., *Comprehensive modeling of microRNA targets predicts functional non-conserved and non-canonical sites.* Genome Biol, 2010. **11**(8): p. R90.

151. Ovcharenko, I., et al., *Mulan: multiple-sequence local alignment and visualization for studying function and evolution.* Genome Res, 2005. **15**(1): p. 184-94.

152. Waterhouse, A.M., et al., *Jalview Version 2--a multiple sequence alignment editor and analysis workbench.* Bioinformatics, 2009. **25**(9): p. 1189-91.

153. Murray, P.J., *The primary mechanism of the IL-10-regulated antiinflammatory response is to selectively inhibit transcription.* Proc Natl Acad Sci U S A, 2005. **102**(24): p. 8686-91.

154. Rossato, M., et al., *IL-10 modulates cytokine gene transcription by protein synthesis-independent and dependent mechanisms in lipopolysaccharide-treated neutrophils.* Eur J Immunol, 2007. **37**(11): p. 3176-89.

155. Alas, S. and B. Bonavida, *Inhibition of constitutive STAT3 activity sensitizes resistant non-Hodgkin's lymphoma and multiple myeloma to chemotherapeutic drug-mediated apoptosis.* Clin Cancer Res, 2003. **9**(1): p. 316-26.

156. Liu, J., et al., *Argonaute2 is the catalytic engine of mammalian RNAi.* Science, 2004. **305**(5689): p. 1437-41.

157. Herrero, C., et al., *Reprogramming of IL-10 activity and signaling by IFN-gamma.* J Immunol, 2003. **171**(10): p. 5034-41.

158. Nylander, S. and C. Mattsson, *Thrombin-induced platelet activation and its inhibition by anticoagulants with different modes of action.* Blood Coagul Fibrinolysis, 2003. **14**(2): p. 159-67.

159. Benkhart, E.M., et al., *Role of Stat3 in lipopolysaccharide-induced IL-10 gene expression.* J Immunol, 2000. **165**(3): p. 1612-7.

160. Natarajan, K., et al., *Caffeic acid phenethyl ester is a potent and specific inhibitor of activation of nuclear transcription factor NF-kappa B.* Proc Natl Acad Sci U S A, 1996. **93**(17): p. 9090-5.

161. Cuzzocrea, S., et al., *Pyrrolidine dithiocarbamate attenuates the development of acute and chronic inflammation.* Br J Pharmacol, 2002. **135**(2): p. 496-510.

162. Auwerx, J., *The human leukemia cell line, THP-1: a multifacetted model for the study of monocyte-macrophage differentiation.* Experientia, 1991. **47**(1): p. 22-31.

163. Ostuni, R., I. Zanoni, and F. Granucci, *Deciphering the complexity of Toll-like receptor signaling.* Cell Mol Life Sci, 2010. **67**(24): p. 4109-34.

164. Qi, X.F., et al., *Essential involvement of cross-talk between IFN-gamma and TNF-alpha in CXCL10 production in human THP-1 monocytes.* J Cell Physiol, 2009. **220**(3): p. 690-7.

165. Heagy, W., et al., *Evidence for a CD14- and serum-independent pathway in the induction of endotoxin-tolerance in human monocytes and THP-1 monocytic cells.* Shock, 2003. **19**(4): p. 321-7.

166. West, M.A. and A. Koons, *Endotoxin tolerance in sepsis: concentration-dependent augmentation or inhibition of LPS-stimulated macrophage TNF*

secretion by LPS pretreatment. J Trauma, 2008. **65**(4): p. 893-8; discussion 898-900.

167. Melo, E.S., et al., *Gene expression reprogramming protects macrophage from septic-induced cell death.* Mol Immunol, 2010. **47**(16): p. 2587-93.

168. Randow, F., et al., *In vitro prevention and reversal of lipopolysaccharide desensitization by IFN-gamma, IL-12, and granulocyte-macrophage colony-stimulating factor.* J Immunol, 1997. **158**(6): p. 2911-8.

169. Bundschuh, D.S., et al., *Granulocyte-macrophage colony-stimulating factor and IFN-gamma restore the systemic TNF-alpha response to endotoxin in lipopolysaccharide-desensitized mice.* J Immunol, 1997. **158**(6): p. 2862-71.

170. Varma, T.K., et al., *Cellular mechanisms that cause suppressed gamma interferon secretion in endotoxin-tolerant mice.* Infect Immun, 2001. **69**(9): p. 5249-63.

171. Randow, F., et al., *Mechanism of endotoxin desensitization: involvement of interleukin 10 and transforming growth factor beta.* J Exp Med, 1995. **181**(5): p. 1887-92.

172. Schroder, M., et al., *Different modes of IL-10 and TGF-beta to inhibit cytokine-dependent IFN-gamma production: consequences for reversal of lipopolysaccharide desensitization.* J Immunol, 2003. **170**(10): p. 5260-7.

173. Ajuebor, M.N., et al., *Role of resident peritoneal macrophages and mast cells in chemokine production and neutrophil migration in acute inflammation: evidence for an inhibitory loop involving endogenous IL-10.* J Immunol, 1999. **162**(3): p. 1685-91.

174. Banerjee, S., et al., *miR-125a-5p regulates differential activation of macrophages and inflammation.* J Biol Chem, 2013. **288**(49): p. 35428-36.

175. Baek, D., et al., *The impact of microRNAs on protein output.* Nature, 2008. **455**(7209): p. 64-71.

176. Guo, H., et al., *Mammalian microRNAs predominantly act to decrease target mRNA levels.* Nature, 2010. **466**(7308): p. 835-40.

177. Bystrom, J., et al., *Resolution-phase macrophages possess a unique inflammatory phenotype that is controlled by cAMP.* Blood, 2008. **112**(10): p. 4117-27.

178. Stables, M.J., et al., *Transcriptomic analyses of murine resolution-phase macrophages.* Blood, 2011. **118**(26): p. e192-208.

179. Docke, W.D., et al., *Monocyte deactivation in septic patients: restoration by IFN-gamma treatment.* Nat Med, 1997. **3**(6): p. 678-81.

6. APPENDICES

Negative regulation of Toll-like receptor 4 signaling by IL-10–dependent microRNA-146b

Graziella Curtale[a,b], Massimiliano Mirolo[b], Tiziana Ada Renzi[a,b], Marzia Rossato[c], Flavia Bazzoni[c], and Massimo Locati[a,b,1]

[a]Department of Medical Biotechnologies and Translational Medicine, University of Milan, 20089 Rozzano, Italy; [b]Humanitas Clinical and Research Center, 20089 Rozzano, Italy; and [c]Division of General Pathology, Department of Pathology, University of Verona, 37134 Verona, Italy

Edited by Ruslan Medzhitov, Yale University School of Medicine, New Haven, CT, and approved May 28, 2013 (received for review November 15, 2012)

Toll-like receptors (TLRs) play key roles in detecting pathogens and initiating inflammatory responses that, subsequently, prime specific adaptive responses. Several mechanisms control TLR activity to avoid excessive inflammation and consequent immunopathology, including the anti-inflammatory cytokine IL-10. Recently, several TLR-responsive microRNAs (miRs) have also been proposed as potential regulators of this signaling pathway, but their functional role during the inflammatory response still is incompletely understood. In this study, we report that, after LPS engagement, monocytes up-regulate miR-146b via an IL-10–mediated STAT3-dependent loop. We show evidence that miR-146b modulates the TLR4 signaling pathway by direct targeting of multiple elements, including the LPS receptor TLR4 and the key adaptor/signaling proteins myeloid differentiation primary response (MyD88), interleukin-1 receptor-associated kinase 1 (IRAK-1), and TNF receptor-associated factor 6 (TRAF6). Furthermore, we demonstrate that the enforced expression of miR-146b in human monocytes led to a significant reduction in the LPS-dependent production of several proinflammatory cytokines and chemokines, including IL-6, TNF-α, IL-8, CCL3, CCL2, CCL7, and CXCL10. Our results thus identify miR-146b as an IL-10–responsive miR with an anti-inflammatory activity based on multiple targeting of components of the TLR4 pathway in monocytes and candidate miR-146b as a molecular effector of the IL-10 anti-inflammatory activity.

Toll-like receptors (TLRs) have important roles in detecting pathogens and initiating inflammatory responses that, subsequently, prime specific adaptive immune responses during infection (1). It is therefore important that TLR signaling pathways are tightly regulated. One of the most effective suppressor of TLR-induced inflammatory cytokine production is IL-10, which displays powerful inhibitory actions on innate immune cells (2,3), not only by direct inhibition of cytokine transcription (4,5) but also by destabilizing their coding RNA (6) and blocking their translation (7). MicroRNAs (miRs) are small (22–24 nt) noncoding RNA sequences acting primarily as translational repressors of gene transcripts by interacting with their 3′ UTRs (8,9). In the field of inflammation, miRs are attracting increasingly interest for their ability to regulate strength and timing of TLR responses (10). Although their role in the resolution of inflammation is just beginning to be explored, their emerging importance in the modulation of TLR signaling strongly suggests a possible regulation of their expression by anti-inflammatory stimuli. In this respect, IL-10 has been recently shown to inhibit miR-155 induction by TLRs (11), thus increasing the expression of the miR-155 target gene SH2 domain-containing inositol-5′-phosphatase 1 (SHIP1) and promoting expression of anti-inflammatory genes (12). Moreover, a direct role of miR-187 in IL-10–mediated suppression of proinflammatory cytokines has been recently demonstrated (13), and miR-21 has been reported to promote an anti-inflammatory response by increasing IL-10 production through the down-regulation of programmed cell death 4 (PDCD4) (14). We here report that LPS induces expression of miR-146b via an IL-10–dependent loop, and demonstrate that miR-146b play an anti-inflammatory role in monocytes by direct targeting multiple elements involved in the TLR4 signaling pathway, thus making this miR a candidate feedback modulator of the LPS response potentially involved in inflammation resolution.

Results

MiR-146b Expression Is Induced by IL-10 in Human Monocytes. TLRs have been shown to regulate a distinct panel of miR in monocytes, including miR-155 and miR-146a (15-17). We have here identified miR-146b, a second member of the miR-146 family located within an intergenic region on chromosome 10, as an LPS-responsive miR induced at a later time point compared with miR-146a and miR-155 (Fig. 1*A*). MiR-146b induction by LPS was also mirrored by its enrichment in the RNA-induced silencing complex (RISC), suggesting its functional role in human primary monocytes (Fig. S1*A*). Analysis of miR-146b expression in monocytes stimulated with IL-1β and different TLR agonists, including the TLR2 agonist palmitoyl-3-cysteine-serine-lysine 4 (Pam_3CsK_4), the TLR3 agonist poly(I:C), the TLR7 agonist imiquimod, and the TLR9 agonist synthetic CpG oligonucleotides (ODN), showed that miR-146b induction is restricted to the signaling pathway activated by IL-1β and TLR2/TLR4 (Fig. S2*A*). As the ability of different stimuli to induce miR-146b directly correlates with their ability to induce IL-10 production (Fig. S2*B*), we asked whether IL-10 could be involved in the induction of miR-146b by LPS. As shown in Fig. 1*B*, IL-10 stimulation induced miR-146b but was unable to induce expression of miR-146a and miR-155, and suppressed the LPS-dependent induction of miR-155, as previously reported (11). Consistent with these results, the inhibition of the LPS-induced endogenous IL-10 by using an anti–IL-10 receptor blocking monoclonal antibody or the JAK/STAT inhibitor AG-490 (18) resulted in a significant reduction of miR-146b induction by LPS, whereas miR-146a expression was not affected and miR-155 levels were further increased (Fig. 2 *A*–*C*). Finally, the LPS-dependent induction of miR-146b observed in murine bone marrow-derived macrophages was severely reduced when macrophages were obtained from IL-$10^{-/-}$ animals, indicating that, also in the murine system, miR-146b is induced by LPS via an IL-10–dependent feedback loop. Conversely, miR-146a induction by LPS was not significantly different in WT and IL-$10^{-/-}$ macrophages, further demonstrating the IL-10 dependency of miR-146b and not miR-146a (Fig. 1*C*).

The human mature miR-146b is generated by processing of the premiR-146b molecule transcribed from an intergenic region on chromosome 10, with the predicted transcription start site located 700 bp upstream of the mature miR-146b sequence (15). To gain additional insight into the role of IL-10 in the transcriptional regulation of miR-146b in monocytes, the recruitment of polymerase II (Pol II) to the miR-146b promoter region in the presence of LPS or IL-10 was investigated. As expected, ChIP analysis indicated that, in LPS-stimulated monocytes, Pol II was recruited

Author contributions: G.C. and M.L. designed research; G.C., M.M., and T.A.R. performed research; G.C., M.M., T.A.R., and M.R. analyzed data; and G.C., F.B., and M.L. wrote the paper.

The authors declare no conflict of interest.

This article is a PNAS Direct Submission.

Freely available online through the PNAS open access option.

[1]To whom correspondence should be addressed. E-mail: massimo.locati@humanitasresearch.it.

This article contains supporting information online at www.pnas.org/lookup/suppl/doi:10.1073/pnas.1219852110/-/DCSupplemental.

IMMUNOLOGY

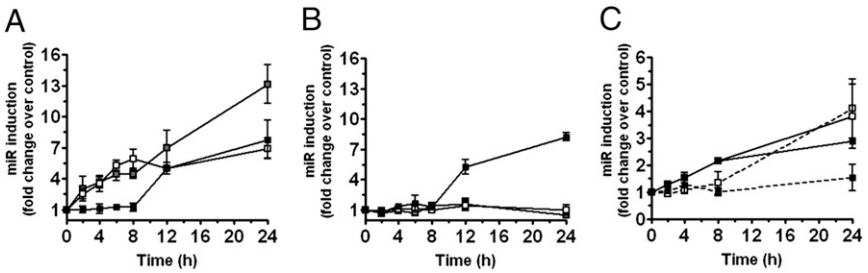

Fig. 1. IL-10 induces miR-146b expression. Expression levels of miR-146a (white symbols), miR-146b (black symbols), and miR-155 (gray symbols) were measured by qPCR in triplicate samples of human monocytes cultured for the indicated times with 100 ng/mL LPS (*A*) or with 20 ng/mL IL-10 (*B*). Results are expressed as fold change vs. untreated cells (mean ± SEM; $n = 3$). (*C*) Bone marrow-derived macrophages from WT (solid line) or IL-10$^{-/-}$ mice (dashed line) were stimulated or not stimulated for the indicated time with 100 ng/mL LPS, and expression of miR-146b (closed symbols) and miR-146a (open symbols) was quantified by qPCR in triplicate samples. Results expressed as fold change vs. untreated cells (mean ± SEM; $n = 3$).

to the miR-146b promoter, as well as to the miR-146a and miR-155 promoters (Fig. 2 *D–F*). Conversely, in monocytes stimulated with IL-10, Pol II recruitment was observed only on the promoter region of miR-146b and not miR-146a or miR-155, consistent with the selective IL-10–mediated up-regulation of miR-146b expression (Fig. 2 *D–F*). To identify putative *cis*-regulatory elements critical for IL-10–dependent gene transcription, a comparative bioinformatic analysis covering 1,000 bp upstream of the premiR-146b coding region was performed. Conserved putative binding sites for STAT3, the main transcription factor mediating the IL-10 anti-inflammatory action in monocytes (19), were predicted on both miR-146a and miR-146b promoter regions (Fig. 2*G*); however, ChIP analysis on monocytes stimulated with IL-10 showed an IL-10–dependent significant recruitment of STAT3 protein on the region encompassing the two predicted STAT3 binding sites exclusively in the miR-146b promoter region, whereas no STAT3 recruitment was found on the miR-146a promoter region (Fig. 2*H*). In the miR-146b promoter region, two putative NF-κB binding sites were also predicted. Interestingly, the NF-κB chemical inhibitors caffeic acid phenetyl ester (CAPE) and pyrrolidine dithiocarbamate (PDTC) significantly inhibited miR-146a expression levels, consistent with previous reports of NF-κB driving the expression of miR-146a in LPS-stimulated monocytes (15), but had no role on miR-146b induction by LPS in monocytes (Fig. 2*I*). These data indicate that miR-146a and miR-146b undergo a profound different regulation in monocytes exposed to pro- and anti-inflammatory stimuli and identify miR-146b, but not miR-146a, as an IL-10–dependent miR, suggesting that miR-146b may play a role in mediating the anti-inflammatory activity of IL-10.

The TLR/IL-1 Receptor Signaling Pathway as a miR-146b Target. To gain insight into the functional role of miR-146b in the context of LPS-mediated inflammation, we chose an *in silico* approach to identify potential miR-146b targets. As algorithms based on seed pairing and evolutionary conservation typically have low specificity predictive value, we combined miRanda (20) predictions with pathways analysis based on the Ingenuity Pathway Analysis database (www.ingenuity.com), mapping biomolecular networks based on known pathways, Gene Ontology, and interactions. Interestingly, miR-146b targets showed significant enrichment in "TLR signaling," "NF-κB signaling," and "IL-1β signaling" pathways (Fig. 3), leading us to investigate the hypothesis that miR-146b may contribute to the IL-10-dependent feedback inhibitory loop fine

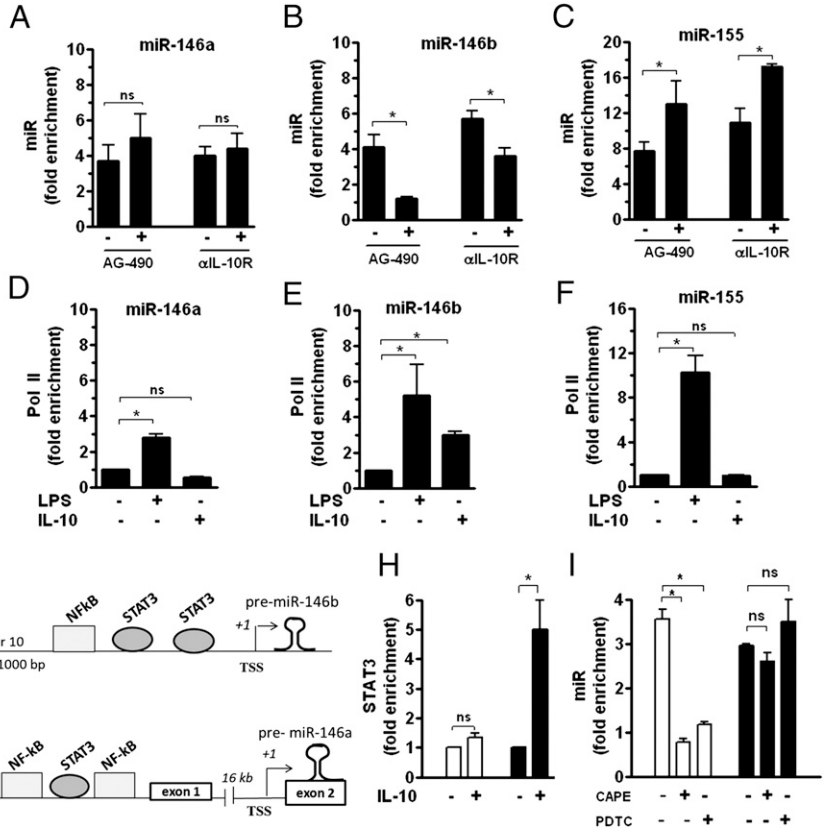

Fig. 2. MiR-146b induction after LPS challenge is driven by IL-10. (*A–C*) Human monocytes were pretreated or not pretreated for 30 min with 5 μM of the JAK/STAT inhibitor AG-490 and then stimulated for 12 h with 100 ng/mL LPS. Alternatively, monocytes stimulated for 12 h with 100 ng/mL LPS were cultured in the presence of 10 μg/mL anti-IL-10 receptor (-αIL-10R) or isotype control mAb. MiR levels were measured by qPCR in triplicate samples and results expressed as fold change vs. control (mean ± SEM; $n = 3$). ChIP assays were carried out by using anti-Pol II Ab and analyzed by qPCR with specific primers binding to the miR-146b, miR-146a, and miR-155 promoters (*D*, *E*, and *F*, respectively). Data from qPCR have been normalized to input DNA and displayed as fold change vs. untreated cells (mean ± SEM; $n = 3$). (*G*) Graphical representation of predicted promoter regions reporting binding sites of transcription factors of potential interest. (*H*) Monocytes were stimulated or not stimulated for 4 h with 20 ng/mL IL-10. ChIP assays were carried out by using anti-STAT3 Ab and analyzed by qPCR with specific primers binding to miR-146a (white columns) and miR-146b (black columns) promoters. (*I*) Cells were pretreated for 1 h with the NF-κB inhibitors PDTC (1 μM) or CAPE (2 μM) and then stimulated for 12 h with 100 ng/mL LPS. MiR-146a (white columns) and miR-146b (black columns) expression levels were measured by qPCR in triplicate samples and results expressed as fold change vs. control (mean ± SEM; $n = 3$).

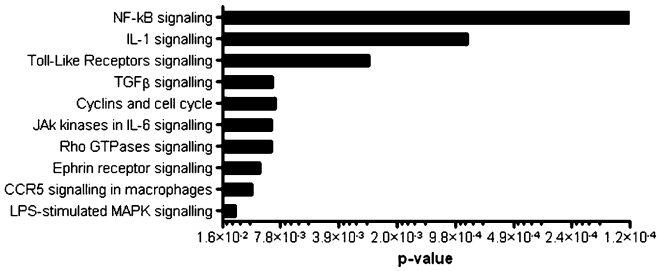

Fig. 3. miR-146b targets the TLR signaling pathway. Canonical pathways significantly enriched for miR-146b predicted target genes as identified by the Ingenuity Pathways Analysis library.

tuning the inflammatory response induced in monocytes by TLR/IL-1 receptor (IL-1R) activation. In particular, miR-146b was predicted to directly target both receptors and key signal transducers of the TLR/IL-1 signaling pathway but not effector molecules, with the remarkable exception of IL-6 (Fig. S3).

TLR4 Is a Direct Target of miR-146b. To validate predictions, the direct targeting of TLR2 and TLR4 by miR-146b was investigated. In 293T cells, miR-146b significantly decreased luciferase activity of a reporter gene containing the TLR4 3′UTR, and the deletion of 5 nt in the 3′UTR seed match sequence abolished the inhibitory effect of miR-146b on luciferase levels, indicating that the observed down-regulation was dependent on the predicted miR-146b target site (Fig. 4*A*). The significant enrichment of TRL4 mRNA in the RISC complexes immunoprecipitated from human monocytic THP-1 cells transduced with the lentiviral-based expression vector pRRL-miR146b, compared with THP-1 cells transduced with the control lentiviral construct pRRL-ctrl, provide direct evidence that miR-146b directly targets TLR4 (Fig. 4*B*). Consistent with this, pRRL-146b–transduced THP-1 cells showed a significant decrease of TLR4 protein levels compared with THP-1 cells transduced with pRRL-ctrl [mean fluorescence intensity (MFI), pRRL-ctrl, 1,117 ± 120; pRRL-146b, 790 ± 98; $P < 0.05$; Fig. 4*C*]. Protein reduction was not mirrored by a corresponding reduction at the transcript level (pRRL-ctrl, 0.040 ± 0.25; pRRL-146b, 0.044 ± 0.19, relative to GAPDH), indicating that miR-146b acts by blocking translation of TLR4 mRNA. As a complementary approach, we used lentiviral expression vectors to obtain a permanent miR-146b inhibition (miRzip-146b), and we found a significant decrease of TLR4 transcript in the RISC complex of LPS-stimulated THP-1 cells (Fig. 4*B*), also mirrored by a corresponding increase of TLR4 protein in miRzip-146b cells compared with miRzip-ctrl THP-1 cells (MFI, miRzip-ctrl, 3,616 ± 98; miRzip-146b, 5,323 ± 111; $P < 0.05$; Fig. 4*D*). Conversely, miR-146b overexpression did not induce any impairment of the TLR2 transcript stability as assessed by luciferase assay (Fig. 4*E*), did not enrich TLR2 transcript in the RISC complex (Fig. 4*F*), and did not reduce TLR2 protein expression (MFI, pRRL-ctrl, 1,671 ± 59; pRRL-146b, 1,530 ± 61; *P* value not significant; Fig. 4*G*). In parallel experiments, THP-1 cells stimulated with LPS in the presence of miRzip-146b did not show any increase of the TLR2 transcript in the RISC complex (Fig. 4*F*), nor a decrease in TLR2 protein expression compared with miRzip-ctrl THP-1 cells (MFI, miRzip-ctrl, 1,001 ± 20; miRzip-146b, 1,186.5 ± 157; *P* value not significant; Fig. 4*H*). Taken together, these results indicate that, contrary to predictions, TLR2 is not a direct target of miR-146b.

Multitargeting of TLR Signaling Pathway by miR-146b. As the TLR/IL-1R signaling pathway scored as a major target of miR-146b, signaling adaptors involved in this pathway were investigated. Luciferase assays validated myeloid differentiation primary response 88 (MyD88), interleukin-1 recpetor-associated kinase 1 (IRAK-1), and TNF receptor-associated factor 6 (TRAF6) as direct targets of miR-146b, and, in all cases, abrogation of miR-146b effects by mutagenesis of its seed match regions in target 3′UTR demonstrated the specificity of its action (Fig. 5 *A*, *E*, and *I*, respectively). Consistent with this, RISC immunoprecipitation (RIP) analysis revealed a significant enrichment of MyD88, IRAK-1, and TRAF6 transcripts in pRRL-146b–transduced THP-1 cells and a corresponding reduction in THP-1 cells transduced with miRzip-146b but not miRzip-ctrl (Fig. 5 *B*, *F*, and *L*, respectively). Western blot analysis confirmed that enforced expression of miR-146b reduced MyD88, IRAK-1, and TRAF6 protein levels (Fig. 5 *C*, *G*, and *M*, respectively), whereas miR-146b inhibition enhanced their protein expression levels (Fig. 5 *D*, *H,* and *N*). Conversely, even though IL-6 was also predicted as a direct target of miR-146b, luciferase assay on the IL-6 3′UTR and RIP assay did not confirm this prediction (Fig. 5 *O* and *P*, respectively). Quantitative real-time PCR (qPCR) experiments revealed that miR-146b targeting affected stability of MyD88 and TRAF6 but not IRAK-1 transcripts, suggesting that, in this latter case, the miR-146b effect is likely mediated by translation repression. Conversely, miR-146a significantly destabilized IRAK-1 and TRAF6 but not MyD88 transcript (Fig. S4 *A–C*). The predicted energy interactions of miR-146a and miR-146b on their corresponding seeds on these targets did not correlate with their effect on the transcripts' stability (Fig. S4 *A–C*), indicating the involvement of other still unknown parameters. Taken together, these results demonstrate that miR-146b targets multiple elements involved in the TLR signaling system, as previously described for miR-146a (15), but also indicate that the two miR-146 isoforms adopt different mechanisms to regulate TLR adaptors, suggesting they may exert different functions on the TLR signaling pathway.

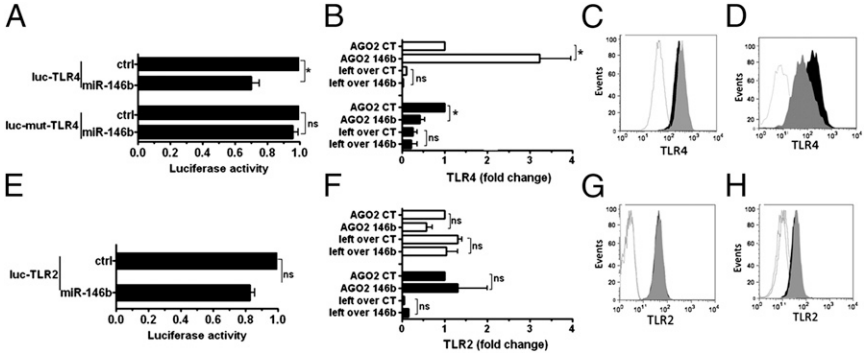

Fig. 4. TLR4 is a direct target of miR-146b. (*A* and *E*) Luciferase constructs with the entire 3′UTR of TLR4 (luc-TLR4) or the corresponding construct mutated in the miR-146b seed region (luc-mut-TLR4) or TLR2 (luc-TLR2) were cotransfected in 293T cells with miR-146b mimic or a negative control mimic (ctrl). Results are expressed as the ratio between *renilla* and *firefly* luciferase activities (mean percent variation ± SEM; $n = 3$). (*B* and *F*) Cell extracts from THP-1 cells transduced with pRRL-ctrl (CT; closed columns) or pRRL-146b (146b; closed columns) or transduced with miRzip-ctrl (CT; open columns) or miRzip-146b (146b; closed columns) were subjected to RIP assay by using anti-Ago2 or IgG control Abs, and levels of TLR4 and TLR2 transcripts (*B* and *F*, respectively) were assayed in triplicate by qPCR in RIP (IP AGO2) and leftover samples. Results are expressed as normalized fold enrichment (mean percent variation ± SEM; $n = 3$). (*C*, *D*, *G*, and *H*) Protein levels were measured by flow cytometry on THP-1 cells transduced with pRRL-ctrl (gray histogram) or pRRL-146b (black histogram) (*C* and *G*, TLR4 and TRL2, respectively) or with miRzip-ctrl (gray) or miRzip-146b (black; *D* and *H*, TLR4 and TRL2, respectively). The isotype control staining is shown by the white histogram. One experiment representative of four performed with similar results is shown.

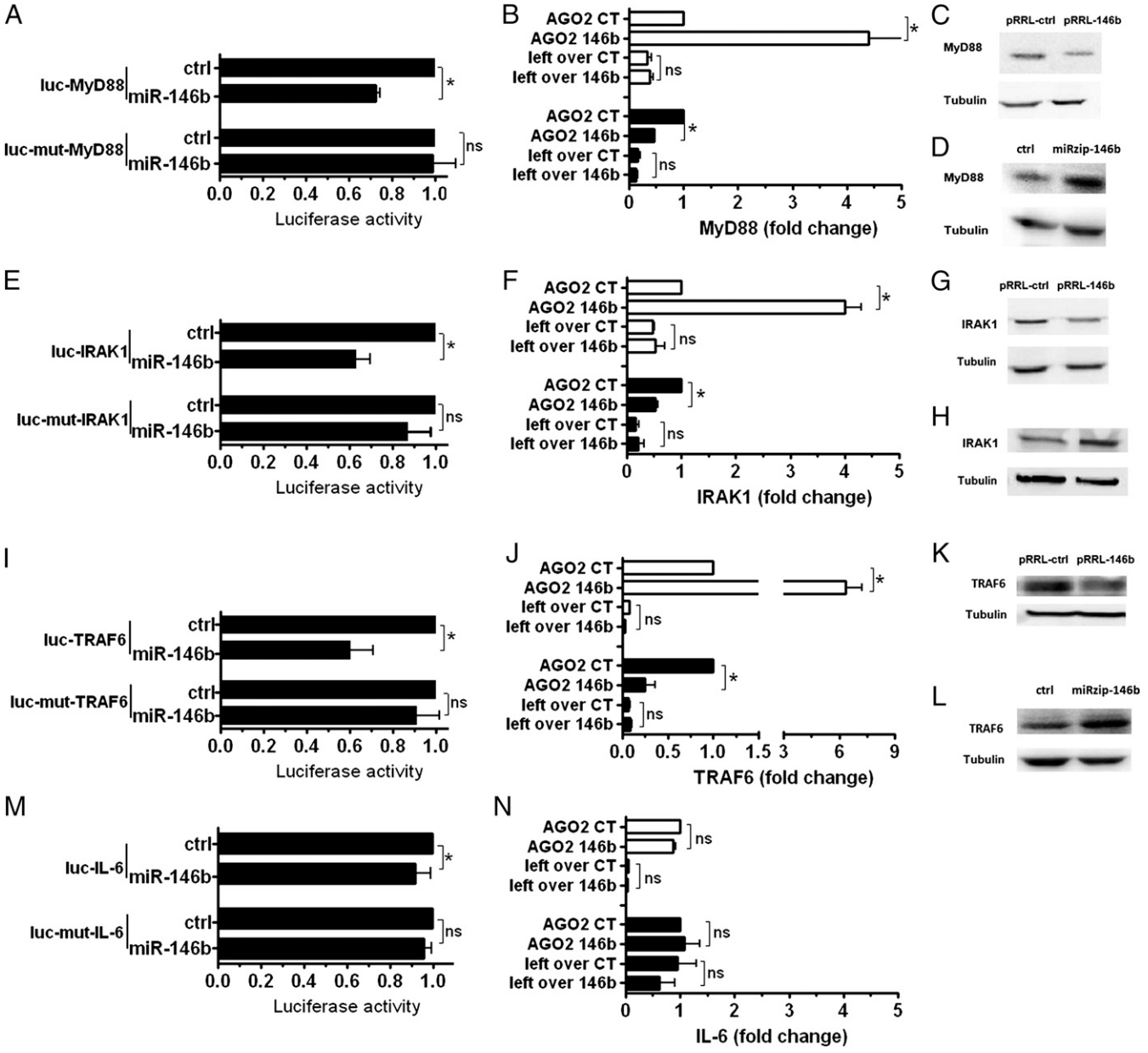

Fig. 5. Multitargeting of the TLR4 signaling pathway by miR-146b. 3′UTR luciferase constructs were cotransfected in 293T cells with miR-146b mimic or a negative control mimic (ctrl). MyD88 (*A*), IRAK-1 (*E*), TRAF6 (*I*), and IL-6 (*M*). Results are expressed as the ratio between renilla and firefly luciferase activities (mean percent variation ± SEM; $n = 3$). Cell extracts from pRRL-ctrl–transduced (CT) or pRRL-146b–transduced (146b) THP-1 cells (white histograms); miRzip-ctrl–transduced or miRzip-146b–transduced THP-1 cells (black histograms) were subjected to RIP assay by using anti-Ago2 or IgG control Abs. Levels of MyD88 (*B*), IRAK-1 (*F*), TRAF6 (*J*), and IL-6 (*N*) mRNAs were assayed in triplicate by qPCR in RIP (IP AGO2) and leftover samples and expressed as normalized fold enrichment. (mean percent variation ± SEM; $n = 3$). Protein levels were analyzed by Western blot and normalized on tubulin, used as loading controls. MyD88 (*C* and *D*), IRAK-1 (*G* and *H*), and TRAF6 (*K* and *L*). One experiment representative of four is shown.

MiR-146b Controls Induction of Proinflammatory Cytokines by TLR Agonists. As we demonstrated a direct targeting of multiple elements involved in the TLR/IL-1R signaling pathway by miR-146b, we investigated its biological impact on the TLR-dependent production of proinflammatory cytokines. In THP-1 cells exposed to LPS, we observed a significant reduction of proinflammatory cytokine and chemokines when miR-146b expression was enhanced by cell transduction with pRRL-146b and a significant enhancement when miR-146b expression was inhibited by cell transduction with miRzip-146b (Fig. 6 *A*–*H*). Similar results were obtained when the TLR2 agonist Pam_3CsK_4 was used (Fig. S5). Finally, we measured the effect of miR-146b on the production of the IFN-inducible CXCL10 induced by LPS, mainly a secondary consequence of TRIF-dependent IFN-β production, or IFN-γ, which operates through the activation of a MyD88/IRAK-1–independent STAT1-dependent pathway (21). Consistent with the notion that miR-146b specifically operates on the TLR/IL-1R signaling pathway, the induction of CXCL10 production by LPS was significantly impaired in pRRL-146b–transduced THP-1 cells and enhanced in miRzip-146b–transduced THP1 cells (Fig. 6*H*), whereas its induction by IFN-γ was unaffected (Fig. 6*I*). Taken together, these data identify miR-146b as an anti-inflammatory miR able to reduce the inflammatory signal transmitted through the engagement of TLR4 by a multiple targeting mechanisms directed to the receptor and its adaptor proteins.

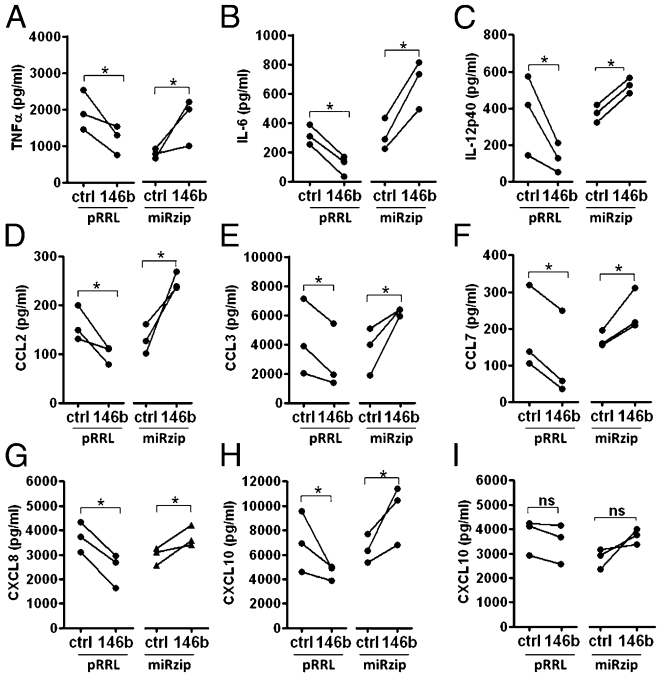

Fig. 6. MiR-146b down-regulates TLR4-dependent production of proinflammatory cytokines. (*A–H*) Proinflammatory cytokine levels measured by ELISA in cell-free supernatants of THP-1 cells transduced with lentiviral vectors overexpressing miR-146b (pRRL-146b and its respective control) or a miR-146b sponge (miRzip-146b and its respective control) after stimulation with 1 μg/mL LPS. (*I*) CXCL10 levels measured by ELISA in cell-free supernatants collected under the same experimental conditions after stimulation with 10 ng/mL IFN-γ.

Discussion

Negative regulation of the immune response plays an important role in controlling homeostasis of the immune system and in preventing development of autoimmune diseases. Multiple regulatory mechanisms, including a complex network of receptors, transcription factors, adaptors, and effector molecules, have evolved to keep activation of the immune system in check. Evidence is now emerging indicating that miR might constitute an additional negative feedback mechanism operating in the innate immune system (22-24). MiR-146a has been the first miR associated to the inflammatory response, described as an miR rapidly induced by proinflammatory stimuli in phagocytes (15), and experimental evidence has clearly defined its role of negative regulator of inflammation (10, 25, 26) and its involvement in endotoxin tolerance (27, 28). The miR-146 family also includes miR-146b, which is encoded by a distinct gene on a separate chromosome and only differs from miR-146a by 2 nt at the 3′ end in its mature sequence. Despite their sequence similarity, it is still unclear whether these two miRs fulfill redundant or distinct functions. Unlike miR-146a, little information is available on the biological role in the context of the immune response of miR-146b, which has been mostly associated with tumor biology, being expressed at lower levels in many human solid tumors compared with normal tissues (29–32).

Here we report that LPS stimulation induces miR-146b expression in human monocytes, with delayed kinetics with respect to miR-146a. Most relevant, our study provides evidence for a link between miR-146b and IL-10, demonstrating that miR-146b induction depends on the activity of IL-10 produced after LPS challenging, whereas, to the contrary, IL-10 does not influence miR-146a expression. This is consistent with ChIP data showing a central role of STAT3 in the induction of miR-146b but not miR-146a, which instead depends upon NF-κB. Bioinformatic analysis revealed a significant enrichment of miR-146b potential targets in the TLR signaling, IL-1 signaling, and NF-kB signaling pathways, which play an essential role in the innate immune response driving transcriptional activation of genes encoding for proinflammatory cytokines and costimulatory molecules, which subsequently control the activation of antigen-specific adaptive immune responses. Luciferase and RIP assays validated the LPS receptor TLR4 and the proximal adaptor molecules MyD88, IRAK-1, and TRAF6 as true miR-146b targets. As these molecules sustain the TLR4 signaling pathway and showed a relatively mild down-regulation at the protein level, these findings are consistent with the present understanding that miRs might conceivably exert their major activities through the subtle individual regulation of multiple targets involved in a common signaling pathway rather then operating a strong repression of isolated targets (29, 30). In keeping with this mechanism of regulation, enforced expression of miR-146b resulted in the marked reduction of proinflammatory cytokines highly expressed upon TLR triggering. These findings suggest that miR-146b mediates some of the anti-inflammatory activities of IL-10 repressing the inflammatory response in monocytes by direct targeting of transcripts encoding TLR4 and key adaptors/signaling molecules.

Although our results leave open the question whether the two miR-146 isoforms are functionally equivalent, their divergent and asynchronous transcriptional regulation suggests they play differential roles during distinct temporal windows of the inflammatory process. During the development of the inflammatory process miR-146a and b may represent the components of a relay team in which one isoform succeeds to other to control expression of proinflammatory genes, first through the activity of the LPS-depend induction of miR-146a, and subsequently during the resolution phase maintaining transcripts repression through the IL-10 dependent induction of miR-146b. In this respect it is worth noticing that miR-146a–deficient mice are indeed overresponsive to bacterial challenge and produce excessive amount of proinflammatory cytokines (31), but they show an autoimmune phenotype with late onset and incomplete penetrance and lack a global change in the expression of putative miR-146 targets (32). This phenotype is suggestive of the existence of a compensatory mechanism operating in miR-146a–deficient animals. Finally, similar to miR-146b, miR-146a has been shown to target IRAK-1 and TRAF6, although in different cellular contexts (15, 29), but its ability to also directly target MyD88 and TLR4 has not been investigated.

Further research is required to understand whether miR-146b truly serves as a molecular switch involved in the resolution of inflammation, but it is interesting to note that this miR has been reported to be expressed during the resolution phase in a murine model of acute inflammation (33). A broader and deeper understanding of how miR-146b acts in concert with the growing number of negative regulators, particularly in the context of complex inflammatory processes involving signaling by multiple receptors, may well lead to novel therapeutic approaches for the rapidly expanding number of diseases driven by dysregulated inflammatory responses.

Materials and Methods

Materials. A detailed list of materials is provided in *SI Materials and Methods*.

Cell Purification and Culture. Human monocytes were obtained from healthy donor buffy coats by two-step gradient centrifugation using Ficoll (Biochrom) and Percoll (Amersham). Human studies were approved by the ethical committee of Istituto Clinico Humanitas, Milan, Italy. Monocytes and THP-1 cell line (American Type Culture Collection) were resuspended in RPMI 1640 (Lonza) supplemented with 10% (vol/vol) heat-inactivated FBS (Lonza), 100 U/mL penicillin/streptomycin (Lonza), and 25 mM L-glutamine (Lonza). The HEK-293T cell line (American Type Culture Collection) was grown in Dulbecco's modified Eagle medium (DMEM) (Cambrex) supplemented with 10% (vol/vol) FBS, 100 U/mL penicillin/streptomycin, and 25 mM L-glutamine. Murine bone marrow-derived macrophages were obtained as described in *SI Materials and Methods*.

ChIP Assay. ChIP experiments were performed as described elsewhere (34) and in *SI Materials and Methods*.

ELISA. Antibodies and detection reagents for ELISAs were purchased from R&D Systems and used according to the manufacturer's instructions. Samples were diluted so that the optical density fell within the optimal portion of a log standard curve.

Quantification of miR and mRNA. Total RNA was purified by using TRIzol Reagent (Ambion), and qPCR was conducted by using a 7900HT Real-Time PCR System. One hundred nanograms of total RNA were reverse-transcribed for quantification of miR expression by using TaqMan MiRNA Reverse Transcription Kit (Applied Biosystems), according to the manufacturer's instructions and as described in detail in *SI Materials and Methods*.

Constructs. The 3′UTR of TLR4, TLR2, MyD88, IRAK-1, TRAF6, and IL-6 were amplified from genomic DNA and cloned in the biosensor psiCHECK-2 vector (Promega). PremiR-146b and premiR-146a were amplified from genomic DNA and cloned in the pcDNA3 expression vector as described in *SI Materials and Methods*. To knock down miR-146b expression, the miRzip lentivector-based construct anti–miR-146b and the relative control were purchased from System Biosciences. The list of oligonucleotides used is reported in Table S1.

Luciferase Reporter Assay. HEK-293T cells were transfected after 24 h with 100 ng psiCHECK-2–3′UTR reporter construct and 700 ng pcDNA3-miR or pcDNA3 as control, by using Lipofectamine 2000 (Invitrogen), according to the manufacturer's protocol, as described in detail in *SI Materials and Methods*.

FACS Analysis. Cells were washed twice with PBS solution containing 1% BSA. Aspecific binding was blocked by using Fc-block (BD Biosciences). Washed cells were resuspended in a 1:200 dilution of APC-conjugated anti-human TLR4 (clone HTA125; eBioscience) or anti-human TLR2 antibody (clone 383936; R&D Systems) or the mouse IgG_{2a} isotype control APC (eBioscience). Stained cells were washed twice with PBS solution containing 1% BSA and analyzed by flow cytometry (FACSCanto; BD Biosciences).

Immunoprecipitation of Ago2-Bound RNAs. Immunoprecipitation of Ago2-bound RNAs (RIP), which contains miRs and their target mRNA, was performed as previously described (35), with minor modifications and as described in detail in *SI Materials and Methods*. Briefly, 30×10^6 pRRL-ctrl and pRRL-146b THP-1 cells were stimulated for 2 h with 1 μg/mL LPS, whereas miRzip-ctrl and miRzip-146b THP-1 cells were stimulated for 12 h with 1 μg/mL LPS. In all experiments, an aliquot of immunoprecipitation supernatants, corresponding to 0.5×10^6 cell equivalent, was removed after immunoprecipitation (indicated as "left over") and used as control for the specificity of the assay. Results were expressed as fold enrichment relative to Ago2-immunoprecipitation control samples.

Statistical Analysis. Statistical evaluation was performed with use of the Student *t* test or one-way ANOVA and reported in figures. *P* values less than 0.05 were considered significant.

ACKNOWLEDGMENTS. This study was conducted in the context of Fondazione Humanitas per la Ricerca and was supported by Ministero dell'Istruzione dell'Università e della Ricerca PRIN (Progetto di Rilevante Interesse Nazionale) Research Grants 2002061255 and FIRB (Fondo per Investimenti in Ricerca di Base) Research Grant RBFR08CW8G, a University of Verona Joint Project Grant, the Italian Association for Cancer Research, Regione Lombardia LIIN (Lombardian Innate Immunity Network) Project, Fondazione Cariplo, and the European Community Seventh Framework Programme TIMER Project.

1. O'Neill LA (2006) How Toll-like receptors signal: What we know and what we don't know. *Curr Opin Immunol* 18(1):3–9.
2. Murthy PK, Dennis VA, Lasater BL, Philipp MT (2000) Interleukin-10 modulates proinflammatory cytokines in the human monocytic cell line THP-1 stimulated with Borrelia burgdorferi lipoproteins. *Infect Immun* 68(12):6663–6669.
3. Siewe L, et al. (2006) Interleukin-10 derived from macrophages and/or neutrophils regulates the inflammatory response to LPS but not the response to CpG DNA. *Eur J Immunol* 36(12):3248–3255.
4. Tebo JM, Kim HS, Gao J, Armstrong DA, Hamilton TA (1998) Interleukin-10 suppresses IP-10 gene transcription by inhibiting the production of class I interferon. *Blood* 9(12): 4742–4749.
5. Zhou L, Nazarian AA, Smale ST (2004) Interleukin-10 inhibits interleukin-12 p40 gene transcription by targeting a late event in the activation pathway. *Mol Cell Biol* 24(6): 2385–2396.
6. Kishore R, Tebo JM, Kolosov M, Hamilton TA (1999) Cutting edge: clustered AU-rich elements are the target of IL-10-mediated mRNA destabilization in mouse macrophages. *J Immunol* 162(5):2457–2461.
7. Knödler A, et al. (2009) Post-transcriptional regulation of adapter molecules by IL-10 inhibits TLR-mediated activation of antigen-presenting cells. *Leukemia* 23(3):535–544.
8. Selbach M, et al. (2008) Widespread changes in protein synthesis induced by microRNAs. *Nature* 455(7209):58–63.
9. Friedman RC, Farh KK, Burge CB, Bartel DP (2009) Most mammalian mRNAs are conserved targets of microRNAs. *Genome Res* 19(1):92–105.
10. O'Neill LA, Sheedy FJ, McCoy CE (2011) MicroRNAs: the fine-tuners of Toll-like receptor signalling. *Nat Rev Immunol* 11(3):163–175.
11. McCoy CE, et al. (2010) IL-10 inhibits miR-155 induction by toll-like receptors. *J Biol Chem* 285(27):20492–20498.
12. O'Connell RM, Chaudhuri AA, Rao DS, Baltimore D (2009) Inositol phosphatase SHIP1 is a primary target of miR-155. *Proc Natl Acad Sci USA* 106(17):7113–7118.
13. Rossato M, et al. (2012) IL-10-induced microRNA-187 negatively regulates TNF-α, IL-6, and IL-12p40 production in TLR4-stimulated monocytes. *Proc Natl Acad Sci USA* 109(45):E3101–E3110.
14. Sheedy FJ, et al. (2010) Negative regulation of TLR4 via targeting of the proinflammatory tumor suppressor PDCD4 by the microRNA miR-21. *Nat Immunol* 11(2): 141–147.
15. Taganov KD, Boldin MP, Chang KJ, Baltimore D (2006) NF-kappaB-dependent induction of microRNA miR-146, an inhibitor targeted to signaling proteins of innate immune responses. *Proc Natl Acad Sci USA* 103(33):12481–12486.
16. O'Connell RM, Taganov KD, Boldin MP, Cheng G, Baltimore D (2007) MicroRNA-155 is induced during the macrophage inflammatory response. *Proc Natl Acad Sci USA* 104(5):1604–1609.
17. Bazzoni F, et al. (2009) Induction and regulatory function of miR-9 in human monocytes and neutrophils exposed to proinflammatory signals. *Proc Natl Acad Sci USA* 106(13):5282–5287.
18. Alas S, Bonavida B (2003) Inhibition of constitutive STAT3 activity sensitizes resistant non-Hodgkin's lymphoma and multiple myeloma to chemotherapeutic drug-mediated apoptosis. *Clin Cancer Res* 9(1):316–326.
19. Benkhart EM, Siedlar M, Wedel A, Werner T, Ziegler-Heitbrock HW (2000) Role of Stat3 in lipopolysaccharide-induced IL-10 gene expression. *J Immunol* 165(3): 1612–1617.
20. Betel D, Koppal A, Agius P, Sander C, Leslie C (2010) Comprehensive modeling of microRNA targets predicts functional non-conserved and non-canonical sites. *Genome Biol* 11(8):R90.
21. Qi XF, et al. (2009) Essential involvement of cross-talk between IFN-gamma and TNF-alpha in CXCL10 production in human THP-1 monocytes. *J Cell Physiol* 220(3):690–697.
22. Zhou R, O'Hara SP, Chen XM (2011) MicroRNA regulation of innate immune responses in epithelial cells. *Cell Mol Immunol* 8(5):371–379.
23. Perry MM, et al. (2008) Rapid changes in microRNA-146a expression negatively regulate the IL-1beta-induced inflammatory response in human lung alveolar epithelial cells. *J Immunol* 180(8):5689–5698.
24. O'Connell RM, Rao DS, Chaudhuri AA, Baltimore D (2010) Physiological and pathological roles for microRNAs in the immune system. *Nat Rev Immunol* 10(2):111–122.
25. Etzrodt M, et al. (2012) Regulation of monocyte functional heterogeneity by miR-146a and Relb. *Cell Rep* 1(4):317–324.
26. Jurkin J, et al. (2010) miR-146a is differentially expressed by myeloid dendritic cell subsets and desensitizes cells to TLR2-dependent activation. *J Immunol* 184(9):4955–4965.
27. Nahid MA, Pauley KM, Satoh M, Chan EK (2009) miR-146a is critical for endotoxin-induced tolerance: IMPLICATION IN INNATE IMMUNITY. *J Biol Chem* 284(50):34590–34599.
28. Quinn EM, Wang J, Redmond HP (2012) The emerging role of microRNA in regulation of endotoxin tolerance. *J Leukoc Biol* 91(5):721–727.
29. Bhaumik D, et al. (2008) Expression of microRNA-146 suppresses NF-kappaB activity with reduction of metastatic potential in breast cancer cells. *Oncogene* 27(42):5643–5647.
30. Baek D, et al. (2008) The impact of microRNAs on protein output. *Nature* 455(7209): 64–71.
31. Boldin MP, et al. (2011) miR-146a is a significant brake on autoimmunity, myeloproliferation, and cancer in mice. *J Exp Med* 208(6):1189–1201.
32. Zhao JL, et al. (2011) NF-kappaB dysregulation in microRNA-146a-deficient mice drives the development of myeloid malignancies. *Proc Natl Acad Sci USA* 108(22): 9184–9189.
33. Recchiuti A, Krishnamoorthy S, Fredman G, Chiang N, Serhan CN (2011) MicroRNAs in resolution of acute inflammation: Identification of novel resolvin D1-miRNA circuits. *FASEB J* 25(2):544–560.
34. Tamassia N, et al. (2010) Uncovering an IL-10-dependent NF-kappaB recruitment to the IL-1ra promoter that is impaired in STAT3 functionally defective patients. *FASEB J* 24(5):1365–1375.
35. Hendrickson DG, Hogan DJ, Herschlag D, Ferrell JE, Brown PO (2008) Systematic identification of mRNAs recruited to argonaute 2 by specific microRNAs and corresponding changes in transcript abundance. *PLoS ONE* 3(5):e2126.

Supporting Information

Curtale et al. 10.1073/pnas.1219852110

SI Materials and Methods

Reagents. LPS from *Escherichia coli* (serotype 055:B5), Pam_3CsK_4, imiquimod, synthetic CpG oligonucleotides (ODN) and poly(I:C) were purchased from Enzo Life Sciences. Human IL-10 and IL-1β were purchased from R&D Systems. AG-490 was purchased from Calbiochem. Rabbit anti-Myd88 antibody was purchased from Enzo Life Science, and rabbit anti–IRAK-1 and rabbit anti-TRAF6 antibodies from Cell Signaling Technology. Other antibodies were purchased from Biolegend unless specified otherwise.

Purification of Murine Macrophages. Mouse macrophages, obtained from 6- to 8-wk C57BL/6 mice, were plated in six-well plates at a density of 1 to $2 \times 10^5/cm^2$. Femora and tibiae of hind legs were flushed with PBS solution and cells were resuspended in Iscove's modified Dulbecco's medium (IMDM) medium with L-glutamine, 10% (vol/vol) FCS, 100 U/mL penicillin, and 100 mg/mL of streptomycin and cultured for 7 d with 10 ng/mL macrophage colony-stimulating factor (MCSF). Macrophages were detached using PBS solution containing 10 mM EDTA, washed, and resuspended in IMDM medium supplemented with, 10% heat-inactivated FCS, 100 U/mL of penicillin, and 100 mg/mL of streptomycin.

Lentiviral Constructs. The pCR2.1 vector (Invitrogen) was used as subcloning vector. For THP-1 cells transduction, the microRNA (miR)/lentiviral-based expression vector pRRL-miR-146b and premiR-146a were generated cloning a 500-bp region encompassing the premiR-146b and premiR-146a in the pRRLSIN.cPPT. PGK-GFP.WPRE vector (plasmid 12252; Addgene). The lentiviral construct pRRL-ctrl, encoding for a hairpin yielding a 22-mer RNA with no homology to any human gene, was used as mock construct.

ChIP Assay. Sheared chromatin from 5×10^6 monocytes was immunoprecipitated overnight (ON) at 4 °C by using polyclonal antibodies against polymerase II (N-20; sc-899; Santa Cruz Biotechnology), STAT3 (C-20; sc-482; Santa Cruz Biotechnology). One percent of starting chromatin was used, not immunoprecipitated, and used as input. Quantitative real-time PCR (qPCR) was performed in triplicate by using promoter-specific primers (Table S1). Signals obtained from the ChIP samples were normalized on signals obtained from corresponding input samples, according to the formula $100 \times 2^{\wedge(\text{input Ct} - \text{sample Ct})}$. Results were expressed as fold enrichment relative to untreated cells.

Quantification of miR and mRNA. Total RNA was reverse transcribed and quantification was performed by using Power SYBR Green Mix (Applied Biosystems) with specific primer pairs (Table S1). Experimental data were then analyzed using the SDS2.2 software, and the relative expression values were calculated according to the "comparative Ct" method using U6 as endogenous control for miR and GAPDH for mRNA.

Luciferase Reporter Assay. HEK-293T cells were plated in 24-well plates in 500 μL of D-MEM supplemented with 10% FBS and 1% of L-glutamine at 16×10^4 per well. After 24 h, cells were transfected with 100 ng psiCHECK-2–3′UTR reporter construct and 700 ng pcDNA3-miR or pcDNA3 as control by using Lipofectamine 2000 (Invitrogen). After 48 h, cells were lysed, and *firefly* and *renilla* luciferase activities were determined by using the Dual-Glo Luciferase Assay System (Promega). The enzymatic activities of both luciferases were quantified by using a MultiDetection Microplate Reader Synergy 2 luminometer (BioTek). The values of *renilla* luciferase activity were normalized by *firefly* luciferase activities, which served as internal control. Normalized values were expressed as fold changes relative to the value of the negative control.

***In Silico* Prediction of miR-146b Targets.** The list of miR-146b predicted targets with their probability (mirSVR) score was obtained from the microRNA database (www.microrna.org) (1). The relative enrichment of biological functions and associated networks was determined calculating the *P* value associated to the Fisher exact test built into the Ingenuity Pathway Analysis software (Ingenuity Systems).

Immunoprecipitation of Ago2-Bound RNAs. Immunoprecipitations were carried out ON at 4 °C by using Magna Chip Protein A+G magnetic beads (Millipore) conjugated with anti-Ago2 (EIF2C2 monoclonal antibody, clone 2E12-1C9; Abnova) or isotype IgG_{1k} control Abs (Abnova). A total of 30×10^6 pRRL-ctrl and pRRL-146b THP-1 cells were stimulated for 2 h with 1 μg/mL LPS, whereas miRzip-ctrl and miRzip-146b THP-1 cells were stimulated for 12 h with 1 μg/mL LPS. In all experiments, an aliquot of immunoprecipitation supernatants, corresponding to 0.5×10^6 cell equivalent, was removed after immunoprecipitation (indicated as "left over") and used as control for the specificity of the assay. Results were expressed as fold enrichment relative to Ago2-IP CT samples. Sequences of 3′UTR mRNA-specific primers used in qPCR are listed in Table S1. The miR/mRNA enrichment to the RNA-induced silencing complex was calculated according to the formula $2^{-(\text{CtAgo} - \text{CtIgG})}$ and normalized over GAPDH for mRNA and U6 for miR.

Prediction of miRNA–mRNA Duplex Secondary Structure. The RNAhybrid Web server (http://bibiserv.techfak.uni-bielefeld.de/rnahybrid) (2) was used to predict multiple binding sites of miRNAs in large target RNAs, calculating the minimum free energy related to the secondary structure of the miRNA–mRNA duplex.

1. Hendrickson DG, Hogan DJ, Herschlag D, Ferrell JE, Brown PO (2008) Systematic identification of mRNAs recruited to argonaute 2 by specific microRNAs and corresponding changes in transcript abundance. *PLoS ONE* 3(5):e2126.

2. Rehmsmeier M, Steffen P, Hochsmann M, Giegerich R (2004) Fast and effective prediction of microRNA/target duplexes. *RNA* 10(10):1507–1517.

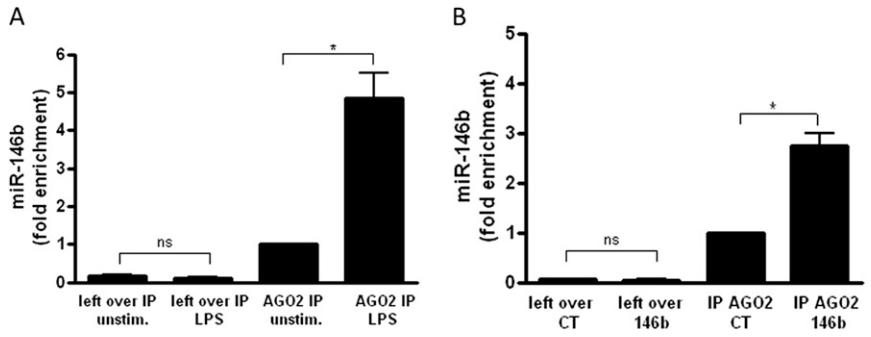

Fig. S1. MiR-146b enrichment in the RISC complex. (*A*) Human monocytes were stimulated or not with 100 ng/mL LPS for 16 h. Cell extracts were subjected to RIP assay using anti-Ago2 or IgG control Abs and levels of miR-146b were assayed in triplicate by Q-PCR in RIP (IP AGO2) and left over samples and expressed as normalized fold enrichment of miR-146b. (*B*) Cell extracts from pRRL-ctrl transduced (CT) and pRRL-146b transduced (146b) THP-1 cells were subjected to RIP assay using anti-Ago2 or IgG control Abs and levels of miR-146b were assayed in triplicate by Q-PCR in RIP (IP AGO2) and left over samples and expressed as normalized fold enrichment of miR-146b. Results are shown as normalized fold enrichment (mean ± SEM).

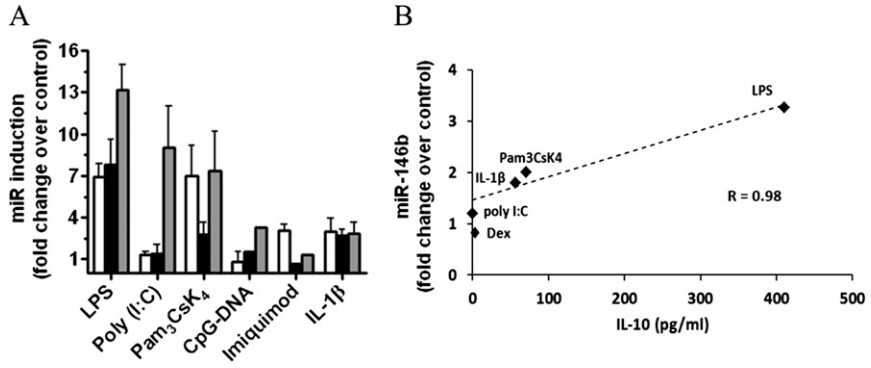

Fig. S2. MiR-146b induction by different stimuli correlates with IL-10 expression. (*A*) Expression levels of miR-146a (white columns), miR-146b (black columns), and miR-155 (grey columns) were measured by Q-PCR in triplicate samples of human monocytes cultured for 24 h with TLR/IL-1R agonists (100 ng/mL LPS, 5 μg/mL poly(I:C), 1 μg/mL Pam_3CsK_4, 1μM CpG-DNA, 100 ng/mL imiquimod, 100 ng/mL IL-1β). Results are expressed as fold change over untreated cells (mean ± SEM; $n = 3$). (*B*) Monocytes were cultured for 24 h with 100 ng/mL LPS, 1 μg/mL Pam_3CsK_4, 5 μg/mL poly(I:C), 100 ng/mL IL-1β, or 200 ng/mL dexamethasone. IL-10 release in cell-free supernatants was analyzed by ELISA and correlated to the expression of miR-146b, quantified by Q-PCR. Dotted line represents the linear regression curve correlating miR-146b expression levels with IL-10 release in the indicated experimental conditions. Results shown are from one representative of three independent experiments.

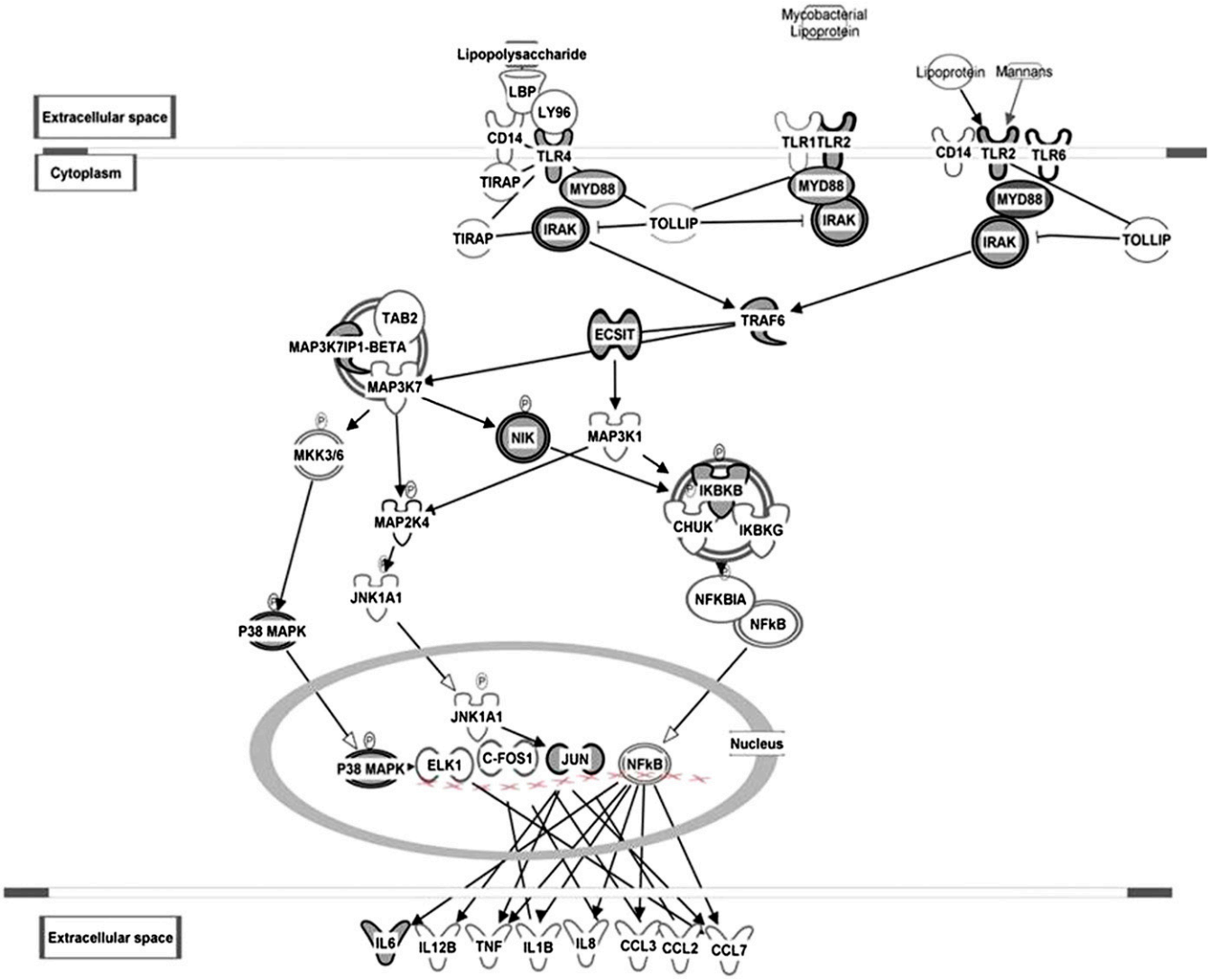

Fig. S3. Predicted miR-146b targets in the TLR pathway. Graphic representation of the TLR4/TRL2 pathway with predicted miR-146b target genes highlighted.

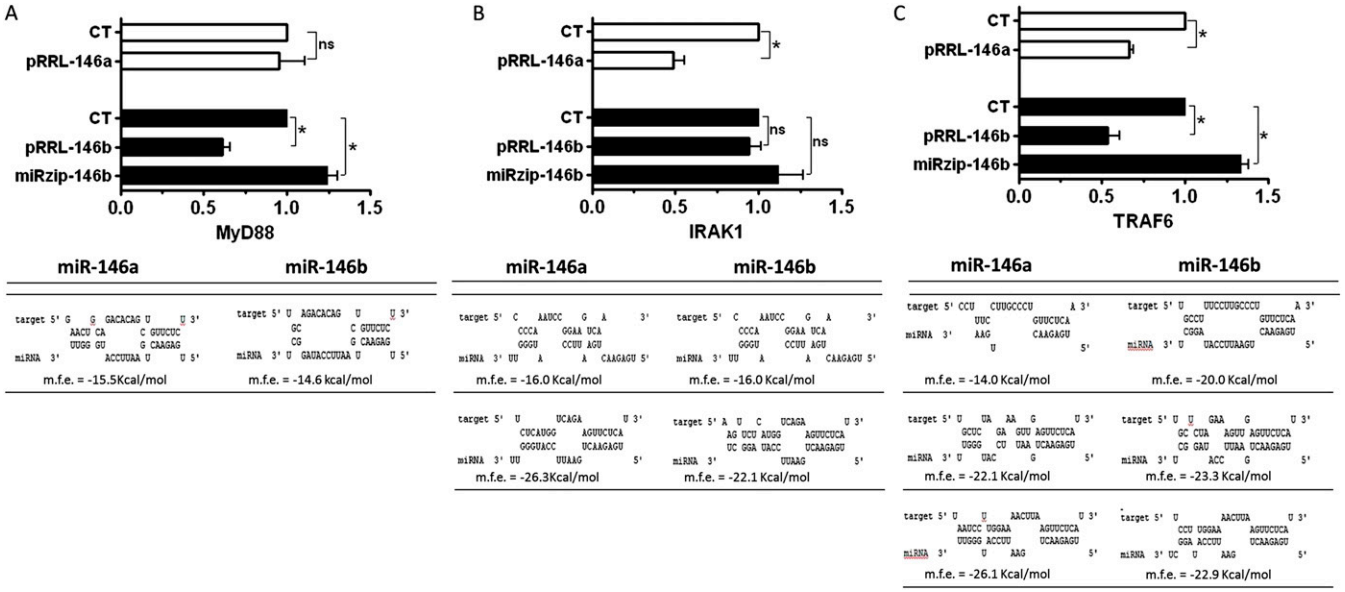

Fig. S4. Differential effect of miR-146a and miR-146b on transcripts of TLR signalling adaptors. Relative MyD88 (*A*), IRAK-1 (*B*), and TRAF6 (*C*) mRNA levels were measured by Q-PCR in pRRL-ctrl, pRRL-146b, miRzip-ctrl and miRzip-146b THP-1 cells and normalized to GAPDH. Results are shown as fold change over nonstimulated control (mean ± SEM). The predicted structure of the miRNA-mRNA target duplex is graphically visualized, according to RNA hybrid algorithm (see *SI Materials and Methods*) and the corresponding minimum free energy (m.f.e.) is also reported.

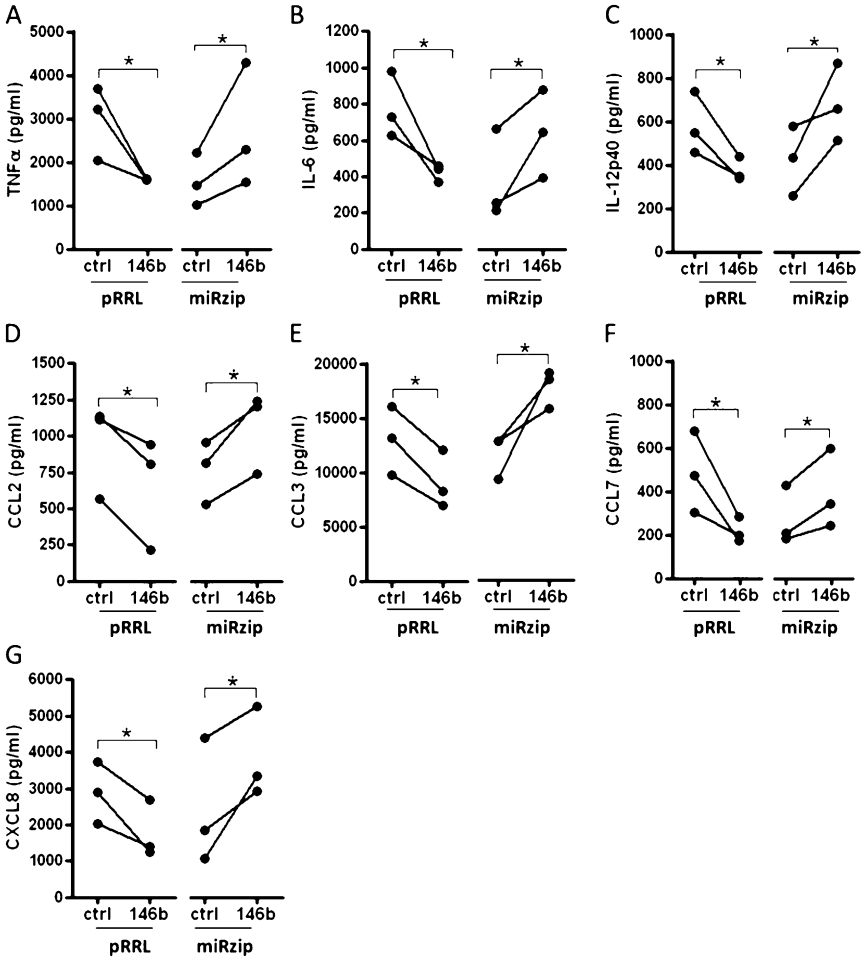

Fig. S5. MiR-146b down-regulates TLR2-dependent production of pro-inflammatory cytokines. (*A–G*) Pro-inflammatory cytokine levels measured by ELISA in cell-free supernatants of THP-1 cells transduced with lentiviral vectors overexpressing miR-146b (pRRL-146b and its respective control) or a miR-146b sponge (miRzip-146b and its respective control) after stimulation with 1 μg/mL Pam_3CsK_4.

Table S1. List of oligonucleotides used

Type	Oligonucleotide
Cloning	
TLR4 3′UTR	5′-GTCAGAAACCTGTCCACT-3′
	5′-TGTGCCTAATTCAGAAGATG-3′
TLR2 3′UTR	5′- GTTCCCATATTTAAGACCAG-3′
	5′- TCTCATCCTGTAAAGTTTAA-3′
IL-6 3′UTR	5′-GTCAGAAACCTGTCCACT-3′
	5′-AATATGTATAAGTTAGCCAT-3′
IRAK-1 3′UTR	5′-ATCATTTATGCTTGGGAGGT-3′
	5′-AAGAGGACACTCGGTTACA-3′
MyD88 3′UTR	5′-GCAAATATCGGCTTTTCTCA-3′
	5′-GACTCTCTTTGGAGCATA-3′
TRAF6 3′UTR	5′-TTGCCCTCACTTGCTCAA-3′
	5′-AGATGCTACTTCGTAACCTC-3′
miR-146b	5′-TGGAATAGGAGTTCTCTTG-3′
	5′-TAGTGGCAGGTTATGAGCA-3′
miR-146b seed mutagenesis	
TLR4	5′-TGTCTATGGCTGTTTGAGATTCTCTACTCTTGTGCTTG-3′
	5′-CAAGCACAAGAGTAGAGAATCTCAAACAGCCATAGACA-3′
IRAK-1 (seed 1)	5′-GATCCCCCAAATCCGGCAAAGTTCTCATGGTC-3′
	5′-GACCATGAGAACTTTGCCGGATTTGGGGGATC-3′
IRAK-1 (seed 2)	5′-GCAAAGTTCTCATGGTCGTTCTCATGGTGCACGA-3′
	5′-TCGTGCACCATGAGAACGACCATGAGAACTTTGC-3′
MyD88	5′-GAACTGCAGACACAGCTTCTCCCTCTCTCCTT-3′
	5′-AAGGAGAGAGGGAGAAGCTGTGTCTGCAGTTC-3′
TRAF6 (seed 1)	5′-CCTGGAGAAAACAGTGTCCTTGCCCTGTTCTC-3′
	5′-GAGAACAGGGCAAGGACACTGTTTTCTCCAGG-3′
TRAF6 (seed 2)	5′-CTCGAGAAGAGTTATTGCTCTAGTTGAGTTCTCATTTTTTTAACC-3′
	5′-GGTTAAAAAAATGAGAACTCAACTAGAGCAATAACTCTTCTC-3′
TRAF6 (seed 3)	5′-ATTTGAACCATAATCCTTGGATTAAGTTCTCATTCACCCCAG-3′
	5′-CTGGGGTGAATGAGAACTTAATCCAAGGATTATGGTTCAAAT-3′
qPCR	
MyD88	5′-GCACATGGGCACATACAGAC-3′
	5′-GACATGGTTAGGCTCCCTCA-3′
IL-6	5′-TACCCCCAGGAGAAGATTCC-3′
	5′-TTTTCTGCCAGTGCCTCTTT-3′
TLR4	5′-CACCTGATGCTTCTTGCTG-3′
	5′-TCCTGGCTTGAGTAGATAA-3′
TRAF6	5′-GTCCCTTCCAAAAATTCCAT-3′
	5′-CACAAGAAACCTGTCTCCTT-3′
IRAK-1	5′-TGAAGAGGCTGAAGGAGAA-3′
	5′-CACAATGTTTGGGTGACGAA-3′
ChIP assay	
Pol-II on miR-146b	5′-AATAGGAGTTCTCTTGGTAT-3′
	5′-AATTCAGTTCTCAGTGCC-3′
Pol-II on miR-146a	5′-GAGGAAGTGACATTGAAAGC-3′
	5′-TGTATGGTAGACACACACAT-3′
Pol-II on miR-155	5′-ACCATTTCTTCCTCTCTTAG-3′
	5′-GGCTCCAACCTTTGTTCTT-3′
STAT3 in miR-146b	5′-CTCGGCTGAACTCTCCAGA-3′
	5′-GCAAACCAAGGGGCTTTCT-3′
STAT3 in miR-146a	5′-GCACTTGAAAAGCCAACAGG-3′
	5′-CACAGCGAGGGAGGAAGA-3′
RIP assay	
IRAK-1	5′-CTCTTTGCCCATCTCTTTG-3′
	5′-GCCACACTTTTCCAAATTGT-3′
TRAF6	5′-TAAGTTCTCATTCACCCCAG-3′
	5′-AGGAAATAAGTAAGCAAGGC-3′
MYD88	5′-GCTTGGGCTGCTTTTCATT-3′
	5′-CCTGCTCACATCATTACAGT-3′
TLR4	5′-CCTCCTCAGAAACAGAACAT-3′
	5′-TCATAACGGCTACACCATTT-3′
TLR2	5′-CAACTGTAATCTGTAGCAAC-3′
	5′-TAGCAGGAAGAAAGAATGAC-3′
IL-6	5′-GCATTCCTTCTTCTGGTCA-3′
	5′-ATAGTGTCCTAACGCTCATA-3′